2016-04

Structure, Vibrational Spectra, and Thermodynamic Properties of Cluster Ions over Cesium Halides

Mwanga, Stanley Ferdinand

STRUCTURE, VIBRATIONAL SPECTRA, AND THERMODYNAMIC PROPERTIES OF CLUSTER IONS OVER CESIUM HALIDES

Stanley Ferdinand Mwanga

A Dissertation Submitted in Partial Fulfillment of the Requirements for the Degree of Doctor of Philosophy in Materials Science and Engineering at the Nelson Mandela African Institution of Science and Technology

Arusha, Tanzania

April, 2016

ABSTRACT

The geometrical parameters, vibrational spectra and thermodynamic properties of molecular and ionic clusters of cesium halides, Cs_nX_n, $Cs^+(CsX)_n$, $X^-(CsX)_n$, where X = F, Cl, Br, I, n=1-4, have been studied using electron density functional theory (DFT) with the Beck–Lee–Yang–Parr functional (B3LYP5) and second and fourth order Møller–Plesset perturbation theory (MP2 and MP4). The relativistic effective core potential (ECP) with Def2-QZVP for cesium and SDB-aug-cc-pVTZ for bromine and iodine, as well as full-electron basis set with aug-ccpVTZ for fluorine and cc-pVTZ for chlorine were employed. Geometrical parameters of the species have been optimized and vibrational spectra calculated. The IR spectra have been analyzed and assignment of vibrational modes performed. Various configurations of the species have been considered and existence of isomers revealed for trimers (Cs_3X_3), pentaatomic ions ($Cs_3X_2^+$ and $Cs_2X_3^-$) and heptaatomic positive ions ($Cs_4F_3^+$, $Cs_4Cl_3^+$). Using thermodynamic approach the relative abundances of isomers have been evaluated.

Enthalpies of dissociation reactions $\Delta_r H°(0)$ of molecular and ionic clusters have been determined theoretically and on the basis of the experimental equilibrium constants measured earlier for selected reactions. Both theoretical and based on experiment values of $\Delta_r H°(0)$ appeared to be in agreement. The enthalpies of formation $\Delta_f H°(0)$ of the species have been determined (in kJ mol^{-1}): −1384 ± 8 (Cs_3F_3); −996 ± 9 (Cs_3Cl_3); −858 ± 11 (Cs_3Br_3); −698 ± 15 (Cs_3I_3); −1949 ± 13 (Cs_4F_4); −1453 ± 16 (Cs_4Cl_4); −1265 ± 23 (Cs_4Br_4); −1038 ± 23 (Cs_4I_4); −97 ± 4 (Cs_2F^+); 101 ± 5 (Cs_2Br^+); 160 ± 10 (Cs_2I^+); −774 ± 4 (CsF_2^-); −552 ± 5 ($CsBr_2^-$);−478 ± 10 (CsI_2^-); −581 ± 7 ($Cs_3F_2^+$), 202 ± 10 ($Cs_3Br_2^+$); −88 ± 15 ($Cs_3I_2^+$); −1255 ± 7 ($Cs_2F_3^-$); −858 ± 10 ($Cs_2Br_3^-$); −729 ± 15 ($Cs_2I_3^-$); −1142 ± 12 ($Cs_4F_3^+$); −727 ± 17 ($Cs_4Cl_3^+$); −1632 ± 17 ($Cs_5F_4^+$); −1119 ± 36 ($Cs_5Cl_4^+$).

The Gibbs free energies $\Delta_r G°(T)$ calculated for the dissociation reactions of trimer and tetramer molecules have indicated that these molecules are resistive in narrow temperature range only and decompose spontaneously with temperature increase with elimination of dimer molecules.

DECLARATION

I, **STANLEY FERDINAND MWANGA** do hereby declare to the Senate of the Nelson Mandela African Institution of Science and Technology that this dissertation is my own original work and that it has neither been submitted nor being concurrently submitted for degree award in any other institution.

_____ _____

Name and signature of candidate **Date**

The above declaration is confirmed

_____ _____

Name and signature of supervisor (1) **Date**

_____ _____

Name and signature of supervisor (2) **Date**

COPYRIGHT

CERTIFICATION

The undersigned certify that they have read dissertation titled "***Structure***, ***Vibrational Spectra, and Thermodynamic Properties of Cluster Ions over Cesium Halides***" and recommend for examination in fulfillment of the requirements for the degree of Doctor of Philosophy in Materials Science and Engineering of the Nelson Mandela African Institution of Science and Technology.

_____

Professor Tatiana P. Pogrebnaya

(Supervisor)

_____

Professor Alexander M. Pogrebnoi

(Supervisor)

ACKNOWLEDGEMENT

I am pleased to have this opportunity to thank all those people who have guided, inspired and helped me to complete my studies at The Nelson Mandela Institution of Science and Technology (NM-AIST). First of all, I would like to express my deep gratitude to my supervisors: Prof. **Tatiana P. Pogrebnaya** and Prof. **Alexander M. Pogrebnoi** for their invaluable time, tremendous support, constant guidance, comments, endless patience and encouragement. They were always there to help, and I am so grateful to have the opportunity to work with them and to be part of their computational research group. I would like also to thank Mr. **Adam Mawenya** an IT member in the School of Computational and Communication Sciences and Engineering (CoCSE) of NM-AIST laboratory for his precious assistance and services.

I'm indebted too, to the **United Republic of Tanzania** through NM-AIST, for granting me financial support to pursue my studies without which the study would not have been possible. I, also acknowledge the permission of study leave given by The University of Dodoma for me to undertake this study.

Last but not least, I thank my family, my wife **Maryline**, and my daughters: **Doreen**, **Dorice** and **Dorcas** for their patience especially during the time they missed my love. No words can express my gratitude to my late father **Ferdinand Remy Mwanga (+1997)** and my mother **Leah Raphael Msuya** for all they have given me throughout my entire life and academic career. I would have not made this far without their guidance, patience, moral and financial support and encouragement.

I pray to The Almighty God to bless everyone abundantly.

DEDICATION

I dedicate this work to my wife **Maryline**, and my daughters **Doreen**, **Dorice** and **Dorcas**

TABLE OF CONTENTS

LIST OF TABLES

LIST OF FIGURES

LIST OF APPENDICES

LIST OF ABBREVIATIONS AND SYMBOLS

$\Delta\varepsilon$	Zero point vibration energy (ZPVE) correction
$\Delta_f H°(0)$	Enthalpy of formation
$\Delta_r E$	Dissociation energies
$\Delta_r E_C$	Energies of dissociation reaction computed using counterpoise correction
ΔE_{iso}	Isomerisation energies
$\Delta_r G°(T)$	Change in Gibbs free energies
$\Delta_r H°(0)$	Enthalpy of dissociation reaction
$\Delta_r \Phi°(T)$	Reduced Gibbs energy of the reaction
$\Sigma\omega_{i\ prod}$	Sums of the products of vibrational frequencies
$\Sigma\omega_{i\ react}$	Sums of the reactants of vibrational frequencies
k_p°	Equilibrium constant
Å	Angstrom
B1	First basis set
B2	Extended basis set
B3LYP5	Becke-Lee-Yang-Parr DFT functional
B3P86	Becke-Perdew DFT functional
BSSE	Basis set superposition error
c	Speed of light in the free space
CC	Coupled cluster
cc-pVTZ	Correlation consistent, polarized valence triple zeta basis set
CCSDT	Coupled cluster single, double and triple excitations
CI	Configuration interaction
CP	Counterpoise method
CPC	Counterpoise correction
DFT	Density functional theory
ECP	Effective core potential
EMSL	The Environmental molecular science laboratory US
GAMESS	General Atomic and Molecular Electronic Structure System

GGA	Generalized gradient approximation
h	Planck constant
HF	Hartee-Fock theory
LDA	Local density approximation
MBPT	Many body perturbation theory
MO	Molecular orbital
MP2	2^{nd} order Møller-Plesset perturbation theory
MP4	4^{th} order Møller-Plesset perturbation theory
PES	Potential energy surface
p_I	Partial pressure of reactants
p_{II}	Partial pressure of the products
R	Gas constant
SCF	Self consistent field
SDB-aug-cc-pVTZ	Stuttgart–Dresden–Bonn–augmented correlation consistent polarization valence triple zeta basis
T	Temperature

CHAPTER ONE

Introduction

1.1. Background Information on molecular and ionic clusters

Cluster is a group of atoms or molecules combined together by the interaction ranging from weak van der Waals to strong covalent bonds (Castleman *et al.*, 2006), usually are within sub-nanometre to nanometre range whereby the number of atoms or molecules are defined accurately. The most interesting behaviour of clusters is that their composition can be selectively chosen by changing the number of atoms or geometry and the individual characteristics might be retained when assembled into single nanoscale composites (Khanna *et al.*, 1993, 1995; Woodruff, 2007). The possibility of tuning properties of clusters through size and composition make them to serve as a source of new materials with tailored properties.

Alkali halides are among the group of species that show the promising characteristics of cluster ions; for instance, Kumar and Misra (Srivastava *et al.*, 2014a, b) theoretically synthesized supersalts by simply combining two cluster ions. Similarly cluster ions with the unique physical and chemical properties are useful in elaboration of ionic thrusters (Patterson, 2004), and magneto-hydrodynamic generators (Kay, 2011). Moreover, mixed alkali halide and lanthanide trihalide are used in the production of metal-halide lamps as the energy saving light sources (Hilpert *et al.*, 1997; Miller *et al.*, 1994). Apart from these, cesium halide in particular has been identified with several possible scientific applications: cesium chloride through ion implantation and chemical vapor deposition technique (Michael *et al.*, 1994) have made feasible for a number of modern electronic devices and novel materials being fabricated (Lee *et al.*, 2010; Liao *et al.*, 2011; Liu *et al.*, 2013a; Liu *et al.*, 2012; Zhang *et al.*, 2014; Zhang *et al.*, 2012). Besides, cesium and iodine are proved to exist among the fission products that can be released in nuclear power plants (Lennart *et al.*, 1994; Roki *et al.*, 2014; Roki *et al.*, 2013). They have major impact on ground contamination and radiation doses in environment in case of accidents such as containment building leakages. The essential properties involved in all processes are the enthalpy of formation of the gaseous species and their thermodynamic functions, usually derived by statistical thermodynamics from their molecular geometry and vibrational frequencies.

Molecular and ionic clusters over cesium halides have been detected under high temperature mass spectrometry (Dunaev *et al.*, 2013; Gorokhov, 1972; Gusarov, 1986; Hilpert, 1990; Lisek *et al.*, 1998; Pogrebnoi *et al.*, 2000; Sidorova *et al.*, 1979). For some species such as Cs_2Cl^+, $CsCl_2^-$, $Cs_3Cl_2^+$, $Cs_2Cl_3^-$, $Cs_4Cl_3^+$ and $Cs_5Cl_4^+$ (Pogrebnoi *et al.*, 2000), and Cs_2I^+, CsI_2^-, $Cs_3I_2^+$ and $Cs_2I_3^-$ (Sidorova *et al.*, 1979) their equilibrium constants of ion-molecular reactions involving these ions had been measured. Thermodynamic properties were estimated using the third law of thermodynamics. Moreover, the quantum chemical calculations have shown to be promising techniques for estimating geometrical parameters and vibrations spectra of the molecules and cluster ions which are essential in the evaluation of thermodynamic functions. Previously quantum chemical methods were used to determine the geometrical parameters, vibration frequencies and thermodynamic properties of cluster ions existing in saturated vapors over NaX (X = F, Cl, Br, I) and MCl (M = K, Rb, Cs) (Pogrebnaya *et al.*, 2007, 2008, 2010; Pogrebnaya *et al.*, 2012). Experimental techniques are available for determining the geometrical parameters and vibrational frequencies however, for higher molecules and cluster ions are difficult to be measured directly (Castleman *et al.*, 2006). Thus, theoretical calculations play a vital role to supplement the missing data.

1.2. Quantum Chemical Methods

The improvement of computational techniques and basis sets offers a possibility of producing computed structural parameters that is compatible with the level of precision experimental data. The advantage of chemical computational methods is the ability of providing information not only about stable, but also unstable molecules as intermediate or even transition state which is difficult to obtain through experiment. Therefore, the overall computational chemistry is very important adjunct to experimental chemistry.

Molecular mechanics and electronic structure theory are two theoretical methods. They basically concern the structure of molecules and related properties. Both approaches can predict energies, geometries and frequencies of the molecular or ionic clusters. Molecular mechanics uses classical mechanics to model molecular systems whereas the electrons are not explicitly treated in calculations. The energy of a system is calculated as a function of the position only. While electronic structure methods use laws of quantum mechanics in their computations and are of

two major classes: semiempirical methods which use parameters derived from experimental data to simplify computations and *ab initio* based only on the laws of quantum mechanics and fundamental physical constants (Jensen, 2007).

In quantum computation the central idea is to solve the Schrödinger equation to get the information about the energy and their related properties of the molecule. The time-independent, non-relativistic Schrödinger equation is given by:

$$H\Psi = E\Psi \tag{1.1}$$

where $\boldsymbol{H}$ is the Hamiltonian operator which include the kinetic and potential energies of the nuclei and electrons, Ψ is the total wavefunction and E is the total energy. The Hamiltonian operator comprises five energies contributions: kinetic energies of the electrons and nuclei ($\boldsymbol{T}_{\mathbf{e}}$ and $\boldsymbol{T}_{\mathbf{n}}$), the attraction of electrons to the nuclei ($\boldsymbol{V}_{\mathbf{en}}$), and the interelectronic and internuclear repulsion ($\boldsymbol{V}_{\mathbf{ee}}$ and $\boldsymbol{V}_{\mathbf{nn}}$), which can be symbolically represented as:

$$\boldsymbol{H} = \boldsymbol{T}_e + \boldsymbol{T}_n + \boldsymbol{V}_{en} + \boldsymbol{V}_{ee} + \boldsymbol{V}_{nn} \tag{1.2}$$

For a system with N_{nuclei} nuclei and N_{elec} electrons, the electronic Hamiltonian operator after application of Born-Oppenheimer approximation is written as:

$$\boldsymbol{H}_e = -\sum_{i=1}^{N_{elec}} \frac{1}{2}\nabla_i^2 - \sum_{i=1}^{N_{elec}} \sum_{A=1}^{N_{nuclei}} \frac{Z_A}{|R_A - r_i|} + \sum_{i=1}^{N_{elec}} \sum_{j>1}^{N_{elec}} \frac{1}{|r_i - r_j|} + \sum_{A=1}^{N_{nuclei}} \sum_{B=1}^{N_{nuclei}} \frac{Z_A Z_B}{|R_A - R_B|} \tag{1.3}$$

where the first term on the right hand is the electronic kinetic energy and other terms stand for the nuclear-electron attraction, electron-electron repulsion and the nuclei-nuclei repulsion potential energies; R and r represent the nuclear positions (A, B) and (i, j) are electronic coordinates corresponding to different centres; Z is the atomic number and ∇ is the gradient operator.

Within the Born-Oppenheimer approximation the last term is a constant as the nuclei are fixed and the Hamiltonian operator is determined by the number of electrons and the potential created

by the nuclei in terms of charges and positions. The changes in electronic energies as a function of nuclear positions give the potential energy surface (PES) of a molecule. The global minimum of energy on the PES gives the most stable structure of the molecule. The second derivatives of the energy with respect to the nuclear positions provide the Hessian which can be transformed into the harmonic vibrational modes of the molecule. Our aim is to solve the Schrödinger equation to obtain information about the structure and properties of the molecules and ions.

The Schrödinger equation can be solved exactly for one-electron atoms like hydrogen atom. For multy-electron systems approximation methods are required. Currently, there are two distinct approaches for solving the Schrödinger equation: molecular orbital theory (MO) which include Hartree-Fock (HF) or post Hartree-Fock methods and density function theory (DFT) (Trapp *et al.*, 2006).

1.2.1. *Ab initio* Molecular Orbital Theory

This is one of the earliest approaches used to solve Schrödinger equation for the electronic structure of the molecules in molecular orbital theory (Grant *et al.*, 1995; Hehre, 1986). The simplest approach used in solving Schrödinger equation is the Hartree-Fock (HF) theory, whereas each electron in an *n*-electrons system move in an average field created by the *n*-1 other electrons and the nuclei. The *n*-electrons repulsion is considered as the average of all electrons, thus the electron correlation is neglected. Each MO is constructed as a linear combination of atomic orbitals, expressed as a set of one electron atomic functions known as a basis functions (χ_μ) usually centred on a nuclei. An individual molecular orbital may then be expressed as:

$$\phi_i = \sum_{\mu=i}^{N} C_{\mu\, i}\, \chi_\mu \qquad (1.4)$$

where $C_{\mu\, i}$ are the molecular orbital coefficients. Using HF approach, the Schrödinger equation is reduced to a set of Fock equations by variational principle (Cramer, 2004; Dorsett *et al.*, 2000), the solution of which gives the above MO coefficients. Iteratively, the HF equations is solved to optimize the coefficients and minimize the electronic energy, this procedure is called the self consistent field (SCF) method.

For a sufficient large basis set, the total energy which can be computed using HF wavefunction can account up to 99%, however the remaining energy is very important in explaining chemical phenomena. The difference between the HF and the exact energy is a result of electron correlation, and is simply explained by the motion of electron as they interact with each other. In HF theory the motion of electrons with the opposite spin is uncorrelated. Thus, according to HF theory for double occupied orbital, the electron of opposite spin does not feel the repulsion of the other rather the average of *n*-1 electrons. In reality both electrons in the orbital must feel the influence of each other, so their motion is correlated. The methods which include explicitly the electron correlation energies are known as post-HF methods. They are usually begin with HF wave function and include electron correlation, thus much better energies are obtained.

The three main methods incorporate the electron correlation energy are configuration interaction (CI), many body perturbation theory (MBPT) and coupled cluster (CC) method. Configuration interaction methods (Pople *et al.*, 1977) are based on constructing a linear combination of determinants by replacing one or more occupied orbitals within the HF determinant with virtual orbital and their coefficients are solved by minimizing the energy of the total wave function. Full CI method corresponds to all allowed possible excitations, however, it scales as $N!$, where N is the number of bases functions, and usually CI method is restricted to single, double and triple excitations, abbreviated as CIS, CISD and CISDT methods respectively. Full CI is both variational and size-consistent, but it is extremely expensive computationally. Truncated CI methods are variational, but they are neither size consistent nor size extensive (Szalay, 2005) thus, the other two methods are preferable as they are size consistent and size extensive.

Many body perturbation theories (MBPT) include the electron correlation by treating it as a perturbation to the HF wavefunction. The MBPT also account for corrections to the energy obtained by adding higher excitation to the HF determinant non-iteratively. In perturbation theory, the Hamiltonian is divided into two parts:

$$H = H_0 + \lambda H' \tag{1.5}$$

where H_0 is unperturbed Hamiltonian operator and H' is a perturbation. The coefficient λ is used to generate power series expansion of energy and molecular wavefunction, which determines the

strength of perturbation. Second order Møller-Plesset perturbation theory (Møller *et al.*, 1934) is the simplest treatment of electron correlation. The methods of Møller-Plesset are indexed as MP_n whereby n represent the order of perturbation. MP_2 scales as N^5 (Cramer, 2004) due to the integral transformation step, and this recovers around 90% of the correlation energy (Jensen, 2007), whereas this is the most cheap correlated *ab initio* method. MP_3 does not improve significantly compare with the result of MP_2. The higher perturbation based method usually used is MP_4 and recovers about 98% of the correlation energy, but is computationally very expensive as it scales up to N^6. In this work, MP_4 method was used in the energy calculations whereby is not much time consuming.

Coupled-cluster (CC) theory (Bartlett, 1989; Purvis III *et al.*, 1982; Watts *et al.*, 1993) is based on the assumption that the wavefunction can be approximated as:

$$\Psi_{CC} = e^{T}\Phi_{HF} \tag{1.6}$$

$$e^{\boldsymbol{T}} = 1 + T + \frac{1}{2}\ T^2 + \frac{1}{6}\ T^3 + \cdots = \sum_{k=0}^{\infty} \frac{1}{k!} T^k \tag{1.7}$$

where we have expanded the exponential in a Taylor series form. T is the cluster operator and Φ_{HF} is the HF reference configuration, and T is defined as:

$$T = T + \ T^2 + \ T^3 + \cdots + T_n \tag{1.8}$$

and n describes a specific degree of excitation: $n = 1$ are singles, $n = 2$ are doubles, $n = 3$ are triple excitation and so on. The CC equations are solved iteratively. In practice, the cluster operator must be truncated at some level of excitation; otherwise it scales as in the full CI method.

Unlike CI, the CC methods and *MP* theory are size-consistent. The fraction of correlation energy recovered and the accuracy of the results obtained by CC method is significantly higher than for MP_n methods for the same order. However, coupled-cluster calculations are computationally expensive and extremely time consuming with N^7 scaling. Thus, our studied are limited to MP_2 and MP_4. On the other hand DFT methods are cheap but still provide a good solution with scaling around N^3.

1.2.2. Density Function Theory

The basis for DFT which is pioneered by Hohenberg and Kohn (1964) is that the ground state electronic energy is determined completely by the electron density. The DFT methods incorporate the effects of electron correlation without dramatically increasing the computational cost and provides a good description of the geometries and frequencies of a wide range of molecules. The main task of DFT is to design the functionals that connect the electron density with the energy (Holthausen *et al.*, 2000; Parr *et al.*, 1989). Kohn and Sham (1965) suggested the method for calculating electron kinetic energy from an auxilary set of orbitals that uses electron density. This approach simplified the approximation and made it possible. The DFT method has computational cost similar to HF but rather provide much more accurate results. The electronic energy of the DFT comprising several terms:

$$E[\rho(r)] = E^T + E^V + E^J + E^{XC} \tag{1.9}$$

where E^T is the kinetic energy, E^V is the electronic-nuclear potential energy, E^J is the coulombic interaction of electrons and E^{XC} is the exchange correlation energy including the remaining part of the electron-electron interactions. All terms except nuclear-nuclear repulsions are functions of the electron density. The terms $E^T + E^V + E^J$ represent the classical energy of the electrons distributions, while E^{XC} represents both the quantum mechanical exchange energy, which accounted for electron spin (Bergman *et al.*, 1993), and the dynamic correlation energy due to the concerted motion of individual electrons. If the exact form of E^{XC} is known, the DFT can give the exact energy in contrast to the HF theory. However, this is not possible because E^{XC} is not explicitly defined. So, a major task of using DFT is choosing the proper form of the exchange-correlation functional. Several exchange correlation functionals are available, thus making DFT calculations fall under three general categories: local density approximations (LDA) which depend only on the electron density, generalized gradient approximations (GGA) also depend on the gradient of the electron density and the last one is 'hybrid' which is formed by combining DFT and HF terms. In this study, B3LYP5 and often B3P86 methods are used to calculate the geometries and frequencies of the molecules and cluster ions.

1.3. Energy Calculations

Accurate prediction of energy is very important for thermodynamic properties. In actual calculations of energy in quantum mechanics, as the inter-molecules distance is reduced from infinity to the equilibrium distance, R_e whereby the energy reaches minimum, the relative energy is lowered. This is because as R decreases the interactions between the molecules is switched on. On the other hand as two interacting molecules approaches each other, they also borrow the basis function from each other to compensate for the incompleteness of their own basis set (Frank, 1999). As a result errors occurs due to these interactions between the molecules which is known as basis set superposition error $BSSE$ (Liu *et al.*, 1973). The $BSSE$ in the solution of Schrödinger equation was first addressed by Jansen (Jansen *et al.*, 1969) in the calculation of accurate intermolecular potential. Counterpoise (CP) method by Boys and Bernardi (Boys *et al.*, 1970) was introduced to overcome such problem. The interaction energy between two molecules A and B calculated using CP method is given as the differences:

$$\Delta E^{CP}(R) = E^{AB}(R) - E^{A\{AB\}}(R) - E^{B\{AB\}}(R) \qquad (1.10)$$

where R is the *A*–*B* distance, and $E^{A\{AB\}}$ and $E^{B\{AB\}}$ are fragments energies obtained using the full molecule basis $\{AB\}$ at a particular *AB* geometry of interest, the above formulae are described in detail by van Duijneveldt *et al*., (1994). Although, there has been some arguments questioning about the validity of *CP* method in calculating the interaction energies of the complex compound (Frisch *et al.*, 1986; Mayer *et al.*, 1991; Yang *et al.*, 1991), it has been generally considered that counterpoise correction *CPC* is fundamental and necessary for the accurate determination of interaction energies. It has been proved that interaction energies calculated by *CP* method are closer to experimental data compared to uncorrected values (Peterson *et al.*, 1995; Tao *et al.*, 1991; Woon *et al.*, 1996).

1.4. Research Problem and Justificaction of Study

Stability of molecular and ionic clusters is but one of the factors that are paramount for these species to be considered as a fundamental building block, it must meet additional requirement that observed property persists after the species is assembled into a bulk material. Very limited

studies on molecular and ionic clusters of cesium halides exist. It is of best interest to every scientist to have knowledge on thermodynamic properties such as enthalpies of molecular reaction and enthalpies of formation of these species before embarking on the designing and synthesizing novel materials. But due to lack of accurate information on geometrical parameters and vibrations frequencies, the knowledge of their thermodynamic properties is unavailable. Therefore, this research studied the geometrical structure, vibrations spectra and their related thermodynamic functions of cluster molecules and ions of cesium halides using quantum chemistry computational methods.

The research findings will contribute to a pool of knowledge on geometrical structure, vibrations frequencies and thermodynamic properties of molecular and ionic clusters over cesium halides. Also, the research may lead to identification of possible candidates that may be considered as fundamental building blocks of new materials based on the stability of the ionic clusters. These results will be used for further research particularly in designing and synthesizing new material such as super and hyper salts (Bartlett, 1962; Knight *et al.*, 2013), fabrication of modern electronic devices (Lee *et al.*, 2010; Liu *et al.*, 2013a; Zhang *et al.*, 2014; Zhang *et al.*, 2012). Also another fields of interest where the cluster ions can be used is on the designing of the materials for environmentally friendly like lithium-ion batteries Li^+ (Giri *et al.*, 2014; Unemoto *et al.*, 2014). The electrolytes currently used in these batteries composed of Li^+ cation and halogen-containing complex anions. Thus this research is important since is in line with the development of advanced industries.

1.5. Objectives

1.5.1. General Objective

To investigate the geometrical structure, vibrational spectra, and thermodynamic properties of molecular Cs_2X_2, Cs_3X_3 and Cs_4X_4 and ionic clusters Cs_2X^+, CsX_2^-, $Cs_3X_2^+$, $Cs_2X_3^-$ (where X is a halogen) and more complex species $Cs_4F_3^+$, $Cs_5F_4^+$, $Cs_4Cl_3^+$ and $Cs_5Cl_4^+$ of cesium halides.

1.5.2. Specific Objectives

Specific Objectives are:

i. To choose appropriate computational methods through comparison of theoretical results and the experimental data available in the literature
ii. To determine the geometrical structure and vibration frequencies of molecular and ionic clusters using appropriate quantum computational methods
iii. To identify the possible isomers among the alternative structures for complex molecules and ions
iv. To determine thermodynamic properties: enthalpies of dissociation reactions and enthalpies of formation of the species
v. To examine the general conception about the structure and properties of the molecular ionic clusters of cesium halides

1.6. Research Questions

The following were the questions that guided this research:

i. What are the appropriate computational methods to obtain the reliable information on the structure and properties of the gaseous cesium halides species?
ii. What are the geometrical structure and vibration frequencies of the cluster ions and molecules considered?
iii. Which isomers if any are the most stable and abundant?
iv. What are the enthalpies of dissociation and enthalpies of formation of each cluster ions over cesium halides?
v. What is the trend of structure and properties for the ions of similar composition but different halides?

CHAPTER TWO

Structure and Properties of Molecular and Ionic Clusters in Vapor over Cesium Fluoride[1]

Abstract: The properties of neutral molecules Cs_2F_2, Cs_3F_3, Cs_4F_4 and positive and negative cluster ions Cs_2F^+, CsF_2^-, $Cs_3F_2^+$, $Cs_2F_3^-$, $Cs_4F_3^+$, and $Cs_5F_4^+$ were studied by several of quantum chemical methods implementing density function theory and Møller–Plesset perturbation theory of the 2nd and 4th order. For all species, the equilibrium geometrical structure and vibrational spectra were determined. Different isomers have been revealed for the trimer neutral molecule Cs_3F_3, pentaatomic both positive and negative, $Cs_3F_2^+$, $Cs_2F_3^-$, and heptaatomic $Cs_4F_3^+$ ions. The most abundant isomers in the saturated vapor were determined. Enthalpies of dissociation reactions and enthalpies of formation of the species were obtained.

2.1. Introduction

The properties of alkali halides clusters ions have been extensively studied during past decades (Aguado, 2001; Alexandrova *et al.*, 2004; Castleman *et al.*, 1996; Castleman Jr *et al.*, 2009; Fernandez-Lima *et al.*, 2012; Huh *et al.*, 2001; Sarkas *et al.*, 1995). The electronic, optical, magnetic, and structural properties of clusters strongly depend on their size and composition (Khanna *et al.*, 1993, 1995) thus, the possibility that materials with desired properties can be made is accustomed by changing the magnitude and structure of the cluster aggregates. The ability to use clusters for making new materials rely on very stable clusters that can maintain their form when assembled (Rao *et al.*, 1999).

The combination of positive and negative clusters, $M^+(MX)_n$ and $X^-(MX)_n$, where M is an alkali metal, X is a halogen, n is a number of MX molecules, results in formation of neutral particles, called supersalts (Srivastava *et al.*, 2014a, b). In the simplest case M_2X^+ and MX_2^- can be

[1]Stanley F. Mwanga, Tatiana P. Pogrebnaya and Alexander M. Pogrebnoi, Structure and Properties of Molecular and Ionic Clusters in Vapor over Cesium Fluoride, *Molecular Physics*, **2015**, *113*(12): 1485−1500, DOI: 10.1080/00268976.2015.1007104

combined to form M_3X_3 (Srivastava *et al.*, 2014b). Supersalts may be considered as fundamental building blocks of new collection of nanostructural materials with tailored properties.

Moreover, similar charged particles were proved to be of significant importance in various applications such as ions implantation (Michael *et al.*, 1994), ions thrusters (Benson *et al.*, 2009), magnetohydrodynamic (MHD) generators (Kay, 2011), etc. For example, in ion implantation, energetic ion beam is injected into the surface of solid material as a result the composition and structure of the near-surface region of targeted material is changed. The advent of this technique enables the fabrication of different electronic devices.

Mass spectrometry is a prominent suitable experimental technique used for investigation of ions in gaseous phase. Different cluster molecules like $(MX)_n$ and positive and negative ions $M^+(MX)_n$ and $X^-(MX)_n$ had been detected in vapors over alkali halides experimentally by high temperature mass spectrometry (Chupka, 1959; Dunaev *et al.*, 2013; Gusarov, 1986; Kudin *et al.*, 1990; Motalov *et al.*, 2001; Pogrebnoi *et al.*, 2000; Sidorova *et al.*, 1979). For treatment of experimental mass spectrometric data, the thermodynamic functions of ions and molecules are necessary. The experimental data about geometric structure and vibrational spectra of the alkali halide cluster ions are unavailable. However, the development of theoretical methods aided by powerful computers codes and high-performance computers have made possible to analyze complex structure and vibrational spectra and also can predict properties that can be verified experimentally. The geometric structure, vibrational frequencies and thermodynamic properties of cluster ions existing in saturated vapors over NaX (X = F, Cl, Br, I), KCl, RbCl and CsCl had been studied using quantum chemical methods previously (Pogrebnaya *et al.*, 2007, 2008, 2010; Pogrebnaya *et al.*, 2012).

The positively charged ions Cs_2F^+, $Cs_3F_2^+$, $Cs_4F_3^+$, and $Cs_5F_4^+$ had been registered in the saturated vapor over cesium fluoride using high temperature mass spectrometric technique as reported in (Dunaev *et al.*, 2013). The present study was aimed to determine the characteristics of these ions as well as negatively charged CsF_2^-, $Cs_2F_3^-$ and neutral molecules Cs_2F_2, Cs_3F_3, Cs_4F_4 related to this system by using quantum chemical methods, to calculate thermodynamic

properties of the species and find out the possible isomers amongst the pentaatomic and more complex compounds.

2.2 Computational Details

The calculations were executed using the GAMESS program (Schmidt *et al.*, 1993), Firefly version 8.0.0 (Granovsky, 2012b) implementing the following methods: electron density functional theory (DFT) with the Becke–Lee–Yang–Parr functional (B3LYP5), second order and fourth order Møller–Plesset perturbation theory (MP2 and MP4). Two basis sets have been utilised. The first basis set denoted as B1 was midsized: the TZV+spd 5s3p1d+sp for F implemented in (Schmidt *et al.*, 1993) and the relativistic effective core potential (ECP) with valence correlation consistent cc-pVTZ basis set (5s4p1d) for Cs (Feller, 1996; Leininger *et al.*, 1996; Schuchardt *et al.*, 2007). The second basis set denoted as B2 was extended and taken from EMSL (The Environmental Molecular Sciences Laboratory, U.S.): the full-electron basis set aug cc-pVTZ (4s3p2d1f) for F (Feller, 1996; Schuchardt *et al.*, 2007) and ECP with valence cc-pVTZ (6s5p4d1f) for Cs (Feller, 1996; Leininger *et al.*, 1996; Schuchardt *et al.*, 2007). No core electrons were frozen in MP2 and MP4 methods. The combination of the two methods (B3LYP5 and MP2) and two basis sets (B1 and B2) provided us with four theoretical approximations: B3LYP5 B1, MP2 B1, B3LYP5 B2, and MP2 B2 to optimize geometric parameters of the species and calculate vibrational frequencies. The vibrational analyses were performed, and all converged structures were confirmed as true energy minima by the absence of any imaginary frequencies. All four theoretical approximations were applied to calculate the characteristics of CsF, Cs_2F_2, Cs_2F^+, CsF_2^-, $Cs_3F_2^+$, $Cs_2F_3^-$. For the heaver particles, Cs_3F_3, Cs_4F_4, $Cs_4F_3^+$, and $Cs_5F_4^+$, B3LYP B1 and MP2 B1 methods were used. The geometrical parameters and vibrational frequencies obtained by MP2 method were used for the calculations of the thermodynamic functions of the molecular and ionic clusters considered using the rigid rotator-harmonic oscillator approximation.

To obtain more accurate values of dissociation energy of the molecules and ions, further computation was performed with higher theoretical levels MP4 B1 and MP4 B2 and here the basis set superposition error (BSSE) (Boys *et al.*, 1970) was taken into account as well using the

procedure proposed by Solomonik and co-workers (Solomonik *et al.*, 2005). Enthalpies of molecular dissociation are calculated by combining the computed interaction energies (using *CPC* method) denoted as $\Delta_r E_C$ and zero point vibration energy ($ZPVE$) correction $\Delta\varepsilon$ given as:

$$\Delta_r H^{\circ}(0) = \Delta_r E_C + \Delta\varepsilon \tag{2.1}$$

and the $ZPVE$ are evaluated using the following formulae:

$$\Delta\varepsilon = \frac{1}{2} hc \left(\sum \omega_{i\,prod} - \sum \omega_{i\,react} \right) \tag{2.2}$$

where h is the Planck constant, c is the speed of light in the free space, $\sum \omega_{i\,prod}$ and $\sum \omega_{i\,react}$ are sums of the vibrational frequencies for products and reactants respectively. The calculations of $\Delta_r E_C$ followed the procedure proposed by Solomonik and co-worker (Solomonik *et al.*, 2005). This can be described simply by considering the dissociation reaction of triatomic positive ion:

$$M_2X^+ \rightarrow MX + M^+ \tag{2.3}$$

whereby the dissociation energies of triatomic ion and monomer molecule is computed by employing MP4 level as illustrated in the following reaction equations:

$$\Delta E = 2E\{M^+(M_2X^+)\} + E\{X^-(M_2X^+)\} - E(M_2X^+) \tag{2.3 a}$$

$$\Delta E = E\{M^+(MX)\} + E\{X^-(MX)\} - E(MX) \tag{2.3 b}$$

$$\Delta E_{MP4C} = E(2.3\,a) - E(2.3\,b) \tag{2.4}$$

ΔE_{MP4C} is the energy of dissociation reaction obtained using BSSE correction. The energies of cation M^+, $E\{M^+(M_2X^+)\}$, and anion X^-, $E\{X^-(M_2X^+)\}$, are obtained using the full basis set of triatomics as if those ions are within the M_2X^+ at the particular optimized geometry. Alike the energies of $E\{M^+(MX)\}$ and $E\{X^-(MX)\}$ are obtained using the full basis set of diatomic as if those ions are within the MX molecule at the particular optimized geometry. Through these calculations the only electrons of M^+ (or X^-) are considered as real ones while the rest atoms of M_2X^+/MX are called ghost atoms because no electrons but only the basis functions are included. The dissociation energies were calculated using MP4 (SDQ) with optimized coordinates determined by MP2 method as input parameters. Furthermore, the enthalpies of formation of

molecular and ionic clusters were evaluated using calculated enthalpies of molecular dissociation with the known enthalpies of formation of the diatomic molecules CsX accessed from IVTANTHERMO Database (Gurvich *et al.*, 2000).

2.3. Results and discussion

2.3.1. Geometrical structure and vibrational frequencies of the neutral molecules, Cs_nF_n, n = 1–4

It is known that the evaporation of an alkali metal halides MX yields a mixture of monomers and smaller amounts of dimers, trimers, and tetramers (Haaland, 2008; Hargittai, 2000). In this section, the calculated properties of the neutral molecules Cs_nF_n, n = 1–4 are considered.

2.3.1.1. Monomer and dimer molecules, CsF and Cs_2F_2

The molecular properties of CsF and Cs_2F_2 molecules such as equilibrium geometric parameters, normal vibrational frequencies, dipole moments and ionization energies were computed through different approaches as shown in Tables 1 and 2. To examine the reliability of the calculated results found by B3LYP5 B1, MP2 B1, B3LYP5 B2 and MP2 B2 levels, a comparison with the available experimental data has been made.

As it is indicated in Table 1 the internuclear distance of diatomic CsF molecule found by the four computational levels were longer than the reference data. The MP2 B2 method fairs better, but still overrates the experimental values of R_e(Cs−F) by ∼0.03Å. The theoretical values of the vibrational frequency ω_e correlate with the internuclear separation, and again the MP2 B2 method gives the best agreement with the reference value. This result is analogous to the results obtained previously for MCl (M = K, Rb, Cs), (Pogrebnaya *et al.*, 2012). The ionization energies were calculated as energy differences between the parent and ionized species. The results obtained agree well with each other and do not contradict to the experimental value (Huber *et al.*, 1976). As for the dipole moment, calculations using the basis set two give the better agreement with the experimental value.

Several structures of dimeric Cs_2F_2 molecule were considered (Fig. 1): linear ($C_{\infty v}$), planar cycle (rhomb) with symmetry D_{2h}, and non-planar cycle (C_{2v}). The only stable structure confirmed was rhomb (D_{2h}), no isomers were found. The calculated results of the dimeric Cs_2F_2 molecule are listed in Table 2. The results computed by four methods do not contradict to each other. As is seen the calculated internuclear distance is longer than the experimental one. The difference between the theoretical and experimental values of the internuclear distances is about 0.09 Å for the basis set B1 (both B3LYP5 and MP2), about 0.05 Å (B3LYP5 B2) and 0.02 Å (MP2 B2). Thus the values obtained by MP2 B2 fits better the experimental data. The calculated values of the valence angle α_e(F–Cs–F) agree well with the experimental one (Krasnov *et al.*, 1979). The experimental data on the vibrational frequencies are restricted by two values of ω_5 (B_{2u}) and ω_6 (B_{3u}) obtained in IR spectra by the matrix isolation technique (Bruce *et al.*, 1976); the theoretical values of these frequencies agree with them within 10% uncertainty.

Table 1: Properties of the monomer molecule CsF.

Property	B3LYP5 B1	MP2 B1	B3LYP5 B2	MP2 B2	Experimental
R_e(Cs–F), Å	2.452	2.465	2.384	2.374	2.345[a,b,c,d]
E, au	–120.03821	–119.66558	–120.04256	–119.85638	
ω_e, cm^{-1}	335	330	342	348	353[a,b]
μ_e, D	8.7	9.1	7.94	8.17	7.61[a]
IP, eV	5.9	10.9	6.3	11.1	9.0 ± 0.2[a]

Notes: R_e(Cs–F) is the equilibrium internuclear distance, E is the total electron energy; ω_e is the frequency of normal vibration, μ_e is the dipole moment, IP is the ionization potential. Reference values: [a]Huber *et. al.*, 1976; [b]Törring *et. al.*, 1996; [c]Krasnov *et. al.*, 1979; [d]Gowda *et. al.*, 1983.

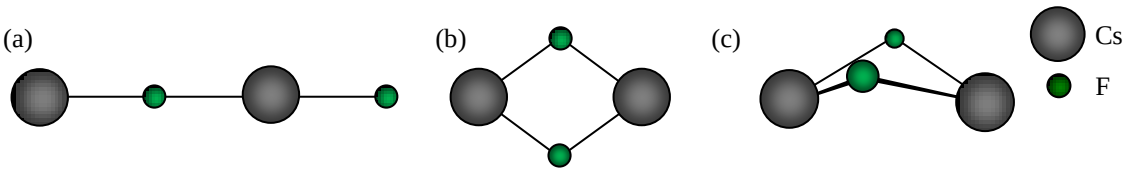

Figure 1: Alternative structures of the dimer Cs_2F_2 molecules: (a) linear, $C_{\infty v}$ symmetry; (b) rhomb, D_{2h}; (c) nonplanar cycle, C_{2v}.

Table 2: Properties of the dimer molecule Cs_2F_2 (D_{2h}).

Property	B3LYP5 B1	MP2 B1	B3LYP5 B2	MP2 B2	Experimental
R_e(Cs−F)	2.674	2.673	2.632	2.611	2.587[a]
α_e(F–Cs–F)	78.3	76.9	78.3	78.5	79.4[b]
E	–240.14022	–239.40156	–240.14338	–239.77839	
ω_1 (A_g)	229	227	231	234	
ω_2 (A_g)	84	82	85	82	
ω_3 (B_{1g})	206	217	195	207	
ω_4 (B_{1u})	80	80	78	77	
ω_5 (B_{2u})	209	207	212	219	207[b,c]
ω_6 (B_{3u})	262	270	263	272	248[b,c]
I_4	1.27	1.33	1.11	1.17	
I_5	2.81	2.85	2.80	2.91	
I_6	4.22	4.30	4.54	4.62	

Notes: 1) Here and hereafter R_e(Cs–F) is the equilibrium internuclear distance, Å; α_e is the valence angle, degrees; E is the total electron energy, au; ω_i are the frequencies of normal vibrations, cm^{-1}; I_i are the IR intensities, $D^2 \cdot amu^{-1} \cdot Å^{-2}$; 2) The reducible vibration representation breaks down into irreducible ones as follows: $\Gamma = 2A_g + B_{1g} + B_{1u} + B_{2u} + B_{3u}$. Reference values: [a]Gowda *et. al.*, 1983; [b]Krasnov *et. al.*, 1976; [c]Bruce *et. al.*, 1976.

Completing the comparison of the theoretical and experimental data, for CsF and Cs_2F_2, we can state the accuracy of the calculated properties of the species. The uncertainties in the internuclear separation are about 0.10 Å for basis B1 (B3LYP5 and MP2), ∼0.04 Å (B3LYP5 B2), and for MP2 B2 ∼0.03 Å. The inaccuracy in the calculated vibrational frequencies does exceed 10% regarding all the methods applied. We expect the similar uncertainties in the properties of the heavier molecules and ions under consideration if the same computational methods are applied. Based on our previous experience (Pogrebnoi *et al.*, 2013), we also suppose that in the case of species with a rigid compact structure, the computed geometric parameters and vibrational frequencies are not so sensitive to the theoretical approaches considered here. This allows us to apply the B3LYP5 B1 and MP2 B1 method to the heavier clusters when the usage of higher levels is difficult.

2.3.1.2 Trimer Cs_3F_3 and tetramer Cs_4F_4 molecules

Different possible shapes of the trimer and tetramer molecules were investigated. For the Cs_3F_3 molecule, the configurations considered were hexagonal planar (D_{3h}), hexagonal non-planar

(C_{3v}), and prismatic (C_s). During optimization the hexagonal non-planar structure converged into the planar one and the prismatic converged into a 'butterfly-shaped' structure (C_s). Thus, two isomeric configurations were confirmed to exist: the hexagonal planar and butterfly-shaped (Figs. 2 a, b). The geometrical parameters and vibrational frequencies are shown in Table 3. The first shape is of high symmetry and only two parameters, R_e(Cs−F) and α_e(F−Cs−F), are needed to describe it. The second one has only one symmetry element, the mirror plane, and is described by four non-equivalent distances Cs−F, two valence angles F−Cs−F and Cs−F−Cs and a dihedral angle Cs_1−F_2−Cs_2−F_1. The butterfly-shaped structure possesses a bit higher energy by 5.7 kJ·mol^{-1} (B3LYP B1) and of 1.3 kJ·mol^{-1} (MP2 B1) compared to hexagonal one. It appeared that the C_s isomer was not planar with the dihedral angle 159°. It was interesting to determine the inversion barrier as energy difference between the planar and equilibrium non-planar butterfly-shaped structures. The planar C_{2v} configuration of Cs_3F_3 was optimised, and the inversion barrier was found to be very small and equal to ~0.06 kJ·mol^{-1} (B3LYP5 B1). Hence the butterfly configuration is non-rigid with rather floppy potential regarding bending

For the Cs_4F_4 the configurations considered were slightly distorted cubical (T_d), pyramidal (C_{3v}), octagonal structure (D_{4h}), planar ladder-shaped (C_{2h}). The pyramidal structure converged, in the optimization procedure, into the tetrahedral (Fig. 2 c), which was confirmed as having minimum at the potential energy surface (PES). For the octagonal structure and planar ladder-shaped, imaginary frequencies were found. Therefore only one structure was proved as equilibrium, of T_d symmetry; the geometrical parameters and vibrational frequencies of the tetramer molecule are shown in Table 4.

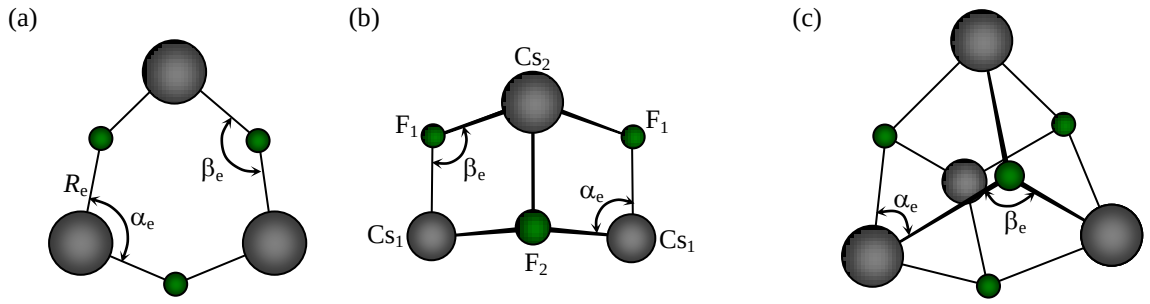

Figure 2: Geometrical structures of the trimer Cs_3F_3 and tetramer Cs_4F_4 molecules: (a) planar hexagonal Cs_3F_3 of D_{3h} symmetry; (b) 'butterfly-shaped' Cs_3F_3, C_s; (c) distorted cubic Cs_4F_4, (T_d).

Table 3: Properties of the trimer molecule Cs_3F_3.

	Cs_3F_3 (planar hexagon, D_{3h})			Cs_3F_3 ("butterfly-shaped", C_s)	
Property	**B3LYP5**	**MP2**	**Property**	**B3LYP5**	**MP2**
R_e(Cs−F)	2.676	2.674	$R_{e1}(Cs_1–F_1)$	2.611	2.612
			$R_{e2}(Cs_1–F_2)$	2.726	2.719
			$R_{e3}(Cs_2–F_1)$	2.774	2.774
			$R_{e4}(Cs_2–F_2)$	3.098	3.030
			$\alpha_e(F_1–Cs_1–F_2)$	84.7	82.8
α_e(F−Cs−F)	104.3	103.3	$\beta_e(Cs_1–F_1–Cs_2)$	105.3	105.8
β_e(Cs−F−Cs)	135.7	136.7	$\chi_e(Cs_1–F_2–Cs_2–F_1)$	158.4	159.1
E	−360.22761	−359.16974	E	−360.22543	−359.16924
ω_1 (A_1')	257	269	ω_1 (A')	266	273
ω_2 (A_1')	152	151	ω_2 (A')	194	196
ω_3 (A_1')	79	81	ω_3 (A')	106	121
ω_4 (A_2'')	74	73	ω_4 (A')	102	102
ω_5 (E')	297	306	ω_5 (A')	74	80
ω_6 (E')	149	149	ω_6 (A')	47	50
ω_7 (E')	36	36	ω_7 (A')	18	15
ω_8 (E')	40	38	ω_8 (A'')	285	295
			ω_9 (A'')	238	247
			ω_{10} (A'')	185	189
			ω_{11} (A'')	64	64
			ω_{12} (A'')	42	42
			μ_e	7.3	7.8

Notes: The data were obtained with the basis set B1. The vibrational representations are as follows: $\Gamma = 3A_1' + A_2'' + 3E' + E''$ for Cs_3F_3 (D_{3h}) and $\Gamma = 7A' + 5\,A_2''$ for Cs_3F_3 (C_s).

Table 4: Properties of the tetramer molecule Cs_4F_4 (T_d).

Property	B3LYP5	MP2	Property	B3LYP5	MP2
R_e(Cs−F)	2.809	2.792	ω_5 (T_1)	154	170
α_e(F−Cs−F)	81.3	79.8	ω_6 (T_2)	217	229
β_e(Cs−F−Cs)	98.1	99.3	ω_7 (T_2)	169	169
E	−480.3406875	−478.875925	ω_8 (T_2)	60	58
ω_1 (A_1)	191	189	I_6	3.36	3.60
ω_2 (A_1)	99	103	I_7	1.65	1.57
ω_3 (E)	162	177	I_8	0.01	0.01
ω_4 (E)	53	50			

Notes: The data were obtained with the basis set B1. The vibrational representation is $\Gamma = 2A_1 + 2E + T_1 + 3T_2$.

2.3.2. Geometrical structure and vibrational frequencies of the ionic clusters

2.3.2.1. Triatomic ions, Cs_2F^+ and CsF_2^-

According to the calculations done using the basis sets B1 and B2 and both methods, B3LYP5 and MP2, the structure of the positive triatomic ion is linear of $D_{\infty h}$ symmetry and that of the negative one is bent of C_{2v} symmetry (Figs. 3 a, b) with the angle α_e(F−Cs−F) = 150° (MP2 B2). The linear structure for the negative triatomic ion CsF_2^- appeared to be not stable due to the presence of imaginary frequencies; the decrease in energy of the bent configuration was about 1 kJ·mol^{-1} compared with the linear structure. The properties of the triatomic ions, the equilibrium internuclear distances R_e(Cs−F), the total electron energies E, the frequencies of normal vibrations ω_i, and the intensities of vibrations in IR spectra I_i were determined. In Table 2.5, the results obtained with the basis set B2 are represented.

For both positive and negative ions, the values of equilibrium internuclear distance by B3LYP5 B2 method are slightly longer than by MP2 B2 method, this result is similar to that obtained for the neutral molecules considered above. There is an increase in R_e(Cs−F) by ~0.05 Å from positive to negative ions, that is due to an extra negative charge in the CsF_2^- ion. This increase in the distance correlates with the decrease in the antisymmetric valence vibration frequency: ω_2 = 333 cm^{-1} in Cs_2F^+ and ω_3 = 227 cm^{-1} in CsF_2^- (MP2 B2).

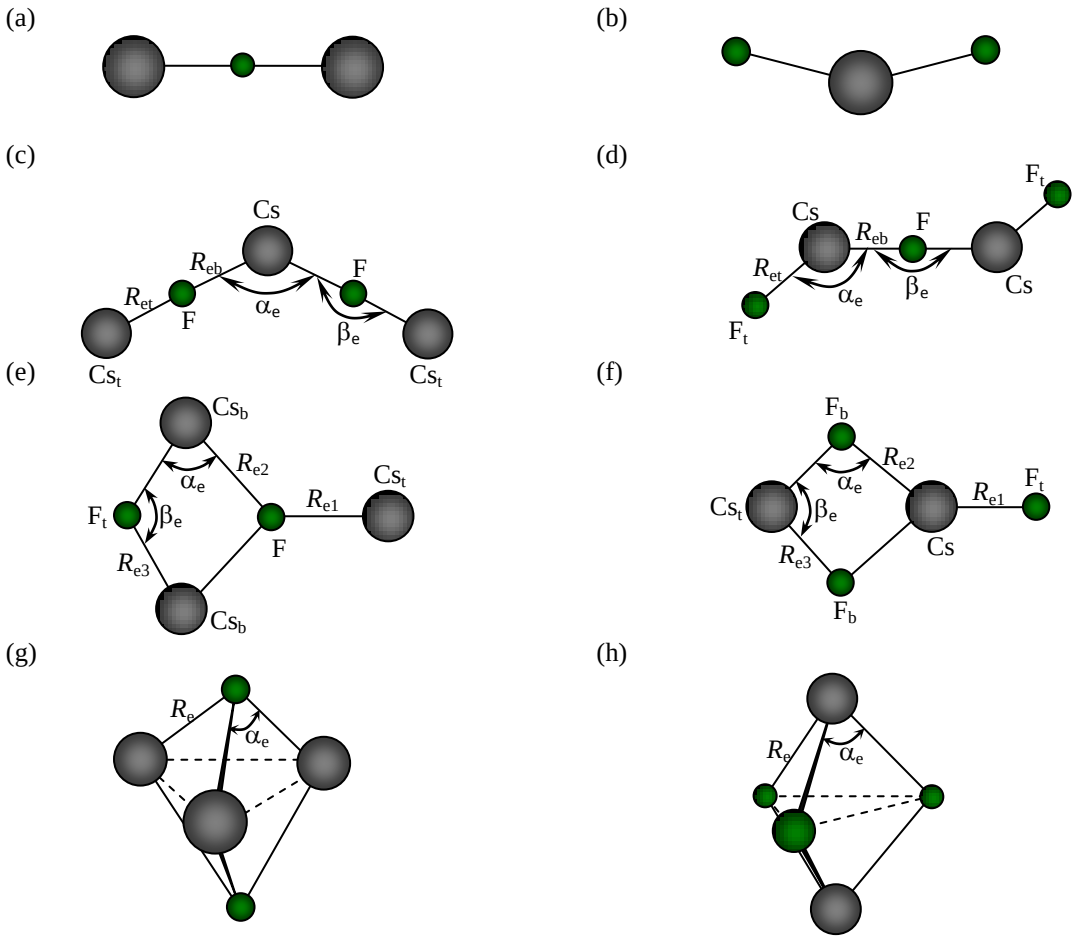

Figure 3: Geometrical configurations of the triatomic and pentaatomic ions: (a) Cs_2F^+, $D_{\infty h}$; (b) CsF_2^-, C_{2v}; (c) $Cs_3F_2^+$ V-shaped, C_{2v}; (d) $Cs_2F_3^-$ Z-shaped, C_{2h}; (e) $Cs_3F_2^+$, planar cyclic, C_{2v}; (f) $Cs_2F_3^-$, planar cyclic, C_{2v}; (g) $Cs_3F_2^+$, bipyramidal, D_{3h}; (h) $Cs_2F_3^-$, bipyramidal of D_{3h}, symmetry.

Table 5: Properties of the triatomic ions Cs_2F^+ ($D_{\infty h}$) linear and CsF_2^- (C_{2v}) V-shaped configurations.

	Cs_2F^+ ($D_{\infty h}$)			CsF_2^- (C_{2v})	
Property	**B3LYP5**	**MP2**	**Property**	**B3LYP5**	**MP2**
R_e(Cs−F)	2.582	2.565	R_e(Cs−F)	2.627	2.618
			α_e(F−Cs−F)	146.5	150.3
E	−140.08798	−139.80881	E	−219.96234	−219.68935
ω_1 ($\sum_g^+$)	95	98	ω_1 (A_1)	243	246
ω_2 ($\sum_u^+$)	320	333	ω_2 (A_1)	39	32
ω_3 (Π_u)	69	87	ω_3 (B_2)	223	227
I_1	0	0	I_1	0.47	0.38
I_2	4.79	4.72	I_2	1.22	1.34
I_3	1.22	1.28	I_3	4.55	4.58
μ_e	0	0	μ_e	5.4	5.1

Notes: The data were obtained with the basis set B_2. The vibrational representations are as follows: $\Gamma = \Sigma_g^+ + \Sigma_u^+ + \Pi_u$ for Cs_2F^+ ($D_{\infty h}$) and $\Gamma = 2A_1 + B_2$ for CsF_2^- (C_{2v}).

2.3.2.2. Pentaatomic $Cs_3F_2^+$ and $Cs_2F_3^-$ ions

Three possible geometric configurations of these ions were considered: $D_{\infty h}$ linear symmetry, planar (kite-shaped or cyclic) with symmetry C_{2v} and bipyramidal symmetry D_{3h} (Figs. 3). For each configuration the geometrical parameters were optimized and the normal vibrations frequencies were calculated. As concerns the linear configuration ($D_{\infty h}$ symmetry) for the positive and negative ions, both B3LYP5 B2 and MP2 B2 methods yield some imaginary deformational frequencies. These observations provided us with a conclusion about the instability of the linear configuration of these ions. Hence, we proceeded with a further optimisation of bent geometrical structures.

The V-shaped for $Cs_3F_2^+$ and Z-shaped for $Cs_2F_3^-$ configurations were found to correspond to the minima on the PES (Fig. 3 c, d). As compared to the $D_{\infty h}$ linear structure, the decrease in energy of these bent configurations appeared to be the same and equal to 3.1 kJ·mol^{-1} (MP2 B2). The properties of the ions $Cs_3F_2^+$ (C_{2v}) and $Cs_2F_3^-$ (C_{2h}) are given in Table 6. There are two different internuclear separations: R_{et}(Cs−F) and R_{eb}(Cs−F), which are the terminal and bridged distances, respectively. For both ions, the terminal distance is shorter: by 0.17 Å in the positive ion and 0.14 Å in negative one (MP2 B2). The equilibrium internuclear distances for the negative ion are slightly greater than those for positive one. The valence angles α_e(F−Cs−F) are obtuse for both ions and more close to straight for the negative ion. The fragments Cs−F−Cs are almost linear

either in the positive and negative ions. Both structures of the ions may be considered as "non-rigid" because they possess the shallow character of PES and low deformational frequencies.

Table 6: Properties of the pentaatomic ions $Cs_3F_2^+$ (V-shaped, C_{2v}) and $Cs_2F_3^-$ (Z-shaped, C_{2h}).

	$Cs_3F_2^+$ (C_{2v})			$Cs_2F_3^-$ (C_{2h})	
Property	**B3LYP5 B2**	**MP2 B2**	**Property**	**B3LYP5 B2**	**MP2 B2**
$R_{et}(Cs_t-F)$	2.518	2.505	$R_{et}(Cs-F_t)$	2.557	2.547
$R_{eb}(Cs-F)$	2.705	2.680	$R_{eb}(Cs-F)$	2.716	2.690
$\alpha_e(F-Cs-F)$	124.6	125.2	$\alpha_e(F-Cs-F_t)$	137.4	138.6
$\beta_e(Cs_t-F-Cs)$	178.0	178.1	$\beta_e(Cs-F-Cs)$	180.0	180.0
E	−260.17749	−259.71637	E	−340.04915	−339.59413
ω_1 (A_1)	330	341	ω_1 (A_g)	260	267
ω_2 (A_1)	87	95	ω_2 (A_g)	77	80
ω_3 (A_1)	63	69	ω_3 (A_g)	29	29
ω_4 (A_1)	8	14	ω_4 (A_u)	34	56
ω_5 (A_2)	55	76	ω_5 (A_u)	5	15
ω_6 (B_1)	65	81	ω_6 (B_u)	280	291
ω_7 (B_2)	305	319	ω_7 (B_u)	242	252
ω_8 (B_2)	99	102	ω_8 (B_u)	58	68
ω_9 (B_2)	52	71	ω_9 (B_u)	9	20
μ_e, D	9.6	9.6	μ_e	0	0

Notes: The vibrational representation is $\Gamma = 4A_1 + A_2 + B_1 + 3B_2$ for $Cs_3F_2^+$ (C_{2v}) and $\Gamma = 3A_g + 2A_u + 4B_u$ for $Cs_2F_3^-$ (C_{2h}).

The other two structures, planar cyclic (C_{2v}) and bipyramidal (D_{3h}), also correspond to the minima on the PES. Table 7 presents the properties of the ions $Cs_3F_2^+$ and $Cs_2F_3^-$ with cyclic structure, the geometrical parameters are specified in Figs. 3 e, f. There are three different internuclear separations Cs−F, which are R_{e1}, R_{e2}, and R_{e3}, and two independent valence angles; α_e and β_e. As is seen the internuclear distances of the negative ion are slightly greater than the correspondent values of the positive one that results in slightly bigger dipole moment of $Cs_2F_3^-$. The vibrational spectra of the ions $Cs_3F_2^+$ and $Cs_2F_3^-$ are quite similar both in frequencies and in the distribution of them among the symmetry irreducible representations. As a whole, the correspondent properties of the cyclic isomers, $Cs_3F_2^+$ and $Cs_2F_3^-$, look alike, except the isomerization energy ΔE_{iso} that is $E(Cs_3F_2^+$, cyclic) – $E(Cs_3F_2^+$, V-shaped) for the positive ion

and $E(Cs_2F_3^-$, cyclic) – $E(Cs_2F_3^-$, Z-shaped) for the negative ion. The positive ion of kite-shaped possesses the higher energy than that of V-shaped (ΔE_{iso} = 4.1 kJ·mol^{-1}, MP2 B2), whereas for the negative ion the planar cyclic configuration appeared to be more stable energetically than the Z-shaped (ΔE_{iso} = −12.2 kJ·mol^{-1}, MP2 B2).

Table 7: Properties of pentaatomic ions with planar cyclic structure of C_{2v} symmetry.

Property	$Cs_3F_2^+$		Property	$Cs_2F_3^-$	
	B3LYP5 B2	**MP2 B2**		**B3LYP5 B2**	**MP2 B2**
$R_{e1}(Cs_t-F)$	2.582	2.570	$R_{e1}(Cs-F_t)$	2.621	2.609
$R_{e2}(Cs_b-F)$	2.962	2.907	$R_{e2}(Cs-F_b)$	2.984	2.938
$R_{e3}(Cs_b-F_t)$	2.559	2.542	$R_{e3}(Cs_t-F_b)$	2.569	2.554
$\alpha_e(F-Cs_b-F_t)$	77.5	77.4	$\alpha_e(Cs-F_b-Cs_t)$	94.3	93.2
$\beta_e(Cs_b-F_t-Cs_b)$	112.9	112.1	$\beta_e(F_b-Cs_t-F_b)$	93.5	94.3
$\gamma_e(Cs_b-F-Cs_t)$	134.0	133.5	$\gamma_e(F_b-Cs-F_t)$	141.1	140.3
E	−260.17393	−259.71482	E	−340.05174	−339.59876
ΔE_{iso}	9.4	4.1	ΔE_{iso}	−6.8	−12.2
ω_2 (A_1)	227	226	ω_2 (A_1)	208	204
ω_3 (A_1)	71	68	ω_3 (A_1)	137	133
ω_4 (A_1)	57	55	ω_4 (A_1)	62	59
ω_5 (B_1)	93	104	ω_5 (B_1)	73	76
ω_6 (B_1)	37	50	ω_6 (B_1)	38	43
ω_7 (B_2)	285	284	ω_7 (B_2)	212	210
ω_8 (B_2)	112	109	ω_8 (B_2)	102	99
ω_9 (B_2)	30	33	ω_9 (B_2)	52	55
μ_e	4.1	4.4	μ_e	5.2	5.5

Notes: ΔE_{iso}= $E(Cs_3F_2^+/Cs_2F_3^-$, cyclic) − $E(Cs_3F_2^+$, V-shaped/$Cs_2F_3^-$, Z-shaped) and ΔE_{iso} is in kJ·mol^{-1}; The vibrational representation is $\Gamma = 4A_1 + 2B_1 + 3B_2$.

For the bipyramidal isomers, the properties are shown in Table 8, only two geometrical parameters, R_e(Cs−F) and α_e, are needed to specify this shape (Figs. 3 g, h). The internuclear distance of the $Cs_3F_2^+$ ion was not shorter but slightly larger than for the $Cs_2F_3^-$ ion unlike other pentaatomic isomers and triatomic ions considered above. It means that the negatively charged bypiramid is more compact as in the base of it there are three F atoms, whereas in base of the positively charged pyramid, there are three cesium atoms which are much bigger than fluorine atoms. The bond angles at the vertices differ, the angle is obtuse for the positive ion, $\alpha_e(Cs-F-Cs) = 96^o$, and acute angle for the negative ion, $\alpha_e(F-Cs-F) = 83^o$. Thus, the bipyramid

is flattened for $Cs_3F_2^+$ but slightly elongated along the z-axis for $Cs_2F_3^-$. The vibrational spectra of the ions $Cs_3F_2^+$ and $Cs_2F_3^-$ of D_{3h} symmetry are rather similar. As is seen from Table 8, the values of the isomerisation energy ΔE_{iso}, that are $E(Cs_3F_2^+, D_{3h}) - E(Cs_3F_2^+$, V-shaped) and $E(Cs_2F_3^-, D_{3h}) - E(Cs_2F_3^-$, Z-shaped), are both negative according to the MP2 B2 calculations. It implies that the bipyramidal isomers are energetically more stable than those of V-shaped and Z-shaped configurations.

Table 8: Properties of the pentaatomic ions with bipyramidal structure of D_{3h} symmetry.

	$Cs_3F_2^+$		$Cs_2F_3^-$	
Property	**B3LYP5 B2**	**MP2 B2**	**B3LYP5 B2**	**MP2 B2**
R_e(Cs−F)	2.800	2.787	2.785	2.779
α_e	96.0	96.1	82.5	82.8
E	−260.16878	−259.24667	−340.05611	−339.13959
ΔE_{iso}	14.9	−4.3	−19.5	−35.9
ω_1 (A_1')	242	249	214	220
ω_2 (A_1')	91	93	97	97
ω_3 (A_2'')	180	186	202	209
ω_4 (E')	195	208	188	197
ω_5 (E')	50	46	108	107
ω_6 (E'')	131	149	126	140

Notes: $\Delta E_{iso} = E(Cs_3F_2^+/Cs_2F_3^-, D_{3h}) - E(Cs_3F_2^+$, V-shaped/$Cs_2F_3^-$, Z-shaped) and ΔE_{iso} is in kJ·mol^{-1}; The vibrational representation is $\Gamma = 2A_1' + A_2'' + 2E' + E''$.

2.3.2.3. Heptaatomic $Cs_4F_3^+$ and nonaatomic $Cs_5F_4^+$ ions

The ions have been detected in vapors over cesium fluoride as it was mentioned above. Similar cluster ions such as $Cs_4Cl_3^+$ and $Cs_5Cl_4^+$ were recorded over cesium chloride (Pogrebnoi *et al.*, 2000). For the ion $Cs_4F_3^+$, five structures were considered: the planar two-cycled, D_{2h}; two-cycled with the mutually perpendicular planes, D_{2d}; Z-shaped of C_{2h} symmetry, and pyramidal with C_{3v} symmetry. Among them only two structures were confirmed to correspond to minima on the PES (Fig. 4); one of them was D_{2d} symmetry and another of C_{3v} symmetry. The properties of two isomers of the heptaatomic ion $Cs_4F_3^+$ with the D_{2d} and C_{3v} symmetry are shown in Table 9.

The first structure of the D_{2d} symmetry is specified by four geometrical parameters: two internuclear separations Cs−F, R_{e1} and R_{e2} and two valence angles α_e(F−Cs−F_b) and β_e(Cs−F_b−Cs). As is seen, the inner distance R_{e2} is noticeably longer, by ~0.35 Å (MP2 B1), than R_{e1}. The angle α_e(F−Cs−F_b) is acute, but β_e(Cs−F_b−Cs) is obtuse. The second structure of the C_{3v} symmetry is described with two distances R_{e1}(Cs−F) and R_{e2}(Cs_t−F), two valence angles α_e(F−Cs_t−F) and β_e(F−Cs−F), and one torsion angle χ_e(Cs−F−Cs−F). The fact that the torsion angle is equal to 77° (MP2) implies that the base of the pyramid is not planar. For the second structure, C_{3v}, there were no low vibrational frequencies in contrast to the first structure, D_{2d}, for which two low deformational frequencies were revealed, $\omega_4(A)$ = 18 and $\omega_{11}(E)$ = 15 cm^{-1}. The second isomer appeared to be much more stable energetically as it possesses much lower energy than the first one, the energy drop being about 80 $kJ \cdot mol^{-1}$ (MP2 B1).

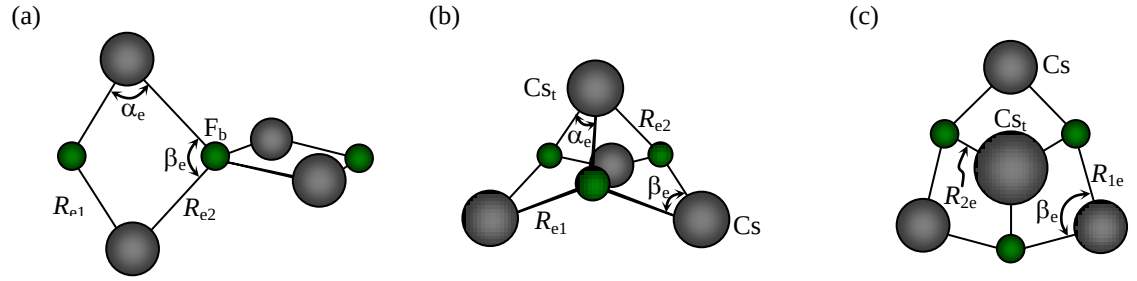

Figure 4: Geometrical structures of the heptaatomic ion $Cs_4F_3^+$: (a) two-cycled with the mutually perpendicular planes, D_{2d}; (b) pyramidal, C_{3v}, side view; (c) pyramidal, C_{3v}, top view.

For the $Cs_5F_4^+$ ion, two structures were investigated: the first one was the pyramid with the CsF-tail of C_{3v} symmetry, and the second one was the inverse bipyramid where two Cs_2F_2 fragments connected through Cs atom (D_{2d} symmetry). Only the first structure of C_{3v} point group symmetry was found to be equilibrium (Fig. 5). This shape may be imagined as a distorted cube of the Cs_4F_4 molecule with one extra Cs atom attached.

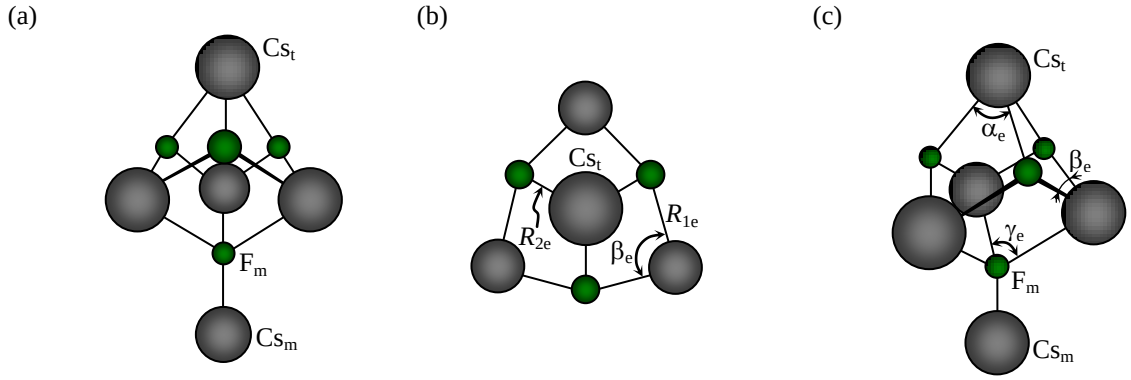

Figure 5: Geometrical structure of the nonaatomic ion $Cs_5F_4^+$, bipyramidal of C_{3v} symmetry: (a) face view; (b) top view; (c) side view.

Table 9: Properties of two isomers of the heptaatomic $Cs_4F_3^+$ ion (D_{2d} and C_{3v} symmetry).

Property	$Cs_4F_3^+$ (D_{2d})		Property	$Cs_4F_3^+$ (C_{3v})	
	B3LYP5 B1	MP2 B1		B3LYP5 B1	MP2 B1
R_{e1}(Cs−F)	2.602	2.602	R_{e1}(Cs−F)	2.760	2.745
R_{e2}(Cs−F)	2.993	2.948	R_{e2}(Cs$_t$−F)	2.852	2.832
α_e(F−Cs−F$_b$)	76.6	75.0	α_e(F−Cs$_t$−F)	75.0	74.0
β_e(Cs−F$_b$−Cs)	93.3	95.7	β_e(F−Cs−F)	78.0	76.8
			χ_e(Cs−F−Cs−F)	75.4	77.0
E	–380.25498	–378.96359	E	–380.281710	–378.99423
ω_1 (A_1)	73	78	ω_1 (A)	203	222
ω_2 (A_1)	38	39	ω_2 (A)	201	211
ω_3 (A_2)	226	226	ω_3 (A)	164	167
ω_4 (B_1)	228	230	ω_4 (A)	95	97
ω_5 (B_2)	179	194	ω_5 (A)	41	41
ω_6 (B_2)	64	70	ω_6 (E)	249	264
ω_7 (B_2)	16	18	ω_7 (E)	156	164
ω_8 (E)	290	300	ω_8 (E)	125	133
ω_9 (E)	123	142	ω_9 (E)	58	56
ω_{10} (E)	43	48	ω_{10} (E)	35	34
ω_{11} (E)	17	15			

Notes: The vibrational representation is $\Gamma = 2A_1 + A_2 + B_1 + 3B_2 + 4E$ for $Cs_4F_3^+$ (D_{2d}) and $\Gamma = 5A + 5E$ for $Cs_4F_3^+$ (C_{3v}).

The geometrical parameters and vibrational frequencies of the $Cs_5F_4^+$ ion are represented in Table 10. There are four non-equivalent internuclear separations Cs–F and three valence angles

were required to describe this configuration. This structure seems to be quite rigid but a few low frequencies are found.

Table 10: Properties of the $Cs_5F_4^+$ ion (C_{3v}).

Property	B3LYP5 B1	MP2 B1	Property	B3LYP5 B1	MP2 B1
$R_e(Cs_t{-}F)$	2.851	2.830	ω_4 (A_1)	94	99
$R_e(Cs{-}F)$	2.738	2.724	ω_5 (A_1)	55	60
$R_e(Cs{-}F_m)$	3.195	3.103	ω_6 (A_1)	42	45
$R_e(Cs_m{-}F_m)$	2.629	2.635	ω_7 (A_2)	191	206
$\alpha_e(F{-}Cs_t{-}F)$	76.6	75.5	ω_8 (E)	236	248
$\beta_e(F{-}Cs{-}F)$	80.4	79.0	ω_9 (E)	176	184
$\gamma_e(Cs{-}F_m{-}Cs)$	87.0	89.5	ω_{10} (E)	150	159
E	−500.36607	−498.71453	ω_{11} (E)	88	107
ω_1 (A_1)	258	269	ω_{12} (E)	57	57
ω_2 (A_1)	215	228	ω_{13} (E)	40	46
ω_3 (A_1)	186	188	ω_{14} (E)	19	20

Notes: The vibrational representation is $\Gamma = 6A_1 + A_2 + 7E$.

2.3.3. Relative abundance of isomers

The existence of different isomers has been disclosed for some compounds considered above. Among the neutral molecules, the trimers may have two equilibrium structures: the planar hexagonal (D_{3h}) and butterfly-shaped (C_s). The three isomers of the pentaatomic ions are proved to exist: V-shaped, kite-shaped (cyclic), and bipyramidal for the positive ion $Cs_3F_2^+$ and Z-shaped, kite-shaped, and bipyramidal for negative $Cs_2F_3^-$. For the heptaatomic ion $Cs_4F_3^+$, two isomeric forms were found: the two-cycled with the mutually perpendicular planes D_{2d}, and pyramidal C_{3v}.

Thermodynamic calculations were performed to evaluate the relative isomer contents in the saturated vapors. We considered the isomerization reactions which are listed in Table 11. The relative concentrations of the isomers in equilibrium vapor were calculated as follows:

$$\Delta_r H°(0\,) = T\Delta_r \Phi°(T) - RTln\left(\frac{p_{II}}{p_I}\right), \tag{2.5}$$

where p_{II}/p_I is the pressure ratio between two isomers: p_I stands for the reactant and p_{II} for product in the isomerization reactions; $\Delta_r H°(0)$ is the enthalpy of the reaction; T is absolute temperature; $\Delta_r \Phi°(T)$ is the change in the reduced Gibbs energy of the reaction.

The values of $\Delta_r \Phi°(T)$ and other thermodynamic functions were computed by the rigid rotator-harmonic oscillator approximation using the geometrical parameters and vibrational frequencies obtained in the MP2 calculations. The enthalpies of the isomerization reactions $\Delta_r H°(0)$ were calculated on the basis of the isomerization energies ΔE_{iso}, and the zero-point vibration energy (ZPVE) correction $\Delta\varepsilon$ as given in Eqs (2.1) and (2.2).

The isomerization energies ΔE_{iso}, zero point vibration energies $\Delta\varepsilon$, enthalpies $\Delta_r H°(0\ )$ of the isomerization reactions, change in the reduced Gibbs energies $\Delta_r \Phi°(T)$, and relative abundance p_{II}/p_I of the isomers at T = 1000 K are presented in Table 11. The values of p_{II}/p_I show which of isomers is predominant. As is seen the "butterfly-shaped" Cs_3F_3 (C_s) is comparable with the hexagonal-shaped (D_{3h}) isomer, as the ratio $p(C_s)/p(D_{3h})$ is about 40%. For the pentaatomic ions, the V-shaped structure for the positive ions and Z-shaped for negative are the predominant structures among three possible isomers considered. The relative fraction of the bipyramidal structure is very small, about 1%, in spite of higher energetical stability of this isomer especially for $Cs_2F_3^-$ ions. For the ion $Cs_4F_3^+$, the pyramidal isomer possesses much lower energy compared to the D_{2d} structure and the former is of much higher relative concentration than the latter.

The temperature effect on the abundance p_{II}/p_I of the isomers has been considered for the temperature range between 800 and 1500 K (Fig. 6). As is seen the relative fraction of the cyclic isomers slightly increases for positive $Cs_3F_2^+$ ion from 13% to 18% and decreases for negative $Cs_2F_3^-$ from 10% to 4% (Fig. 6 a). The relative concentration of the bipyramidal isomers remains very small, about 1% at T = 1000 K, and decreases in the temperature range considered (Fig. 6 b). The relative fraction of the minor isomer of neutral trimer slightly decreases as the temperature rise, still being rather high (Fig. 6 c). For the heptaatomic ion $Cs_4F_3^+$, the relative concentration of the D_{2d} isomer is increasing with temperature increase (Fig. 6 c) from 0.05% at 800 K up to 15% at 1500 K. Thus the general conclusion about the most abundant isomers made

above for T = 1000 K is not changed for temperature interval relevant to the experimental conditions.

Table 11: The isomerization energies ΔE_{iso}, zero point vibration energies $\Delta\varepsilon$, enthalpies $\Delta_r H^o(0)$ of the isomerization reactions, change in the reduced Gibbs energies $\Delta_r\Phi^o(T)$ and relative abundance p_{II}/p_I of the isomers at T = 1000 K.

Isomerization reaction	ΔE_{iso}, kJ·mol^{-1}	$\Delta\varepsilon$, kJ·mol^{-1}	$\Delta_r H^o(0)$, kJ·mol^{-1}	$\Delta_r\Phi^o$(1000 K), J·mol^{-1}·K^{-1}	p_{II}/p_I at 1000 K
Cs_3F_3 (C_s) = Cs_3F_3 (D_{3h})	−1.33	−0.24	−1.6	−9.7	0.37
$Cs_3F_2^+$ (V-shaped, C_{2v}) = $Cs_3F_2^+$ (cyclic, C_{2v})	4.08	0.14	4.2	−11.6	0.15
$Cs_3F_2^+$ (V-shaped, C_{2v}) = $Cs_3F_2^+$ (bipyramid, D_{3h})	−4.28	1.00	−3.3	−40.3	0.01
$Cs_2F_3^-$ (Z-shaped, C_{2h}) = $Cs_2F_3^-$ (cyclic, C_{2v})	−12.16	0.26	−11.9	−33.8	0.07
$Cs_2F_3^-$ (Z-shaped, C_{2h}) = $Cs_2F_3^-$ (bipyramid, D_{3h})	−35.90	2.07	−33.8	−70.6	0.01
$Cs_4F_3^+$ (C_{3v}) = $Cs_4F_3^+$ (D_{2d})	80.40	−1.04	79.4	36.6	0.006

Thermodynamic calculations of the relative abundance of isomers confirm that the entropy factor is significant in determining which of the isomer is predominant. For example, in spite of the higher energetic stability of the hexagonal Cs_3F_3 or the bipyramidal form of the pentaatomic ions, these isomers do not predominate. The minor concentration of these isomers may be explained by the superior effect of the entropy factor. The relatively decrease in entropy as well as reduced Gibbs energy $\Delta_r\Phi°(T)$ in the isomerization reaction is prevailing over the energy factor and lead to higher abundance of the butterfly-shaped structure Cs_3F_3 or V-shape $Cs_3F_2^+$ and Z-shape of the $Cs_2F_3^-$ ions. The thermodynamic functions of the species considered are given for selected temperatures in Appendix 1.

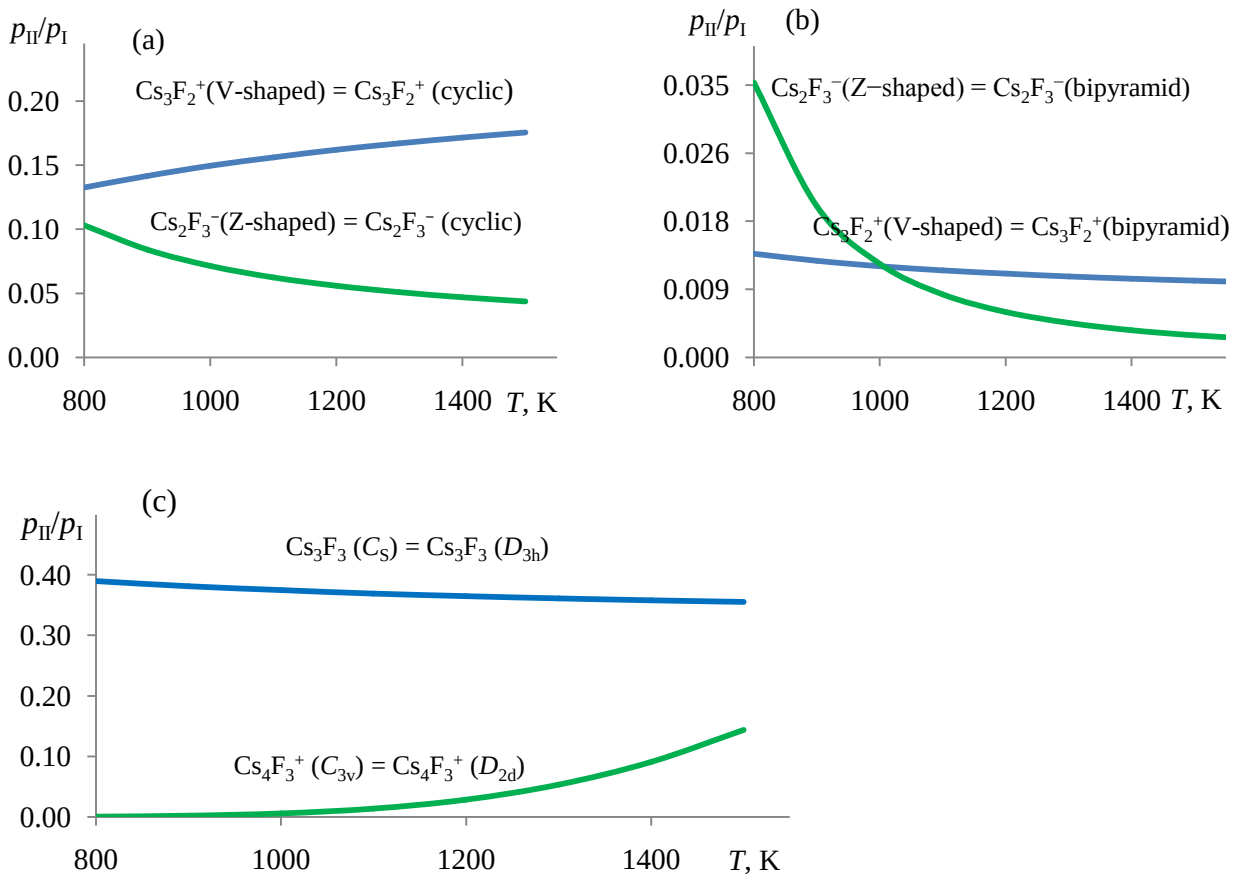

Figure 6: Temperature dependence of the relative amount of isomers p_{II}/p_I: (a) pentaatomic ions, cyclic (C_{2v}) regarding V-shaped (positive) and Z-shaped (negative); (b) pentaatomic ions, bipyramid (D_{3h}) regarding V-shaped (positive) and Z-shaped (negative); (c) heptaatomic ions, pyramid (C_{3v}) regarding two-cycled with the mutually perpendicular planes (D_{2d}), and neutral trimer, hexagonal (D_{3h}) regarding butterfly-shaped (C_s).

2.3.4. The enthalpies of the dissociation reactions and enthalpies of formation of molecules and ions

The dissociation energies $\Delta_r E$ of molecules and ions, with the elimination of the CsF molecule, were calculated employing basis sets B1 and B2. The basis set superposition error (BSSE) (Boys *et al.*, 1970; Solomonik *et al.*, 2005) was taken into account as well; hereafter the dissociation energies with the BSSE corrections included were denoted as $\Delta_r E_c$. The enthalpies of the

dissociation reactions $\Delta_r H°(0\ )$ were calculated using Eq. (2.1). To evaluate the reliability of number of methods applied, B3LYP B1, B3LYPC B1, MP2 B1, MP4 B1, MP4C B1, B3LYP B2, B3LYPC B2, B3LYP B2, MP4 B2, and MP4C B2 (capital letter "C" symbolizes that the BSSE correction was included), the values of the dissociation enthalpy $\Delta_r H°(0)$ were analysed.

For the dimer molecule Cs_2F_2, the theoretical values of the dissociation enthalpy were compared with the reference magnitude $\Delta_r H°(0) = 163.5$ kJ·mol^{-1} available in the IVTANTHERMO Database (Gurvich *et al.*, 2000). This comparison is shown in Fig. 7, where the reference value is taken as a benchmark, and the differences Δ between the theoretical values and reference one are displayed in the bar diagram. The highest level of computation MP4C B2 gives the lowest difference $\Delta = 1.4$ kJ·mol^{-1} that is in the best agreement with the reference value. The maximum error approaches 20 kJ·mol^{-1} for the methods MP2 B1 and MP4 B1 whereas MP4C B1 improves the results decreasing the value of Δ up to 5–6 kJ·mol^{-1}. Worth to note that the lowest level of computation, B3LYP B1, demonstrates surprisingly good result ($\Delta = 1.6$ kJ·mol^{-1}), which may be explained by a mutual error compensation due to an incompleteness of the basis set on one side and method used on the other side. Based on the difference Δ found for the MP4C B2 level, the uncertainty in the theoretical enthalpy of the dissociation reaction of the dimeric molecule was accepted to be $\pm$ 2 kJ·mol^{-1} (Table 12).

As regards, the BSSE correction itself, Δ_C, that is the difference between $\Delta_r H°(0)$ computed without and with the BSSE correction. The values of the Δ_C determined through the MP4–MP4C methods are equal to 11 5 kJ·mol^{-1} (B1) and 5 kJ·mol^{-1} (B2) while through the B3LYP – B3LYPC methods are equal to 4 (B1) and 3 kJ·mol^{-1} (B2). Thus the value of Δ_C obtained by MP4 and MP4C is higher compared with that by B3LYP and B3LYPC method.

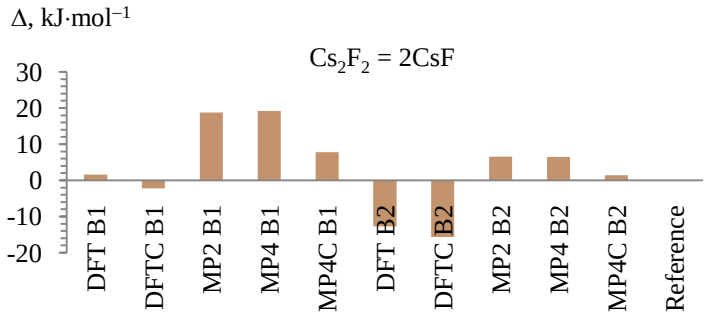

Figure 7: Analysis of the calculated enthalpies of dissociation reactions $\Delta_r H°(0)$ of the dimeric molecule Cs_2F_2. Differences Δ between $\Delta_r H°(0)$ found theoretically and the reference value (Gurvich *et al.*, 2000) are displayed versus different computational methods.

The results for other species, triatomic and pentaatomic ions are shown in Fig. 8. In absence of available experimental data, the value of $\Delta_r H°(0)$ obtained using the MP4C B2 level was considered here as a benchmark. Generally, the trends of these figures for the ions are similar to that for the Cs_2F_2 molecule. The recommended values of $\Delta_r H°(0)$ are presented in Table 12 with the uncertainties estimated on the basis of the error found for the dimer Cs_2F_2.

Concerning the reliability of the method MP4C B1, it provides with a rather good result, as it may be noted from Figs. 7 and 8, as deviations do not exceed 8 kJ·mol^{-1} regarding the reference value (Fig. 7) and 5 kJ·mol^{-1} regarding the MP4C B2 (Fig. 8). This value of 8 kJ·mol^{-1} has been taken for the estimation of the uncertainties in $\Delta_r H^o(0)$ for the dissociation reactions of the trimer Cs_3F_3, tetramer Cs_4F_4, heptaatomic ion $Cs_4F_3^+$, and nonaatomic $Cs_5F_4^+$ where the calculations were limited by the method MP4C B1. Recommended energies and enthalpies of the dissociation reactions are given in Table 12.

Recommended energies and enthalpies of the dissociation reactions and enthalpies of formation of molecules and ions are given in Table 12. The enthalpies of formation were calculated on the basis of the values $\Delta_r H^o(0)$; the required enthalpies of formation of the ions Cs^+, F^-, and molecules CsF, Cs_2F_2 were taken from the IVTANTHERMO Database (Gurvich *et al.*, 2000).

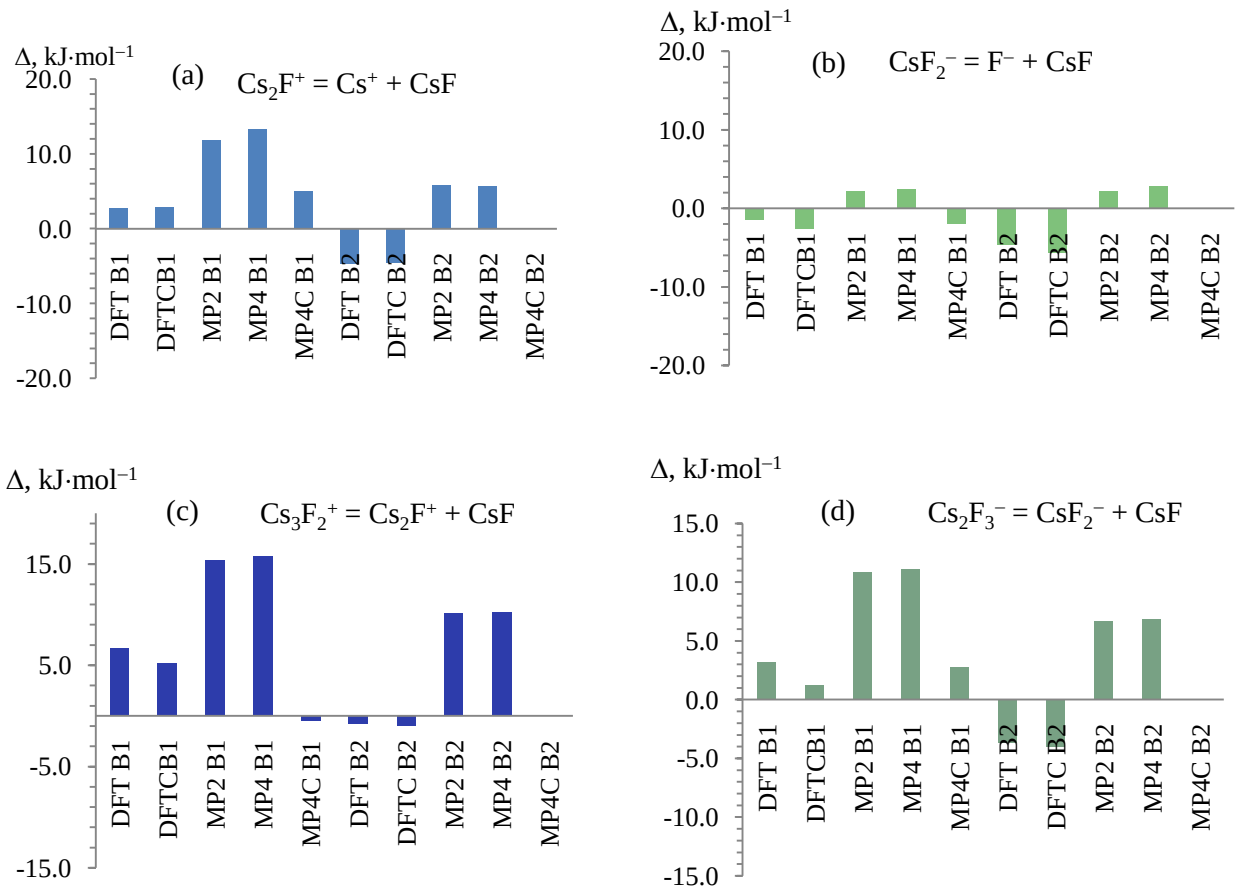

Figure 8: Analysis of the calculated enthalpies of dissociation reactions $\Delta_r H°(0)$ of the triatomic and pentaatomic ions: (a) Cs_2F^+, (b) CsF_2^-, (c) $Cs_3F_2^+$, and (d) $Cs_2F_3^-$. Differences Δ regarding the highest level MP4C B2 are displayed versus other computational methods.

It can be observed in Table 12 that the dissociation enthalpy of the Cs_2F^+ ion is 27 kJ·mol^{-1} higher compared to CsF_2^- and the dissociation enthalpy of $Cs_3F_2^+$ is 4 kJ·mol^{-1} higher compared to $Cs_2F_3^-$. Therefore the positive triatomic ion is much more stable than the negative, whereas pentaatomic ions are comparable in their stabilities. Also, the triatomic ions have higher dissociation enthalpy than pentaatomic: by 66 kJ·mol^{-1} for positive ions and 43 kJ·mol^{-1} for negative ions. Therefore the triatomic ions are more energetically stable than the pentaatomic. The similar results were obtained earlier for cesium chloride (Pogrebnaya *et al.*, 2012): the enthalpies of dissociation had the same trend of decreasing in $\Delta_r H^o(0)$ both from the triatomic to pentaatomic and from positive to negative ions; the values of $\Delta_r H°(0)$ were as follows: 163 ± 4 (Cs_2Cl^+) → 112 ± 7 ($Cs_3Cl_2^+$) and 153 ± 3 ($CsCl_2^-$) → 113 ± 5 kJ·mol^{-1} ($Cs_2Cl_3^-$). As to compare

these data with those in Table 12, we can see that the energetic stability of fluoride-containing ions is higher compared to the corresponding ions over cesium chloride. Apparently it relates to the smaller ionic radius of F^- and the ionic nature of the compounds as well which result in the bond strengthening.

Table 12: The energies, ZPVE, and enthalpies of the dissociation reactions, the enthalpies of formation of the molecules and ions, kJ·mol^{-1}.

No.	Dissociation reaction	$\Delta_r E$	$\Delta_r E_c$	$\Delta\varepsilon$	$\Delta_r H°(0)$	$\Delta_f H°(0)$
1	$Cs_2F_2 = 2CsF$	172.3	167.3	−2.4	165 ± 2	−888 ± 2
2	$Cs_3F_3 = CsF + Cs_2F_2$	141.4	133.6	−1.3	132 ± 8	−1384 ± 8
3	$Cs_4F_4 = CsF + Cs_3F_3$	233.9	210.0	−4.0	206 ± 10	−1949 ± 13
4	$Cs_2F^+ = CsF + Cs^+$	196.2	190.5	−1.5	189 ± 4	−97 ± 4
5	$CsF_2^- = CsF + F^-$	165.5	162.7	−0.9	162 ± 4	−774 ± 4
6	$Cs_3F_2^+ = CsF + Cs_2F^+$	134.5	124.3	−1.3	123 ± 6	−581 ± 7
7	$Cs_2F_3^- = CsF + CsF_2^-$	127.3	120.4	−1.4	119 ± 6	−1255 ± 7
8	$Cs_4F_3^+ = CsF + Cs_3F_2^+$	217.0	197.7	−3.3	194 ± 10	−1142 ± 12
9	$Cs_5F_4^+ = CsF + Cs_4F_3^+$	143.3	130.6	−2.4	128 ± 12	−1632 ± 17

Notes: ΔE is the energy of the reaction; $\Delta_r E_c$ is the energy of the reaction with the BSSE correction; $\Delta\varepsilon$ is the ZPVE correction. The enthalpies of formation correspond to the species given in the left hand side of the reactions. The reference values for the Cs_2F_2 are $\Delta_r H°(0) = 163.5$ kJ·mol^{-1} and $\Delta_f H°(0) = -887$ kJ·mol^{-1} (Gurvich *et al.*, 2000).

It is worth to note a saw-shaped dependence of $\Delta_r H°(0)$ in the rank either of the neutral molecules Cs_2F_2 – Cs_3F_3 – Cs_4F_4 and positive ions Cs_2F^+ – $Cs_3F_2^+$ – $Cs_4F_3^+$ – $Cs_5F_4^+$, that is 165 – 132 – 206 and 189 – 123 – 194 – 128 kJ·mol^{-1} respectively. This behaviour may be explained by the relation of the CsF detachment to the geometrical shape of the molecular or ionic cluster. The lower enthalpy of the reaction is observed where one bond breaks, as for instance in the case of the V-shaped $Cs_3F_2^+$ ion (Fig. 3 c), or where the bonds are relatively weak as in the trimer Cs_3F_3 molecule or in $Cs_5F_4^+$ ion (Figs. 2 b and 5). The tetramer molecule Cs_4F_4 and heptaatomic $Cs_4F_3^+$ ion possess the highest stability against the elimination of the CsF molecule caused by the rather compact structures of these compounds (Figs. 2 c and 4 b, c).

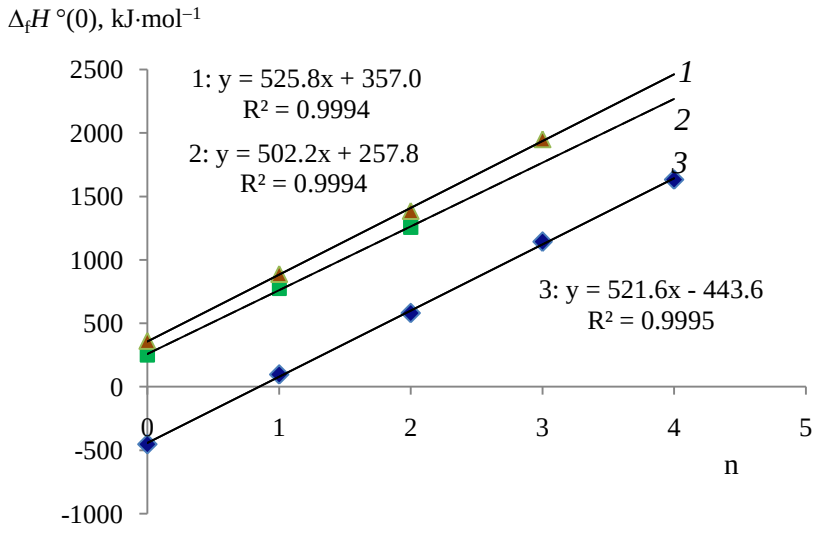

Figure 9: Enthalpies of formation $\Delta_f H°(0)$ of ionic and molecular clusters versus n, the number of CsF molecules attached: 1 – $CsF(CsF)_n$; 2 – $F^-(CsF)_n$;. 3 – $Cs^+(CsF)_n$.

The enthalpies of formation of molecular and ionic clusters (Table 12) were calculated on the basis of the values $\Delta_r H°(0)$; the required enthalpies of formation of the ions Cs^+, F^-, and molecules CsF, Cs_2F_2 were taken from the IVTANTHERMO Database (Gurvich *et al.*, 2000). The enthalpies of formation of the molecules Cs_nF_n and ions $F^-(CsF)_n$ and $Cs^+(CsF)_n$ versus the number n of CsF molecules attached are shown in Fig. 9. The values of $\Delta_f H°(0)$ at n = 0 correspond to the enthalpies of formation of CsF molecule, F^- and Cs^+ ions and were taken from (Gurvich *et al.*, 2000). All three lines demonstrate linear trend with the similar slope and correlation coefficient close to one. These results could be used for the estimation of the enthalpies of formation of the heavier cluster molecules and ions which may be generated under appropriate experimental conditions.

2.4. Conclusion

Theoretical study by the DFT and MP2 methods has confirmed a variety of molecular and ionic species which exist in vapor over cesium fluoride. A comparison of theoretical values of the internuclear separations and vibrational frequencies with the scarce reference data proved the

reliability of both DFT and MP2 methods; the latter being preferable. The existence of isomeric forms is revealed for the trimer Cs_3F_3 molecule, pentaatomic ions $Cs_3F_2^+$, $Cs_2F_3^-$ and heptaatomic ion $Cs_4F_3^+$, and the most abundant isomers are determined. To come to a conclusion which of the isomers is predominant in the saturated vapor, both the energy and the entropy factors must be considered.

The data array on the enthalpies of the reactions obtained by different methods was analyzed. To approach the reliable magnitudes of the enthalpies of the reactions, the BSSE correction has to be taken into account; especially it concerns the calculations by MP2 and MP4 methods. Worth to mention that the simplest level B3LYP B1 considered here, even without the BSSE correction, may bring to a rather good agreement with the reference data in some cases, but does not look sufficiently reliable. In general, the comprehensive analysis of the results by different methods hopefully provides us with the results comparable by the accuracy with the experimental data.

CHAPTER THREE

Molecular and Ionic Clusters Existing in Vapor over Cesium Chloride: Structure and Thermodynamic Properties[2]

Abstract: The properties of neutral molecular Cs_2Cl_2, Cs_3Cl_3 and Cs_4Cl_4 and the positively charged ionic clusters $Cs_4Cl_3^+$ and $Cs_5Cl_4^+$ existing in vapor over cesium chloride have been studied. The DFT method with B3LYP5 and B3P86 functionals, and Møller–Plesset perturbation theory of the second and fourth order have been used. The effective core potential with Def2-QZVP basis set for cesium and full electron basis set cc-pVTZ for chlorine were implemented. The geometrical parameters and vibrational frequencies of species have been determined. Isomers of two kinds have been revealed for Cs_3Cl_3 and $Cs_4Cl_3^+$ species, and their relative concentrations in vapor were evaluated. The dissociation reactions of the clusters with elimination of CsCl molecule were examined and enthalpies of reactions and enthalpies of formation of the species have been determined.

3.1. Introduction

Cluster ions possess unique electronic, optical and magnetic properties (Khanna *et al.*, 1993, 1995; Rao *et al.*, 1999) and serve as fundamental building blocks for new class of materials with desired properties (Castleman Jr *et al.*, 2009; Rao *et al.*, 1999). Particularly cesium chloride is an essential material in manufacturing of different electronic devices. For example, CsCl thin films have been used in fabrication of silicon nanotip arrays (Liao *et al.*, 2011; Zhang *et al.*, 2014) and micro and nano surface of silicon wafer (Liu *et al.*, 2013a) for solar cells. The CsCl ion arrays were used as a resist in reactive ion etching fabrication of certain structures on silicon surfaces (Tsuchiya *et al.*, 2000). Also, light emitting diodes made using self-assembled CsCl nanospheres with nano-textured indium tin oxide (Zhang *et al.*, 2012), and transparent organic light emitting devices prepared by depositing CsCl thin films (Lee *et al.*, 2010) have been proved to enhance the output power of these devices.

---

[2]Stanley F. Mwanga, Tatiana P. Pogrebnaya and Alexander M. Pogrebnoi, Molecular and Ionic Clusters Existing in Vapor over Cesium Chloride: Structure and Thermodynamic Properties *Computational and Theoretical Chemistry*, **2016**, 1078:47−54, DOI: 10.1016/j.comptc.2015.12.013

The vaporization of CsCl by Knudsen effusion mass spectrometry studied by Gorokhov (1972), Hilpert (1990), Lisek *et al*., (1998) where the presence of CsCl and more complicated molecules was observed. In the review by Hargittai (2000) it was reported that in vapors of different alkali halides, monomers presented as the main species, while dimers, trimers and tetramers were detected in a small amount. Similarly, the mixture of CsI, Cs_2I_2 and Cs_3I_3, was detected in the vapor over CsI in (Viswanathan *et al.*, 1984), monomer being the main component. Furthermore, the ionic clusters of cesium chloride such as Cs_2Cl^+, $CsCl_2^-$, $Cs_3Cl_2^+$, $Cs_2Cl_3^-$, $Cs_4Cl_3^+$ and $Cs_5Cl_4^+$ had been registered in saturated vapor over cesium chloride by Knudsen effusion mass-spectrometry (Gusarov, 1986; Pogrebnoi *et al.*, 2000), and the equilibrium constants of ion-molecular reactions involving these ions had been measured.

Accurate experimental data from microwave spectroscopic measurements are available for CsCl diatomic molecule such as internuclear distance and vibrational frequency (Huber *et al.*, 2001), ionization potential (Timoshenko *et al.*, 1974) and dipole moment (Hebert *et al.*, 1968). The molecular parameters and vibrational modes of dimer, trimer and tetramer molecules as well as heptaatomic and nonatomic cluster ions are less well known. For multi-atomic inorganic species, the geometrical parameters and vibration spectra are difficult to be measured directly by experimental techniques (Castleman *et al.*, 2006). Thus theoretical calculations play a vital role in determination of molecular structure and fundamental frequencies for the molecular and ionic clusters.

Previously quantum chemical methods were used to determine the geometrical parameters, vibration frequencies and thermodynamic properties of cluster ions existing in saturated vapors over NaX (X = F, Cl, Br, I) and MCl (M = K, Rb, Cs) (Pogrebnaya *et al.*, 2007, 2008, 2010; Pogrebnaya *et al.*, 2012). The geometrical parameters and vibrational frequencies of tri-and pentaatomic ions of cesium chloride had been studied earlier (Hishamunda *et al.*, 2012; Pogrebnaya *et al.*, 2012) using quantum chemical methods, thermodynamic properties such as enthalpies of ion-molecular reaction and enthalpies of formation of the ions were determined. Moreover, the performance of basis sets and computational methods were examined, whereby MP2 method with extended basis set was found to be more accurate than other methods. Recently quantum chemical calculations have been performed for ionic and molecular clusters of

cesium fluoride, bromide and iodide as in chapter two and four using B3LYP5 and MP2 methods. The aim of this work is to determine geometrical structures, vibrational spectra and thermodynamic properties of Cs_2Cl_2, Cs_3Cl_3, Cs_4Cl_4, $Cs_4Cl_3^+$ and $Cs_5Cl_4^+$ species employing the similar theoretical approaches.

3.2. Computational details

All calculations were performed using the GAMESS(US) software (Schmidt *et al.*, 1993), Firefly version 8.1.0 (Granovsky, 2012a), implementing the electron density functional theory (DFT) with the Becke–Lee–Yang–Parr functional (B3LYP5) (Becke, 1993; Lee *et al.*, 1988) and Becke–Perdew functional (B3P86) (Becke, 1993; Perdew, 1986; Perdew *et al.*, 1981), as well as the second and fourth order Møller–Plesset perturbation theory (MP2 and MP4). The basis sets were employed: for Cs, the effective core potential with 46 electrons in the core and Def2-QZVP basis set (6s5p4d1f) (Leininger *et al.*, 1996), and for Cl, the full-electron basis set cc-pVTZ (5s4p2d1f) augmented with *s*-, *p*-, *d*- and *f*-diffuse functions (Feller, 1996; Schuchardt *et al.*, 2007) both basis sets were accessed from EMSL (The Environmental Molecular Sciences Laboratory, US) . As stated in section 2.2, no core electrons were frozen in MP2 and MP4 methods. The geometry of the species considered was optimized using B3LYP5, B3P86 and MP2 methods. A vibrational analysis was performed at the same level to verify that the optimized structure corresponds to a real minimum at the potential energy surface (PES) by the absence of imaginary frequencies. The dissociation energies $\Delta_r E$ with the elimination of CsCl molecules were calculated by all the methods B3LYP5, B3P86 and MP2 as explained in section 2.2.

3.3. Results and Discussion

3.3.1. Dimer Cs_2Cl_2: structure, vibrational spectrum and enthalpy of dissociation

Different geometrical structures of the Cs_2Cl_2 molecule were considered such as linear ($C_{\infty v}$), planar cycle or rhomb (D_{2h}) and non-planar cycle (C_{2v}). Among these only rhomb with D_{2h} symmetry was found to be equilibrium. This result is similar to other presented on light alkali metal halides (Dickey *et al.*, 1993; Hargittai, 2000). The computed and literature data of geometrical parameters, vibrational frequencies and enthalpy of dissociation reactions of the

Cs_2Cl_2 molecule are compiled in Table 13. The internuclear distance R_e(Cs–Cl) obtained by B3P86 and MP2 methods are in better agreement with literature data, than B3LYP5 result. The fundamental frequencies computed by three methods do not contradict to each other and literature data as well.

The energy of dissociation reaction $\Delta_r E$ of Cs_2Cl_2 into two monomers has been calculated using these three methods, moreover BSSE correction has been taken into account in MP2 and MP4 calculations; thus six methods have been applied: B3LYP5, B3P86, MP2, MP2C, MP4, and MP4C. The enthalpies of reactions $\Delta_r H°(0)$ are calculated using the dissociation energies $\Delta_r E$, and the zero-point vibration energy (ZPVE) correction $\Delta\varepsilon$ as given in Eqs. (2.1) and (2.2).

The enthalpies of the reaction calculated by all theoretical levels were compared with the reference magnitude $\Delta_r H°(0) = 160.9$ kJ·mol^{-1} accessed from IVTANTHERMO database (Gurvich *et al.*, 2000). The theoretical values of enthalpy of dissociation reaction *versus* the level of calculations are shown in Fig. 10 and the reference value (Gurvich *et al.*, 2000) is taken as a benchmark. It can be seen that the results obtained by B3LYP5 and B3P86 methods are underrated essentially (by ~20 kJ·mol^{-1}) compared with the reference datum, while the results by MP2, MP2C, MP4 and MP4C agree much better with the reference value. Our highest level of computation MP4C gives the magnitude of 155 kJ·mol^{-1} which deviates by $\Delta = 6$ kJ·mol^{-1} from the benchmark; this difference was accepted as the uncertainty of the result presented in Table 13.

Concluding this section about dimer molecule, all three methods B3LYP5, B3P86 and MP2 give in general reasonable results on geometrical parameters and vibrational frequencies. For the enthalpy of dissociation reaction, the results by B3LYP5 and B3P86 methods deviate much from the reference value, whereas MP2C and MP4 magnitudes agree well with the benchmark. For the heavier molecular and ionic clusters, the geometrical parameters and vibrational frequencies presented are found by B3P86 method, while MP2 and MP4 methods have been used in the computation of the energies of the dissociation reactions.

Table 13: Properties of the neutral molecule Cs_2Cl_2.

Property[a]	B3LYP5	B3P86	MP2	Literature data
R_e(Cs–Cl)	3.198	3.162	3.155	3.140[b], 3.149[c]
α_e(Cl–Cs–Cl)	87.9	87.8	86.7	87.0[b] 85.6[c]
$-E$	960.831080	961.036916	959.816057	
ω_1 (A_g)	147	154	150	149[b]
ω_2 (A_g)	53	53	53	51[b]
ω_3 (B_{1g})	124	127	133	130[b]
ω_4 (B_{1u})	45	45	44	41[b]
ω_5 (B_{2u})	143	146	146	145[b]
ω_6 (B_{3u})	152	155	159	156[b]
I_4	0.74	0.72	0.77	
I_5	1.68	1.68	1.67	
I_6	1.83	1.86	1.88	
$\Delta_r H°(0)$	140.5	142.7	165	160.9[d]

Notes: [a]Here and hereafter in Tables 2–5, R_e(Cs–Cl) is the equilibrium internuclear distance, Å; α_e(Cl–Cs–Cl) is the valence angle, degrees; E is the total electron energy, au; ω_i are the fundamental frequencies, cm^{-1}; I_i are the IR intensities, $D^2amu^{-1}Å^{-2}$, and $\Delta_r H°(0)$ is the enthalpy of the dissociation reaction $Cs_2Cl_2 = 2CsCl$, $kJ·mol^{-1}$. Besides the values of $\Delta_r H°(0)$ presented, the enthalpy of the reaction has been also calculate by MP4C method and equal to 155 ± 6 $kJ·mol^{-1}$. Reference values: [b]Badawi *et.al.*, 2012; [c]Hargittai., 2000; [d]Gurvich *et.al.*, 2000.

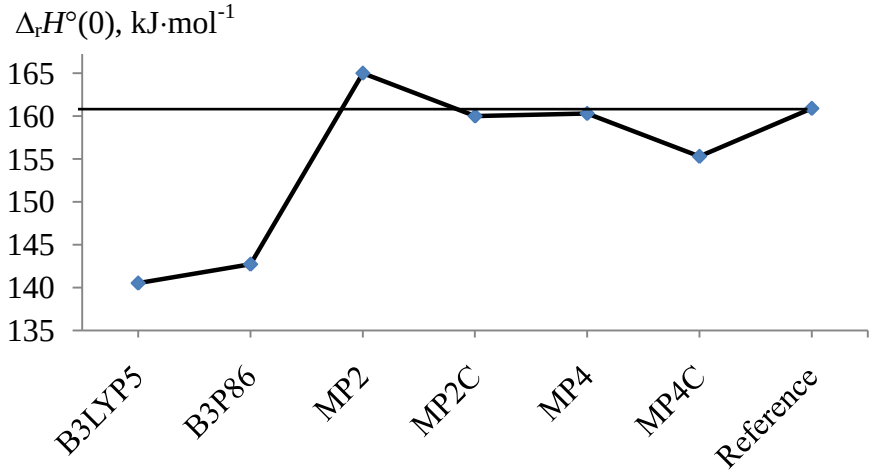

Figure 10: The values of enthalpy of dissociation reaction $Cs_2Cl_2 = 2CsCl$ versus level of calculations.

3.3.2.Trimer Cs_3Cl_3 and tetramer Cs_4Cl_4: structure and vibrational spectra

Several alternative geometrical configurations of the trimer and tetramer were investigated. For Cs_3Cl_3 molecule, three structures were considered: planar hexagonal (D_{3h}), hexagonal non-planar (C_{3v}), and prismatic (C_s). The geometry of these structures was optimized; and through optimization the hexagonal non-planar one converged into planar while prismatic converged into butterfly-shaped structure. Thus for the Cs_3Cl_3 molecule two isomers were confirmed to exist: planar hexagonal and butterfly-shaped (Fig. 11 a, b). Their geometrical parameters and vibrational frequencies are gathered in Table 14. The planar hexagonal shape is of high symmetry and only two parameters R_e(Cs–Cl), and α_e(Cl–Cs–Cl) or β_e(Cs–Cl–Cs) are needed to describe it. The butterfly-shaped isomer possesses a bit lower energy than planar hexagonal by ~ –4.0 kJ·mol^{-1} (B3P86) and ~ –12.0 kJ·mol^{-1} (MP2), the energies by MP2 method for the Cs_3Cl_3 isomers were computed without optimization, but using the parameters obtained by DFT/B3P86 method. This structure is described by four unequal internuclear distances two valence angles and one dihedral angle.

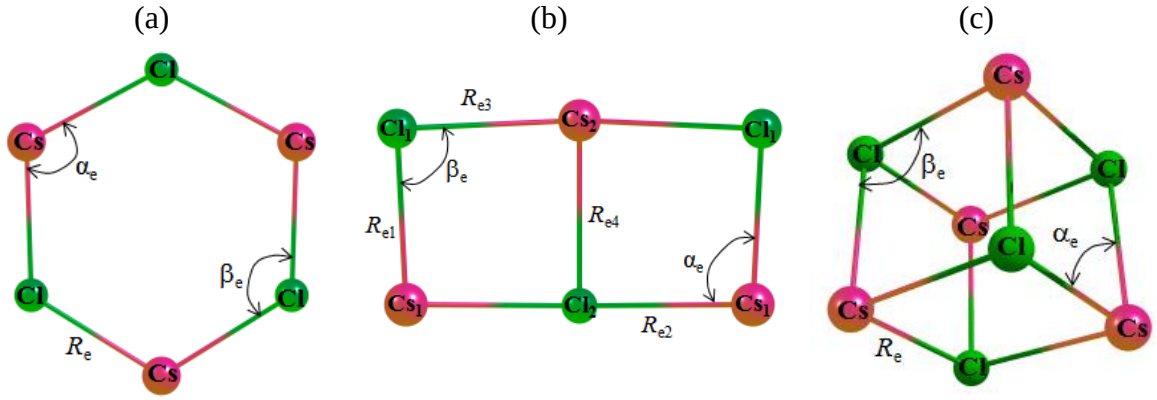

Figure 11: Geometrical structures of the trimer Cs_3Cl_3 and tetramer Cs_4Cl_4 molecules: (a) planar hexagonal Cs_3Cl_3, D_{3h}; (b) butterfly-shaped Cs_3Cl_3, C_s and (c) distorted cube Cs_4Cl_4, T_d.

Table 14: Properties of trimer molecule Cs_3Cl_3.

Cs_3Cl_3 (planar hexagon, D_{3h})		Cs_3Cl_3 ('butterfly-shaped', C_s)	
Property	**B3P86**	**Property**	**B3P86**
R_e(Cs−Cl)	3.169	$R_{e1}(Cs_1-Cl_1)$	3.095
α_e (Cl−Cs−Cl)	116.5	$R_{e2}(Cs_1-Cl_2)$	3.330
β_e(Cs−Cl−Cs)	123.5	$R_{e3}(Cs_2-Cl_1)$	3.501
$-E$	1441.567211	$R_{e4}(Cs_2-Cl_2)$	3.270
ω_1 (A_1')	156 (0.00)	$\alpha_e(Cl_1-Cs_1-Cl_2)$	91.7
ω_2 (A_1')	105 (0.00)	$\beta_e(Cs_1-Cl_1-Cs_2)$	95.4
ω_3 (A_1')	46 (0.00)	$\chi_e(Cs_1-Cl_2-Cs_2-Cl_1)$	160.1
ω_4 (A_2'')	39 (1.09)	ω_1 (A')	161 (2.09)
ω_5 (E')	174 (2.40)	ω_2 (A')	126 (1.10)
ω_6 (E')	113(1.28)	ω_3 (A')	81 (0.39)
ω_7 (E')	19 (0.30)	ω_4 (A')	69 (0.13)
ω_8 (E'')	19 (0.00)	ω_5 (A')	49 (0.57)
		ω_6 (A')	36 (0.17)
		ω_7 (A')	12 (0.06)
		ω_8 (A'')	175 (1.42)
		ω_9 (A'')	153 (0.52)
		ω_{10} (A'')	123 (0.07)
		ω_{11} (A'')	42 (0.10)
		ω_{12} (A'')	23 (0.02)
ΔE_{iso}	0	ΔE_{iso}	–3.98
μ_e	0	μ_e	9.3

Note: ΔE_{iso} is the energy of isomerization reaction Cs_3Cl_3 (D_{3h}) = Cs_3Cl_3 (C_s), kJ·mol^{-1}. Here and thereafter in Tables 3–5, parenthesized values are intensities of *IR* spectrum bands in D^2·amu^{-1}·Å^{-2}, μ_e is the dipole moment in D.

For Cs_4Cl_4 molecule several configurations were considered: slightly distorted cubical (T_d), pyramidal (C_{3v}), planar 'ladder-shaped' (C_{2h}) and octagonal structure (D_{4h}). During optimization, the pyramidal structure converged into the tetrahedral (Fig. 11 c). For the octagonal and planar ladder-shaped structures, imaginary frequencies were found to exist. Therefore only configuration of T_d symmetry corresponds to the minimum at the PES of the Cs_4Cl_4 molecule; geometrical parameters and vibrational frequencies are shown in Table 15.

Table 15: Properties of tetramer molecule Cs_4Cl_4 (T_d).

Property	B3P86
R_e(Cs−Cl)	3.291
α_e(Cl−Cs−Cl)	88.3
β_e(Cs-Cl-Cs)	91.6
$-E$	1922.12887
ω_1 (A_1)	122 (0.00)
ω_2 (A_1)	62 (0.00)
ω_3 (E)	105 (0.00)
ω_4 (E)	37 (0.00)
ω_5 (T_1)	102 (0.00)
ω_6 (T_2)	132 (5.67)
ω_7 (T_2)	120 (1.89)
ω_8 (T_2)	38 (0.03)

3.3.3. Heptaatomic $Cs_4Cl_3^+$ and nonaatomic $Cs_5Cl_4^+$ ions: structure and vibrational spectra

The ions $Cs_4Cl_3^+$ and $Cs_5Cl_4^+$ had been proved to exist in saturated vapor over cesium chloride (Gusarov, 1986; Pogrebnoi *et al.*, 2000) their structural properties are reported in this section.

For the $Cs_4Cl_3^+$ ion, a pool of alternative geometrical configurations such as planar cycled D_{2h}; two-cycled with mutually perpendicular planes, D_{2d}; Z-shaped C_{2h} and pyramidal of C_{3v} symmetry were investigated. Only two structures among them, of C_{3v} and D_{2d} symmetry (Fig. 12), correspond to minima at the PES. The geometrical parameters and vibrational frequencies of these two isomers are gathered in Table 16. The first structure of C_{3v} symmetry is shown in Figure 12 a, b and specified by two internuclear separations, R_{e1} and R_{e2}, two valence angles, α_e and β_e, and a dihedral angle χ_e(Cs−Cl−Cs−Cl). The second D_{2d} structure of the ion $Cs_4Cl_3^+$ is formed by two cycles (Fig. 12 c) which are specified with internuclear separations, R_{e1} and R_{e2} and valence angles, α_e and β_e. The inner distance R_{e2} is much longer, by 0.38 Å, than R_{e1} and both angles are acute. The first isomer (C_{3v}) has lower energy by ~64 kJ·mol^{-1} than two-

cycled one, thus being more stable energetically. Note, that the pyramidal isomer is more "rigid" as its deformational frequencies are bigger compared with the ion of the D_{2d} configuration.

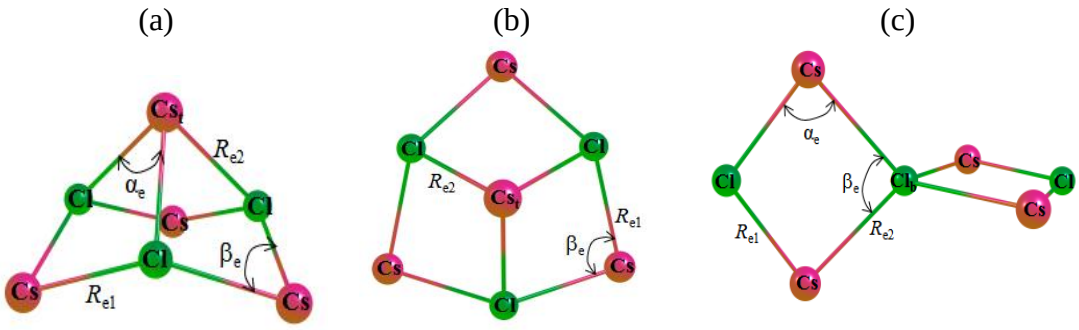

Figure 12: Geometrical structures of the heptaatomic ion $Cs_4Cl_3^+$ (a) pyramidal of C_{3v}, side view; (b) pyramidal of C_{3v}, top view; (c) two-cycled with the mutually perpendicular planes of D_{2d} symmetry.

It is worth to note that the dipole moment of $Cs_4Cl_3^+$ ion (C_{3v}) may seem to be very small, μ_e = 2.0 D, for a pyramidal isomer with highly ionic bonds. This result may be explained if take into account the non-planar shape of the pyramid base (Fig. 12 a). The resultant dipole moment may be considered as a vector sum of all bonds. As is seen the dipole moments of Cs-Cl bonds in the base of the pyramid oppose and hence compensate in large those of the Cs_t-Cl edges. On the other hand the small dipole moment also may be explained by a small separation between centres of positive and negative charges. From these considerations, the small dipole moment of the pyramidal $Cs_4Cl_3^+$ ion looks reasonable.

For the $Cs_5Cl_4^+$ ion, two geometrical structures were examined; the first was the polyhedral and Cs atom attached as a tail (C_{3v} symmetry) and second was inverse bipyramid in which two Cs_2Cl_2 fragments were connected through Cs atom (D_{2d} symmetry). The only one structure of C_{3v} symmetry was found to correspond to the minimum at the PES. This structure may be considered as a distorted cube of Cs_4Cl_4 with an extra Cs atom attached (Fig. 13). The geometrical parameters and vibrational frequencies are gathered in Table 17. This configuration is described by four non-equivalent internuclear separations and three valence angles. The

structure seems to be quite rigid though it has a few low vibrational modes relating to the Cs-tail motion.

Table 16: Properties of two isomers of the heptaatomic $Cs_4Cl_3^+$ ion (D_{2d} and C_{3v} symmetry).

Property	$Cs_4Cl_3^+$ (C_{3v}) B3P86	Property	$Cs_4Cl_3^+$ (D_{2d}) B3P86
R_{e1}(Cs−Cl)	3.237	R_{e1}(Cs−Cl)	3.462
R_{e2}(Cs_t−Cl)	3.321	R_{e2}(Cs−Cl_b)	3.085
α_e(Cl−Cs_t−Cl)	81.9	α_e(Cl−Cs−Cl_b)	83.5
β_e(Cl−Cs−Cl)	84.4	β_e(Cs−Cl_b−Cs)	89.1
χ_e(Cs−Cl−Cs−Cl)	106.8		
$-E$	1461.67647		1461.65227
ΔE_{iso}	0		63.6
ω_1 (A_1)	126 (0.82)	ω_1 (A_1)	55 (0.00)
ω_2 (A_1)	104 (0.66)	ω_2 (A_1)	29 (0.00)
ω_3 (A_1)	62 (0.03)	ω_3 (A_2)	153 (0.00)
ω_4 (A_1)	29 (0.08)	ω_4 (B_1)	152 (1.04)
ω_5 (A_2)	137 (0.00)	ω_5 (B_2)	123 (1.53)
ω_6 (E)	161 (3.68)	ω_6 (B_2)	44 (0.19)
ω_7 (E)	109 (1.34)	ω_7 (B_2)	13 (0.00)
ω_8 (E)	88 (0.03)	ω_8 (E)	172 (2.82)
ω_9 (E)	40 (0.05)	ω_9 (E)	86 (0.86)
ω_{10} (E)	24 (0.05)	ω_{10} (E)	30 (0.16)
μ_e	2.0	ω_{11} (E)	8 (0.32)

Note: ΔE_{iso} is the energy of isomerization reaction $Cs_4Cl_3^+$ (C_{3v}) = $Cs_4Cl_3^+$ (D_{2d}), kJ·mol^{-1}.

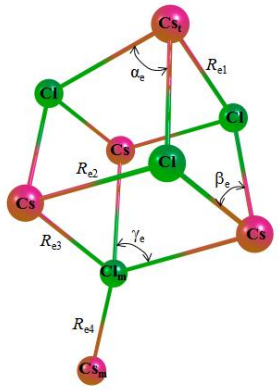

Figure 13: Geometrical structure of the nonaatomic ion $Cs_5Cl_4^+$ of C_{3v} symmetry.

Table 17: Properties of the $Cs_5Cl_4^+$ ion (C_{3v} symmetry).

Property	B3P86
$R_{e1}(Cs_t-Cl)$	3.631
$R_{e2}(Cs-Cl)$	3.333
$R_{e3}(Cs-Cl_m)$	3.221
$R_{e4}(Cs_m-Cl_m)$	3.119
α_e $(Cl-Cs_t-Cl)$	84.1
$\beta_e(Cl-Cs-Cl)$	87.7
$\gamma_e(Cs-Cl_m-Cs)$	85.6
$-E$	1942.207729
ω_1 (A_1)	160 (1.10)
ω_2 (A_1)	136 (2.22)
ω_3 (A_1)	125 (0.17)
ω_4 (A_1)	61 (0.06)
ω_5 (A_1)	46 (0.03)
ω_6 (A_1)	30 (0.02)
ω_7 (A_2)	123 (0.00)
ω_8 (E)	148 (2.34)
ω_9 (E)	125 (1.48)
ω_{10} (E)	101 (0.60)
ω_{11} (E)	63 (0.40)
ω_{12} (E)	40 (0.01)
ω_{13} (E)	30 (0.08)
ω_{14} (E)	14 (0.04)
μ_e	23.5

3.3.4. Relative abundance of Cs_3Cl_3 and $Cs_4Cl_3^+$ isomers

It was revealed that two isomers exist for the Cs_3Cl_3 molecule and $Cs_4Cl_3^+$ ion. Their relative abundance in vapor has been determined through examination of isomerization reactions: Cs_3Cl_3 (D_{3h}) → Cs_3Cl_3 (C_s) and $Cs_4Cl_3^+$ (C_{3v}) → $Cs_4Cl_3^+$ (D_{2d}). The relative concentration of an isomer in equilibrium vapor is calculated using Eq. (2.5). The enthalpies of the isomerization reactions $\Delta_r H°(0)$ were calculated using isomerization energies ΔE_{iso} and the ZPVE corrections $\Delta\varepsilon$ as given in Eqs. (2.1) and (2.2). The values of $\Delta_r\Phi°(T)$ and other thermodynamic functions were evaluated in the rigid rotator-harmonic oscillator approximation using the optimized coordinates and vibrational frequencies obtained by B3P86 method. The thermodynamic functions and the relative abundances of the isomers have been evaluated for the temperature range between 700 K

and 1600 K which may correspond to the experimental conditions. Thermodynamic functions of the species considered are given for the selected temperature in Appendix 2. The results on the relative concentration p_{II}/p_I of the isomers are shown in Table 18 for T = 1000 K.

Table 18: **The energies ΔE_{iso} and enthalpies $\Delta_r H^o(0)$ of the isomerization reactions, change in the reduced Gibbs free energies $\Delta_r\Phi°(T)$, ZPVE corrections $\Delta\varepsilon$, and relative abundances p_{II}/p_I of the isomers (T = 1000 K).**

Isomerization reaction	ΔE_{iso}, kJ·mol^{-1}	$\Delta\varepsilon$, kJ·mol^{-1}	$\Delta_r H°(0)$, kJ·mol^{-1}	$\Delta_r\Phi°(T)$, J·mol^{-1}·K^{-1}	p_{II}/p_I
Cs_3Cl_3 (D_{3h}) = Cs_3Cl_3(C_s)	–3.98	0.32	–3.65	–0.159	1.52
$Cs_4Cl_3^+$ (C_{3v}) = $Cs_4Cl_3^+$ (D_{2d})	63.55	–0.84	62.71	43.530	0.10

As is seen from Table 18, for the Cs_3Cl_3 molecule, the butterfly-shaped isomer (C_s) prevails in vapor as the value of p_{II}/p_I is greater than one. For the heptaatomic $Cs_4Cl_3^+$ ion, the isomer of C_{3v} symmetry dominates that of D_{2d} symmetry as the ratio of the isomers is 0.10 at 1000 K.

Temperature dependence on the ratio p_{II}/p_I of the isomers has been examined for the temperature range between 700 and 1600 K (Fig. 14). It can be seen that for Cs_3Cl_3 molecule the relative concentration of the ion with the butterfly-shaped structure is 1.7 at 800 K and decreases slowly with temperature increase but still is greater than one at 1500 K. Thus, this isomer is prevailing in vapor though it is worth to note a comparable amount of the isomer of hexagonal structure. For the $Cs_4Cl_3^+$ ion of the D_{2d} symmetry, the concentration increases with temperature raise, still remaining less than that of C_{3v} structure at temperatures within the experimental range 832–917 K (Pogrebnoi *et al.*, 2000).

The relative concentration of isomers relates two factors: the isomerisation energy and entropy of species. The lower the ΔE_{iso} and bigger $S°$ of the isomer II, the higher is the ratio p_{II}/p_I. For the Cs_3Cl_3, both of these factors favor the prevalence of the isomer of C_s symmetry. For the $Cs_4Cl_3^+$ ion, the effect of entropy does not compensate that of high energy of the D_{2d} isomer therefore the latter is much less abundant than C_{3v} isomer at moderate temperatures (<1100 K), but at the elevated temperatures both these isomers become comparable in relative concentration.

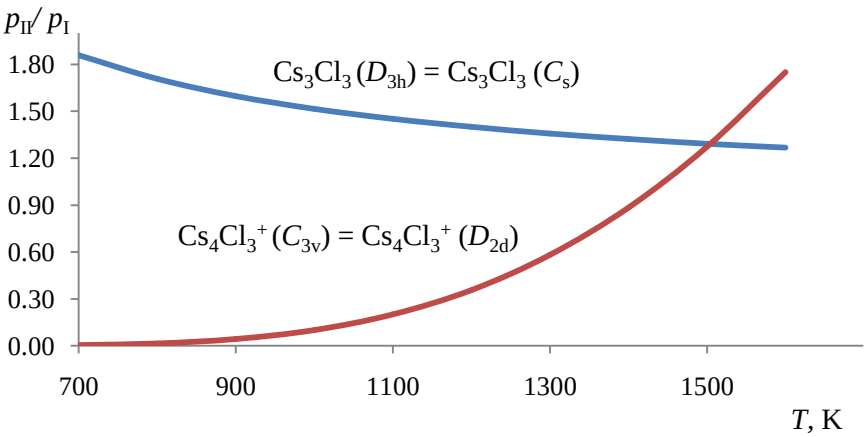

Figure 14: Temperature dependence of the relative concentration of isomers for the trimer Cs_3Cl_3 molecule and heptaatomic ion $Cs_4Cl_3^+$.

3.3.5. The enthalpies of dissociation reactions and enthalpies of formation of the species

In this section we have examined the dissociation reactions of molecular and ionic clusters with the elimination of the CsCl molecule: Cs_nCl_n = CsCl + $(CsCl)_{n-1}$ and $Cs^+(CsCl)_n$ = CsCl + $Cs^+(CsCl)_{n-1}$ (n = 3, 4). For all species the theoretical enthalpies $\Delta_rH°(0)$ of dissociation reactions were calculated using Eqs. (2.1) and (2.2) applying different levels of computation: B3LYP5, B3P86, MP2, MP2C, MP4 and MP4C. Furthermore, we calculated the values of $\Delta_rH°(0)$ for $Cs_4Cl_3^+$ and $Cs_5Cl_4^+$ based on experimental data from (Pogrebnoi *et al.*, 2000) where the equilibrium constants k_p° had been measured; the following formula was applied:

$$\Delta_r H°(0) = -RTlnk_p^\circ + T\Delta_r\Phi°(T) \qquad (3.1)$$

The thermodynamic functions of the species were computed on the base of the geometrical parameters and vibrational frequencies obtained by B3P86 method. The thermodynamic functions of the CsCl molecules and Cs^+ ions were taken from (Gurvich *et al.*, 2000).

The calculated enthalpies $\Delta_rH°(0)$ versus level of computation are presented in Fig. 15. For the dimer Cs_2Cl_2 the enthalpy of dissociation reaction was analyzed in section 3.3.1 above, and the plot for the dimer is inserted in Fig. 15 for comparison with other species. As for the trimer

molecule Cs_3Cl_3, the two isomers were proved to exist, and due to comparable amount of them in vapor, the values of $\Delta_r H°(0)$ for both isomers, of C_s and D_{3h} symmetry, were calculated. The general trend is seen as an oscillating behavior of $\Delta_r H°(0)$ along the plot and the more number of atoms in a species, the higher is the oscillation. For the trimer and tetramer molecules, the values of $\Delta_r H°(0)$ show the character alike to that of Cs_2Cl_2 while for the Cs_4Cl_4 the larger oscillation is observed along the plot. The similar oscillating tendency is also seen for the $Cs_4Cl_3^+$ and $Cs_5Cl_4^+$ ions, although for the latter a jump in the value by MP4 may be noted. For the $Cs_4Cl_3^+$ ion, the value of $\Delta_r H°(0)$ "based on experiment" follows the similar pattern as for Cs_2Cl_2 molecule that is increase of $\Delta_r H°(0)$ magnitude from MP4C to reference. This behavior differs from that of $Cs_5Cl_4^+$ ion, where the theoretical value by MP4C is 8 kJ·mol^{-1} bigger than that "based on experiment".

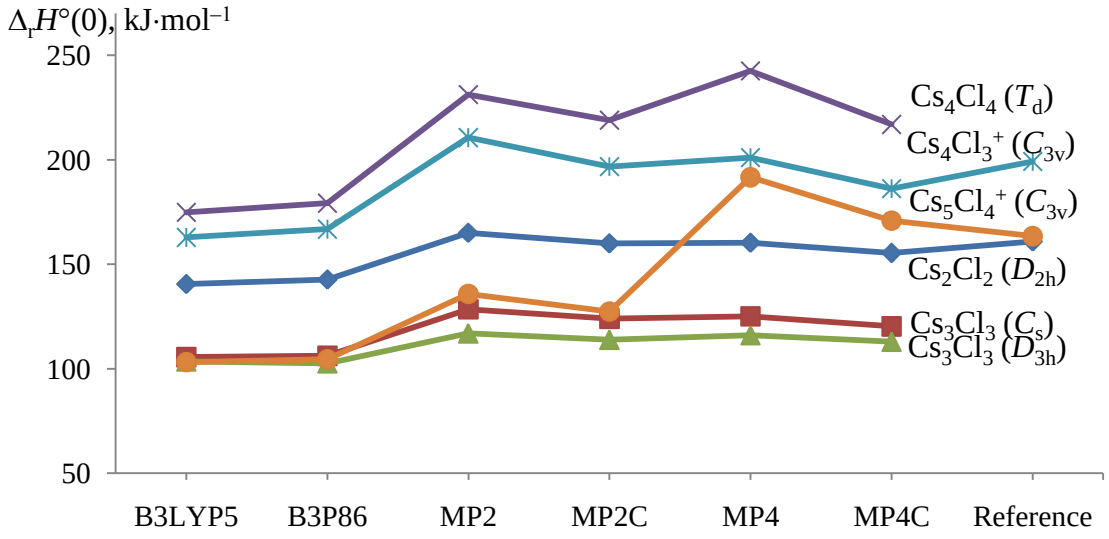

Figure 15: The calculated enthalpies $\Delta_r H°(0)$ of dissociation reactions Cs_nCl_n = CsCl + $(CsCl)_{n-1}$ (*n* = 2–4) and $Cs^+(CsCl)_n$ = CsCl + $Cs^+(CsCl)_{n-1}$ (*n* =3, 4) *versus* level of computation. The reference values for Cs_2Cl_2 are taken from (Gurvich *et al.*, 2000) and for $Cs_4Cl_3^+$ and $Cs_5Cl_4^+$ ions are based on the equilibrium constants from (Pogrebnoi *et al.*, 2000).

The theoretical results (the energies and enthalpies of the dissociation reactions and enthalpies of formation of the species), which were obtained using the method MP4C, are compared with the

"based on experiment" values in Table 19 which also compiles the data for the tri- and pentaatomic ions determined earlier (Hishamunda *et al.*, 2012). The theoretical values of the enthalpies of formation of the molecular and ionic clusters $\Delta_f H°(0)$ were calculated using the correspondent theoretical values of the enthalpies of reactions $\Delta_r H°(0)$ obtained in this work. The data of $\Delta_f H°(0)$ for CsCl and Cs^+ required for calculations were taken from (Gurvich *et al.*, 2000).

The uncertainties of theoretical enthalpies of reactions were estimated as a half-difference between maximum and minimum values obtained by MP2, MP2C, MP4 and MP4C methods, while those of enthalpies of formation included both the uncertainties in $\Delta_r H°(0)$ and $\Delta_f H°(0)$ of the products of the reactions. The uncertainties of the "based on experiment" data for ions were taken from the original paper (Pogrebnoi *et al.*, 2000) and reduced by factor 1.5 due to more accurate thermodynamic functions obtained in present work. Both for the $\Delta_r H°(0)$ and $\Delta_f H°(0)$, the theoretical values and those "based on experiment" are in fair agreement between each other, respectively.

To examine the energetic stability of the clusters, the theoretical values of enthalpies of dissociation reaction were plotted against the size of the species (Fig. 16). There are three types of the species considered: neutral molecules Cs_nCl_n, positive $Cs_nCl_{n-1}^+$, and negative $Cs_{n-1}Cl_n^-$ ions. As is seen, both neutral and ionic clusters show the similar general trend of $\Delta_r H°(0)$: decrease from n = 2 to 3, increase from n =3 to 4, and decrease again from 4 to 5. From these patterns, we can notice that when n is even the stability of molecular or ionic cluster is higher than for the next odd number. That is the "odd-even oscillation behaviour" observed.

Some speculations regarding this behaviour and the relationship between the stability of the species and number of chemicals bonds to be broken may be proposed. For example, in the tetramer molecule the enthalpy of the reaction is highest because four bonds are to be broken to release one CsCl molecule, while in the case of Cs_3Cl_3 or Cs_2Cl_2, the enthalpies are lower as tear of two bonds only is enough. Regarding the cluster ions, the higher values of $\Delta_r H°(0)$, correspond to the heptaatomic and nonaatomic ions and relate to the bigger number of bonds to

disconnect compared to tri- and pentaatomic clusters in which only one bond is to be broken to release CsCl molecule.

Along with the number of bonds, the bond strength and consequently the bond length is an important feature, shorter the length, stronger is the bond. For the neutral molecules, in a series $Cs_2Cl_2 \rightarrow Cs_3Cl_3 \rightarrow Cs_4Cl_4$, as is seen in Fig. 17, minimum of $\Delta_r H^o(0)$ corresponds to the trimer molecule. We may suggest that for the Cs_3Cl_3 (C_s) the most probable route of dissociation is the detachment of a side fragment $Cs_1–Cl_1$ (Fig. 11 b) in which the bond length is shorter (3.095 Å) and, as a result, stronger compared to other three bonds Cs–Cl (Table 11). Two longer and hence weaker bonds with $R_{e2}(Cs_1–Cl_2)$ = 3.330 Å and $R_{e3}(Cs_2–Cl_1)$ = 3.501 Å are easier to be broken. If compare to the dimer molecule Cs_2Cl_2 where also two bonds are destroyed but they are shorter (R_e = 3.149 Å), and therefore the value of $\Delta_r H^o(0)$ is bigger (by ~35 kJ·mol^{-1}) than in trimer. For the tetramer molecule, the enthalpy of dissociation is much bigger (by~100 kJ·mol^{-1}) than for trimer, as now four equivalent bonds with R_e = 3.291 Å are to be torn.

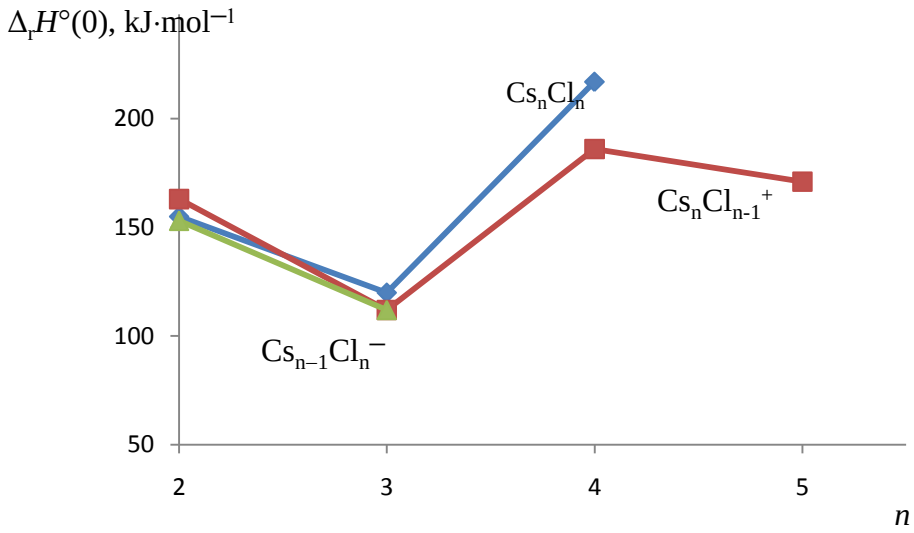

Figure 16: Enthalpies of dissociation reactions with detachment of one CsCl molecule from molecular or ionic clusters versus the size of the cluster.

For negative ions, from $CsCl_2^-$ to $Cs_2Cl_3^-$, the drop by ~40 kJ·mol^{-1} in $\Delta_r H^o(0)$ is seen. The detachment of CsCl molecule from each of negative ions requires the same number of bonds to

be broken, namely only one. The lower enthalpy of dissociation of the $Cs_2Cl_3^-$ obviously relates to the break of the weaker bridged bond unlike to the triatomic ion (R_{eb} = 3.256 Å in $Cs_2Cl_3^-$, R_e = 3.178 Å in $CsCl_2^-$ (Pogrebnaya *et al.*, 2012).

For a series of positive ions, in tri- and pentaatomic ions, Cs_2Cl^+ and $Cs_3Cl_2^+$, similar to negative ions, only one Cs–Cl bond should be disconnected to release CsCl molecule. The decrease in enthalpy by ~50 kJ·mol^{-1} relates to increase in bond length: 3.100 Å (Cs_2Cl^+), 3.228 Å ($Cs_3Cl_2^+$) (Pogrebnaya *et al.*, 2012). The next ascend of $\Delta_r H^o(0)$ by 74 kJ·mol^{-1} at $Cs_4Cl_3^+$ (Fig. 19) obviously relates to a bigger number of bonds to be broken in heptaatomic ion. We can suggest here two possible channels of dissociation: the first is the detachment of Cs-Cl fragment out of the base of the pyramid, and second is the detachment of Cs_t-Cl fragment with Cs_t atom at the top (Fig. 12 a). In first channel three bonds should be destroyed, one Cs_t-Cl and two Cs-Cl. In the second type of dissociation four bonds are disconnected, two Cs-Cl and two Cs_t-Cl. The latter channel seems to be more probable if take into account further transformation into V-shaped configuration of the pentaatomic ion. The V-shaped isomer was proved earlier to prevail among three isomers of the $Cs_3Cl_2^+$ ion in equilibrium vapor over cesium chloride (Pogrebnaya *et al.*, 2012).

From $Cs_4Cl_3^+$ to $Cs_5Cl_4^+$ slight descent in enthalpy of dissociation, by ~15 kJ·mol^{-1}, is observed. We suppose in the nonaatomic ion the Cs_m-Cl_m moiety is more likely to separate as it has the shortest distance, $R_e(Cs_m\text{-}Cl_m)$ = 3.119 Å, while other weaker three bonds Cs-Cl_m with R_e = 3.221 Å are easier to destroy. It is worth to add here that another channel of dissociation $Cs_5Cl_4^+$ = Cs^+ + Cs_4Cl_4 can be suggested as well. The enthalpy of this reaction is equal to 120 ± 40 kJ·mol^{-1}; hence this detachment of Cs^+ ion from $Cs_5Cl_4^+$ is more feasible than detachment of CsCl molecule as the latter requires more energy, $\Delta_r H^o(0)$ = 171 ± 32 kJ·mol^{-1}. The value of $\Delta_r H^o(0)$ was obtained through the enthalpies of formation of $Cs_5Cl_4^+$ and Cs_4Cl_4 (from Table 19) and Cs^+ from (Gurvich *et al.*, 2000).

Other probable routes of dissociation of the clusters may be considered as well where the dimer molecule Cs_2Cl_2 is released. The enthalpies of these reactions are easy to get through the enthalpies of formation of the species listed in Table 19. For the tetramer molecule and

nonaatomic ion, the enthalpies of reactions $Cs_4Cl_4 = 2Cs_2Cl_2$ and $Cs_5Cl_4^+ = Cs_3Cl_2^+ + Cs_2Cl_2$ are equal to 183 ± 18 kJ·mol^{-1} and 183 ± 37 kJ·mol^{-1}, respectively. The equality of these values relates to the same number of bonds to tear, namely four. For reactions $Cs_4Cl_3^+ = Cs_2Cl^+ + Cs_2Cl_2$ and $Cs_3Cl_2^+ = Cs^+ + Cs_2Cl_2$, the values of $\Delta_r H^o(0)$ are equal to 143 ± 18 kJ·mol^{-1} and 120 ± 10 kJ·mol^{-1}, respectively. These magnitudes correlate with number of bonds destroyed: three for $Cs_4Cl_3^+$ and one for $Cs_3Cl_2^+$.

If compare two types of dissociation reactions, with monomer CsCl and dimer Cs_2Cl_2 evolving, one can see that for the latter, the $\Delta_r H^o(0)$ values are remarkably lower which indicates higher probability of dissociation with release of dimer molecules. The statement that the stability of the species relates to the number and strength of chemicals bonds to be broken is also valid for the second type reactions (with dimer molecule release). One more factor which may influence on a reaction energy yield might be mentioned that is a structural rearrangement of product(s). For example, for both types of dissociation of tetramer (into CsCl plus Cs_3Cl_3 or into two Cs_2Cl_2) the same number of bonds is broken but the enthalpies of the reactions are different: 217 and 183 kJ·mol^{-1}, respectively. For the first type the enthalpy is bigger as additional energy is required to rearrange the structure of the Cs_3Cl_3 product into the butter-fly shaped structure, while in the reaction of the second type, two rhombic Cs_2Cl_2 fragments are formed and no structural rearrangement occurs.

Table 19: The energies, $\Delta_r E$, ZPVE corrections, $\Delta\varepsilon$, and enthalpies $\Delta_r H°(0)$ of the dissociation reactions, and enthalpies of formation $\Delta_f H°(0)$ of molecules and ions, all values are in kJ·mol^{-1}.

No	Dissociation reaction[a]	$\Delta_r E$	$-\Delta\varepsilon$[a]	$\Delta_r H°(0)$		$-\Delta_f H°(0)$[d]	
				Theoretical	Based on expt[b]	Theoretical	Based on expt[b]
1	$Cs_2Cl_2 = 2CsCl$	156.9	1.6	155 ± 6	161[c]	635 ± 6	641[c]
2	$Cs_3Cl_3(C_s) = CsCl + Cs_2Cl_2$	121.4	1.6	120 ± 6		996 ± 9	
3	$Cs_3Cl_3(D_{3h}) = CsCl + Cs_2Cl_2$	113.7	0.8	113 ± 3		988 ± 5	
4	$Cs_4Cl_4 = CsCl + Cs_3Cl_3$	219.0	2.2	217 ± 13		1453 ± 16	
5	$Cs_2Cl^+ = CsCl + Cs^+$	164	0.9	163 ± 4	153 ± 7	−51 ± 4	−61 ± 8
6	$CsCl_2^- = CsCl + Cl^-$	153	0.7	152 ± 3	142 ± 4	622 ± 3	611 ± 8
7	$Cs_3Cl_2^+ = CsCl + Cs_2Cl^+$	113	0.7	112 ± 7	110 ± 9	301 ± 8	289 ± 12
8	$Cs_2Cl_3^- = CsCl + CsCl_2^-$	113	0.5	113 ± 5	104 ± 10	975 ± 6	955 ± 12
9	$Cs_4Cl_3^+ = CsCl + Cs_3Cl_2^+$	188.6	2.4	186 ± 15	199 ± 28	727 ± 17	729 ± 30
10	$Cs_5Cl_4^+ = CsCl + Cs_4Cl_3^+$	172.0	1.1	171 ± 32	163 ± 33	1119 ± 36	1133 ± 45

Notes: [a]For reactions 1–4, 9 and 10 the results are calculated in this work; for the reactions 5 – 8 the data were obtained earlier (Hishamunda *et al.*, 2012). [b]For reactions 5–10 the equilibrium constants were taken from (Pogrebnoi *et al.*, 2000). [c]The values for Cs_2Cl_2 are taken from (Gurvich *et al.*, 2000). [d]The enthalpies of formation correspond to the species in the left side of the reactions.

3.4. Conclusions

Various neutral species, positive and negative ions detected earlier experimentally in saturated vapor over cesium chloride have been studied in this work. The geometrical structure, vibrational spectra, and thermodynamic properties of the dimer, trimer and tetramer molecules together with positive heptaatomic and nonaatomic cluster ions of cesium chloride were determined using DFT and MP2 methods. The scrutiny of the results and the comparison with scarce literature data allowed us to conclude that both MP2 and DFT (B3P86 and B3LYP5) methods provide the acceptable accuracy in geometrical parameters and vibrational frequencies. The DFT method is less time consuming and easier to achieve the goal compared to MP2, but in thermochemical calculations the latter gives the better agreement with the data based on experiment. Moreover the advanced theoretical levels like MP4 including the BSSE correction, as well as the experimental data as benchmarks at least for some of the species considered, are needed to ensure reliability of the results. It is worth to note that the existence of isomeric forms was

revealed for the trimer Cs_3Cl_3 molecule and heptaatomic ion $Cs_4Cl_3^+$, and the most abundant isomers in saturated vapor were determined. For the enthalpies $\Delta_r H°(0)$ of dissociation of Cs_nCl_n and $Cs_nCl_{n-1}^+$ species with elimination of CsCl molecules, it was found the "odd-even oscillation behaviour": for n = 2 and 4 the stability is higher than for n = 3 and 5, respectively. The stability of clusters was scrutinized with respect to the strength and number of chemicals bonds to be broken via the dissociation reactions.

CHAPTER FOUR

Theoretical Study of Cluster Ions Existing in Vapors over Cesium Bromide and Iodide[3]

Abstract: The properties of ions Cs_2X^+, $Cs_3X_2^+$, CsX_2^-, and $Cs_2X_3^-$ (X = Br or I) have been studied using the density functional theory and Møller–Plesset perturbation theory of the 2nd and 4th order. For all species the equilibrium geometrical configurations and vibration frequencies were determined. Different isomers of pentaatomic ions were found to exist: the linear ($D_{\infty h}$), V-shaped (C_{2v}), kite-shaped (C_{2v}), and bipyramidal (D_{3h}). The relative abundances of isomers were calculated at temperatures between 700 K and 1600 K. It was found that at about 800 K, the amount of different isomers was comparable for $Cs_3Br_2^+$, $Cs_3I_2^+$ and $Cs_2I_3^-$ ions, while for $Cs_2Br_3^-$ the linear isomer was proved to be predominant. The enthalpies of dissociation reactions with elimination of CsX molecules and the enthalpies of formation of ions were determined.

4.1 Introduction

Alkali halide cluster ions form a potential group for researches due to the possibilities of designing and fabricating new materials. Some of these cluster ions have unique properties such as electronic, optical and magnetic which are function of size and composition (Khanna *et al.*, 1993, 1995; Rao *et al.*, 1999). These species can serve as fundamental building blocks for a new class of materials with desired properties (Castleman Jr *et al.*, 2009; Rao *et al.*, 1999).

Different species composed of cesium and iodine are proved to exist among the fission products that can be released in nuclear power plants (Badawi *et al.*, 2012; Lennart *et al.*, 1994; Roki *et al.*, 2014; Roki *et al.*, 2013). They have major impact on ground contamination and radiation doses in the environment in case of accidents such as containment building leakages. They are highly radioactive in short term for iodine and in middle term for cesium (Badawi *et al.*, 2012; Lennart *et al.*, 1994; Povinec *et al.*, 2013). Thus, evaluations of their thermodynamic properties are essential for safety features of the nuclear pressurized water reactor.

Considerable studies of alkali halide cluster ions have been done in the past decades (Aguado, 2001; Alexandrova *et al.*, 2004; Castleman *et al.*, 1996; Castleman Jr *et al.*, 2009; Huh *et al.*,

[3]Stanley F. Mwanga, Tatiana P. Pogrebnaya and Alexander M. Pogrebnoi, Theoretical Study of Cluster Ions Existing in Vapors over Cesium Bromide and Iodide *British Journal of Applied Science and Technology – BJAST*, **2015**, 9(2): 108−130, DOI: 10.9734/BJAST/2015/17612

2001; Sarkas *et al.*, 1995; Yang *et al.*, 1992). Different analytical procedures have been employed for the investigation of ionic clusters (Anil K. Kandalam *et al.*, 2008; Galhena *et al.*, 2009). Mass spectrometry stands as a major experimental technique which is capable of analyzing a broad characterization of their properties (Bloomfield *et al.*, 1991). Various positive and negative ions had been identified in equilibrium vapors using high temperature mass spectrometry (Chupka, 1959; Dunaev *et al.*, 2013; Gusarov, 1986; Kudin *et al.*, 1990; Motalov *et al.*, 2001; Pogrebnoi *et al.*, 2000; Sidorova *et al.*, 1979). For the treatment of experimental data thermodynamic functions of molecules and ions are required and for the calculation of the thermodynamic functions the geometrical parameters and vibrational frequencies are needed. However they are difficult to be measured by available experimental techniques (Castleman *et al.*, 2006).

Quantum chemical methods are proficient to provide accurate information required. Previously the structure and properties of cluster ions existing in saturated vapors over sodium fluoride (NaF), sodium chloride (NaCl), sodium bromide (NaBr) sodium iodide (NaI), potassium chloride (KCl), rubidium chloride (RbCl) and cesium chloride (CsCl) had been studied by Pogrebnaya *et al*., (2007, 2008, 2010, 2012) using quantum chemical methods.

The ionic species Cs^+, Cs_2I^+, $Cs_3I_2^+$, I^-, CsI_2^-, and $Cs_2I_3^-$ have been detected in the saturated vapor over cesium iodide by high temperature mass spectrometry (Butman *et al.*, 2000; Sidorova *et al.*, 1979). Photoelectron spectroscopy was applied to CsI_2^- (Wang *et al.*, 2010). The ions Cs_2I^+ and CsI_2^- were resulted from collisions of Cs_2I_2 with Xe (Parks *et al.*, 1982). In line to this, we expect similar ions to exist in saturated vapor over cesium bromide. Thus the aims of the present work were to determine the characteristics of the cluster ions of cesium bromide and iodide using quantum chemical methods, as well as to calculate the thermodynamic properties of the ions. To verify the reliability of the results obtained, the properties of neutral species CsX and Cs_2X_2 have been calculated and analyzed through a comparison with the available reference data.

4.2 Computational details

The details of calculations are given in sections 2.2 and 2.3. The relativistic ECP (Br ECP GEN 28 4, 7 electrons in the core; I ECP GEN 46 4, 7 electrons in the core) with SDB-aug-cc-pVTZ basis set (4s4p3d2f) (Martin *et al.*, 2001) taken from EMSL (The Environmental Molecular Sciences Laboratory, U.S.) (Feller, 1996; Schuchardt *et al.*, 2007) were used. No frozen electrons were considered for MP2 and MP4 methods. The B3LYP5 and MP2 methods were applied to compute the geometrical parameters and vibrational spectra of cluster ions. The geometrical structures determined are confirmed as corresponding to minima energy by the absence of imaginary frequencies. The dissociation energies $\Delta_r E$ were calculated by B3LYP5, B3P86 and MP2 methods as explained in the section 2.2.

4.3 Results and discussions

4.3.1 Molecular properties of CsX and Cs_2X_2 (X =Br or I)

For the monomer molecules CsBr and CsI, the properties such as geometrical parameters, normal vibrational frequencies, dipole moments and ionization energies have been computed using the B3LYP5 and MP2 methods. The results are compared with available reference data (Table 20) which include the experimental (Hartley *et al.*, 1987, 1988) and found by a high level quantum chemical calculation (Badawi *et al.*, 2012) as well. For both CsBr and CsI molecules, the internuclear distances R_e(Cs–X) calculated by us are longer than the reference values. The B3P86 method gives better results when comparing with the values obtained from microwave spectrum however overestimating it by 0.02 Å for both CsBr and CsI. While the MP2 method is also close to the experimental value of microwave spectrum since it was longer by 0.03 Å for CsBr and 0.04 Å for CsI. The difference in the reference data themselves are about 0.02 Å for CsBr and 0.01 Å for CsI. The calculated values of the normal vibrational frequencies ω_e are related to the internuclear separations: the bigger is the distance, the smaller the frequency. The values of frequencies computed by all three methods B3LYP5, MP2 and B3P86 are in agreement with the reference values, the MP2 being preferred.

The ionization energies were calculated as energy differences between the parent and ionized species. The results obtained by three theoretical levels are in agreement between each other and

with the experimental values (Hartley *et al.*, 1987, 1988; Huber *et al.*, 2001) as well. As for the dipole moment, the theoretical results do not contradict to the experimental data, the B3LYP5 level being in better agreement.

Table 20: Calculated and literature data of the CsX (X = Br or I) molecules.

Property	CsBr				CsI			
	B3LYP5	**B3P86**	**MP2**	**Reference**	**B3LYP5**	**B3P86**	**MP2**	**Reference values**
R_e(Cs−X), Å	3.124	3.094	3.105	3.072[a,b]	3.372	3.340	3.363	3.315[a,b]
				3.087[d]				3.314[c]
								3.303[d]
ω_e, cm^{-1}	141	144	145	150[b]	111	115	115	119[c]
				144[d]				118[d]
				141[e]				117[e]
μ_e, D	10.9	10.7	11.3	10.8[a,b]	11.6	11.5	12.1	11.6 [b]
IP, eV	7.99	8.21	8.03	8.12[a,b]	7.45	7.68	7.46	7.54[b,c]

Notes: R_e(Cs−X) is the equilibrium internuclear distance; ω_e is the normal mode frequency, μ_e is the dipole moment, IP is the ionization potential. Reference values: [a]Hartley *et. al.*, 1987; [b]Huber *et. al.*, 2001; [c]Hartley *et. al.*, 1988; [d]Badawi *et. al.*, 2012, [e]Groen *et. al.*, 2010.

For the dimer molecules Cs_2Br_2 and Cs_2I_2 the structure was proved to be planar cycle (rhomb) with symmetry D_{2h} (Fig. 17 a) that is in accordance with Hargittai (Hargittai, 2000) and Dickey *et al.*, (Dickey *et al.*, 1993) reported that all dimers geometries of alkali halides have D_{2h} symmetry. The calculated and reference data for Cs_2X_2 molecules are gathered in Table 18: geometrical parameters, vibrational frequencies, IR intensities and enthalpies of dissociation.

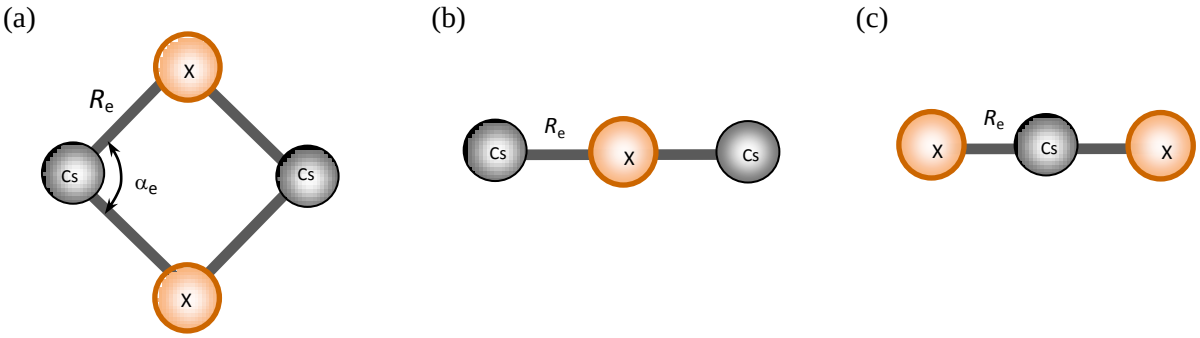

Figure 17: Geometrical equilibrium structures of the dimer molecules (a) Cs_2X_2 and triatomic ions (b) Cs_2X^+ and (c) CsX_2^-.

The internuclear distances R_e(Cs–X) found by MP2 and both B3LYP5 methods are in agreement with the literature values taking into account the scatter of about 0.06 Å of the reference data themselves. It is worth to mention that following the general trend in our data which are usually overrated compared with reference values, the theoretical results by Badawi *et al.* (Badawi *et al.*, 2012), R_e(Cs–Br) = 3.296 Å and R_e(Cs–I) = 3.511 Å, seem to be more realistic and preferable for both dimers while the experimental values of R_e(Cs–Br) = 3.356 Å found by electron diffraction study (Hartley *et al.*, 1987) and R_e(Cs–I) = 3.572 Å (Groen *et al.*, 2010) both look overrated.

The experimental vibrational frequencies are confined by two values of ω_1 (A_g) and ω_6 (B_{3u}) for Cs_2Br_2 (Groen *et al.*, 2010) and four values ω_1 (A_g), ω_4 (B_{1u}), ω_5 (B_{2u}), and ω_6 (B_{3u}) for Cs_2I_2 (Cordfunke *et al.*, 1990; Groen *et al.*, 2010; Konings *et al.*, 1991). The theoretical values of ω_i (Badawi *et al.*, 2012) are taken into account as well. We can notice that theoretical frequencies computed by us are in a good agreement with the reference values.

Concluding this section about the geometrical parameters and frequencies of the dimer molecules, we can state that all three methods, B3LYP5, B3P86 and MP2, give reasonable results in most cases, nevertheless MP2 method provides less deviation from the reference data. Therefore we expect the similar trend to appear in the properties of the ions considered further when the same level of computational method is applied.

Table 21: Calculated and literature data of the Cs_2X_2 (X = Br or I) molecules.

Property	Cs_2Br_2				Cs_2I_2			
	B3LYP5	B3P86	MP2	Reference	B3LYP5	B3P86	MP2	Reference
R_e(Cs−X)	3.373	3.332	3.326	3.356[b] 3.296[d]	3.621	3.578	3.578	3.572[c] 3.511[d]
α_e(X-Cs-X)	90.5	90.3	89.1	85 89.0[b]	94.0	93.7	92.6	92.4[d]
ω_1 (A_g)	111	111	105	108[d] 106[e]	83	87	105	95[e] 90[c] 89[d]
ω_2 (A_g)	41	43	45	41[d]	33	33	35	32[d]
ω_3 (B_{1g})	83	87	93	94[d]	68	73	76	74[d]
ω_4 (B_{1u})	29	29	31	28[d]	22	24	24	29[f] 21[d]
ω_5 (B_{2u})	98	102	104	105[d]	81	85	86	88[d,e]
ω_6 (B_{3u})	100	104	108	109[d] 110[e]	79	83	84	82[d] 76[e]
I_4	0.40	0.39	0.42		0.29	0.28	0.30	
I_5	0.91	0.90	0.89		0.69	0.67	0.65	
I_6	0.91	0.92	0.93		0.61	0.61	0.63	
$\Delta_r H°(0)$	134.7	137.5	160.1 150 ± 5[a]	153.5[g] 154.7[d]	128.6	131.1	153.8 143 ± 13[a]	150.9[g] 147.1[d]

Notes: R_e(Cs–X) is the equilibrium internuclear distance, Å; α_e(X−Cs−X) is the valence angle in degrees; ω_i are the fundamental frequencies, cm^{-1}; I_i are the IR intensities, $D^2 \cdot amu^{-1} \cdot Å^{-2}$; $\Delta_r H°(0)$ is the enthalpy of the dissociation reaction $Cs_2X_2 = 2CsX$, $kJ \cdot mol^{-1}$; [a]obtained by the MP4C method. Reference values: [b]Hartley *et al.*, 1987; [c]Cordfunke *et al.*, 1990; [d]Badawi *et al.*, 2012; [e]Groen *et al.*, 2010; [f]Konings *et al.*, 1991; [g]Gurvich *et al.*, 2000.

The energies of dissociation reactions $\Delta_r E$ of Cs_2X_2 into CsX molecules have been calculated using different theoretical levels: B3LYP5, B3P86, MP2, MP2C, MP4, and MP4C. The enthalpies of reactions $\Delta_r H°(0)$ were obtained using the energies $\Delta_r E$, and the zero-point vibration energy (ZPVE) correction $\Delta\varepsilon$ as given in equations (2.1) and (2.2).

The theoretical enthalpies of dissociations are compared with the reference values $\Delta_r H°(0)$ = 153.5 $kJ \cdot mol^{-1}$ (Cs_2Br_2) and 150.9 $kJ \cdot mol^{-1}$ (Cs_2I_2), accessed from the IVTANTHERMO Database (Gurvich *et al.*, 2000). Beside we take into consideration here the results of a high level quantum chemical computation (Badawi *et al.*, 2012): 154.7 $kJ \cdot mol^{-1}$ (Cs_2Br_2) and 147.1 $kJ \cdot mol^{-1}$ (Cs_2I_2). The comparison is presented in Figs. 18 a, b where the experimental values from (Gurvich *et al.*, 2000) are taken as a benchmark and the differences Δ between the theoretical and reference values are depicted by the bar diagrams. As one can see, B3LYP5 and

B3P86 methods give underrated results for both dimeric species while MP2C and MP4 demonstrate rather good agreement. According to our highest level of computation, MP4C, Δ = −3.5 kJ·mol^{-1} and −8.4 kJ·mol^{-1} for Cs_2Br_2 and Cs_2I_2 respectively. Based on these results, and assuming a factor of 1.5, we estimated uncertainties to be ± 5 kJ·mol^{-1} and ± 13 kJ·mol^{-1} to the corresponding theoretical values of $\Delta_r H°(0)$ calculated by MP4C. It should be noted also that our result found by MP4C method for Cs_2Br_2 is in a good agreement with both reference data (Gurvich *et al.*, 2000) and (Badawi *et al.*, 2012). For Cs_2I_2 the agreement between the value 143 ± 13 and experimental one, 150.9 (Gurvich *et al.*, 2000), is worse, but within the uncertainties, there is no contradiction. If we take into account the data from (Badawi *et al.*, 2012) as a benchmark the agreement appeared to be better as seen in Fig. 18 c. Moreover the bar diagram in Fig. 18 c for cesium iodide now looks alike to that of bromide (Fig. 18 a).

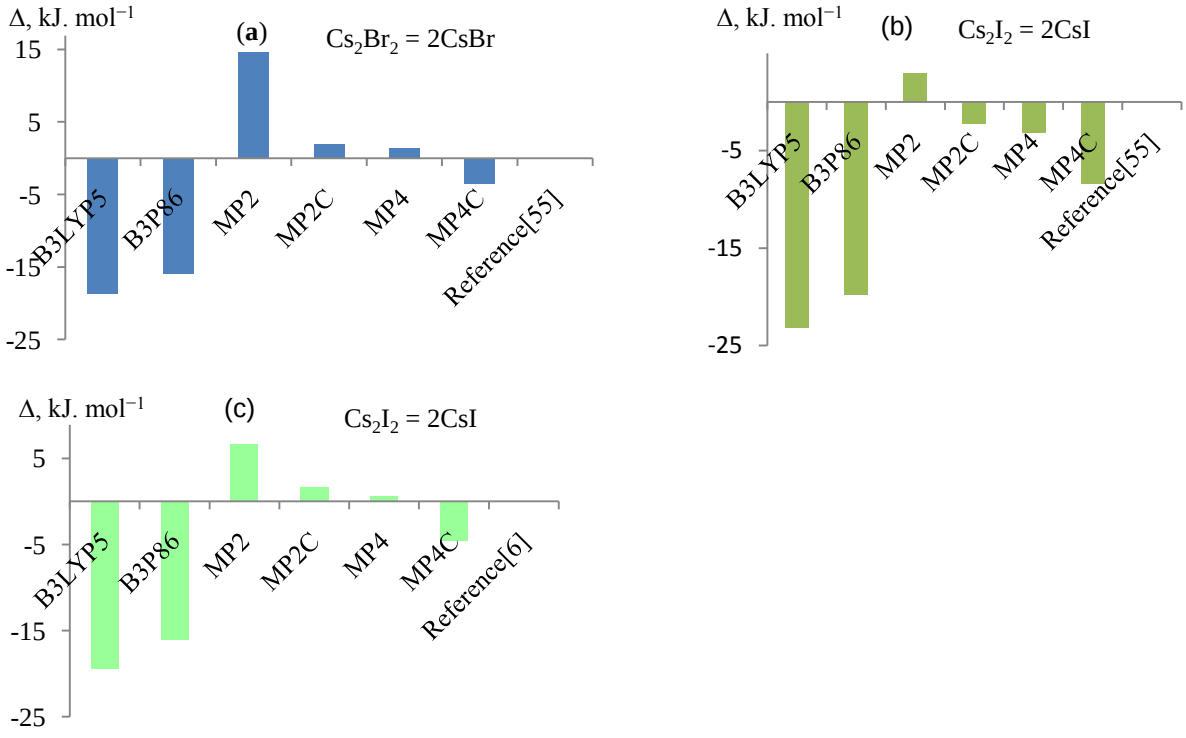

Figure 18: Analysis of the calculated enthalpies of dissociation reactions $\Delta_r H°(0)$ of the dimer molecules Cs_2Br_2 and Cs_2I_2. Values of Δ are displayed *versus* the level of calculation; Δ is the difference between the theoretical $\Delta_r H°(0)$ found by us and reference: (a) Cs_2Br_2, reference (Gurvich *et al.*, 2000); (b) Cs_2I_2, reference (Gurvich *et al.*, 2000); (c) Cs_2I_2, reference (Badawi *et al.*, 2012).

It is also worth to note here that the difference between the enthalpies of dissociation reactions $\Delta_r H°(0)$ for Cs_2Br_2 and Cs_2I_2 is 7 kJ·mol^{-1} according to our results which agrees well with ~8 kJ·mol^{-1} according to (Badawi *et al.*, 2012). The last value seems to be more feasible than 2.6 kJ·mol^{-1} as it comes from (Gurvich *et al.*, 2000). The result of $\Delta_r H°(0)$ = 164.1 kJ·mol^{-1} found for Cs_2I_2 on the base of the data $\Delta_f H°$(CsI, g, 298.15 K) = –153.3 ± 1.8 and $\Delta_f H°$(Cs_2I_2, g, 298.15 K) = –469.2 ± 5 kJ·mol^{-1} reported recently by Roki (Roki *et al.*, 2014) is evidently higher than the enthalpy of dissociation of cesium bromide and therefore looks like overrated.

4.3.2 Geometrical structure and vibrational spectra of the cluster ions

For the calculation of the properties of the cluster ions two methods; (B3LYP5) and MP2 have been used. As a whole array of the data obtained for the neutral species, triatomic and pentaatomic, positive and negative ions demonstrates alike trends from B3LYP5 to MP2 levels, therefore we present hereafter the results found by more reliable MP2 method.

4.3.2.1 Triatomic ions Cs_2X^+ and CsX_2^-

Linear structures with $D_{\infty h}$ symmetry are proved to exist for the triatomic ions (Fig. 17 b, c). The properties such as equilibrium internuclear separations R_e(Cs–X), the frequencies of normal vibrations ω_i, and the intensities of vibrations in IR spectra I_i have been determined and given in Table 22.

It can be observed that internuclear separation R_e(Cs–X) increases by ~0.08 Å from positive to negative ions for both species. Also an increase of internuclear distances by ~0.25 Å has been featured across both positive and negative cesium bromide to cesium iodide. Clearly the increase of internuclear distance from positive to negative ions is due to an excess negative charge in the CsX_2^- ion, and from cesium bromide to cesium iodide is due to an extra shell. This increase in the internuclear distance corresponds to the decrease in the antisymmetric stretching frequency ω_2: 138 cm^{-1} (Cs_2Br^+) to 109 cm^{-1} (Cs_2I^+); and 113 cm^{-1} ($CsBr_2^-$) to 98 cm^{-1} (CsI_2^-).

4.3.2.2 Pentaatomic ions, $Cs_3X_2^+$ and $Cs_2X_3^-$

Three different possible configurations have been considered (Fig. 19): linear of $D_{\infty h}$ symmetry (I), planar cyclic (kite-shaped), C_{2v} (II), and bipyramidal, D_{3h} (III). For each structure, the geometrical parameters were optimized and fundamental frequencies were determined.

As concerns the linear configuration for the $Cs_3Br_2^+$ ion the imaginary frequencies have been revealed. The further optimization showed the bent (V-shaped) structure of C_{2v} symmetry to exist with the valence angle α_e(Br–Cs–Br) = 144° and practically without decrease in energy compared to the linear shape within the accuracy of optimization procedure. Other pentaatomic ions, $Cs_2Br_3^-$, $Cs_3I_2^+$, and $Cs_2I_3^-$, were confirmed to be linear. Note these two equilibrium structures were obtained disregarding initial configuration started from: linear, bent or five-membered ring structures were converted during the optimization into V-shaped for $Cs_3Br_2^+$ or linear for other three ions (Fig. 19 a , b). Here and hereafter we call the isomer I as the ion of the bent (V-shaped) structure (C_{2v}) for the $Cs_3Br_2^+$ ion and linear ($D_{\infty h}$) for $Cs_2Br_3^-$, $Cs_3I_2^+$, and $Cs_2I_3^-$; their properties are given in Table 23. There are two different internuclear separations, terminal and bridge, which are denoted as R_{et}(Cs−X) and R_{eb}(Cs−X), respectively. From positive to negative ions of cesium bromide, there is a slight increase in the internuclear distance by 0.07 Å and 0.05 Å for R_{et}(Cs–Br) and R_{eb}(Cs–Br), respectively. The similar increase is observed for cesium iodide. Regarding terminal and bridge distances, for both ions the first one is shorter than the second, by ~0.16 Å for $Cs_3X_2^+$ and by ~0.13 Å for $Cs_2X_3^-$. In vibrational spectra of the ions with linear or V-shaped structure, several low deformational frequencies are observed, that gives evidence that these structures are floppy regarding to bending of the central moiety.

The isomer II, planar cyclic (C_{2v}), and isomer III, bipyramidal (D_{3h}), were also found to correspond to minima at the potential energy surface (PES). The optimized geometrical parameters were located and all calculated vibrational frequencies were confirmed to be real. Tables 24 and 25 report the properties of the ions $Cs_3X_2^+$ and $Cs_2X_3^-$ for cyclic and bipyramidal structures, their geometrical configurations are shown in Fig. 19 c, d, e, f.

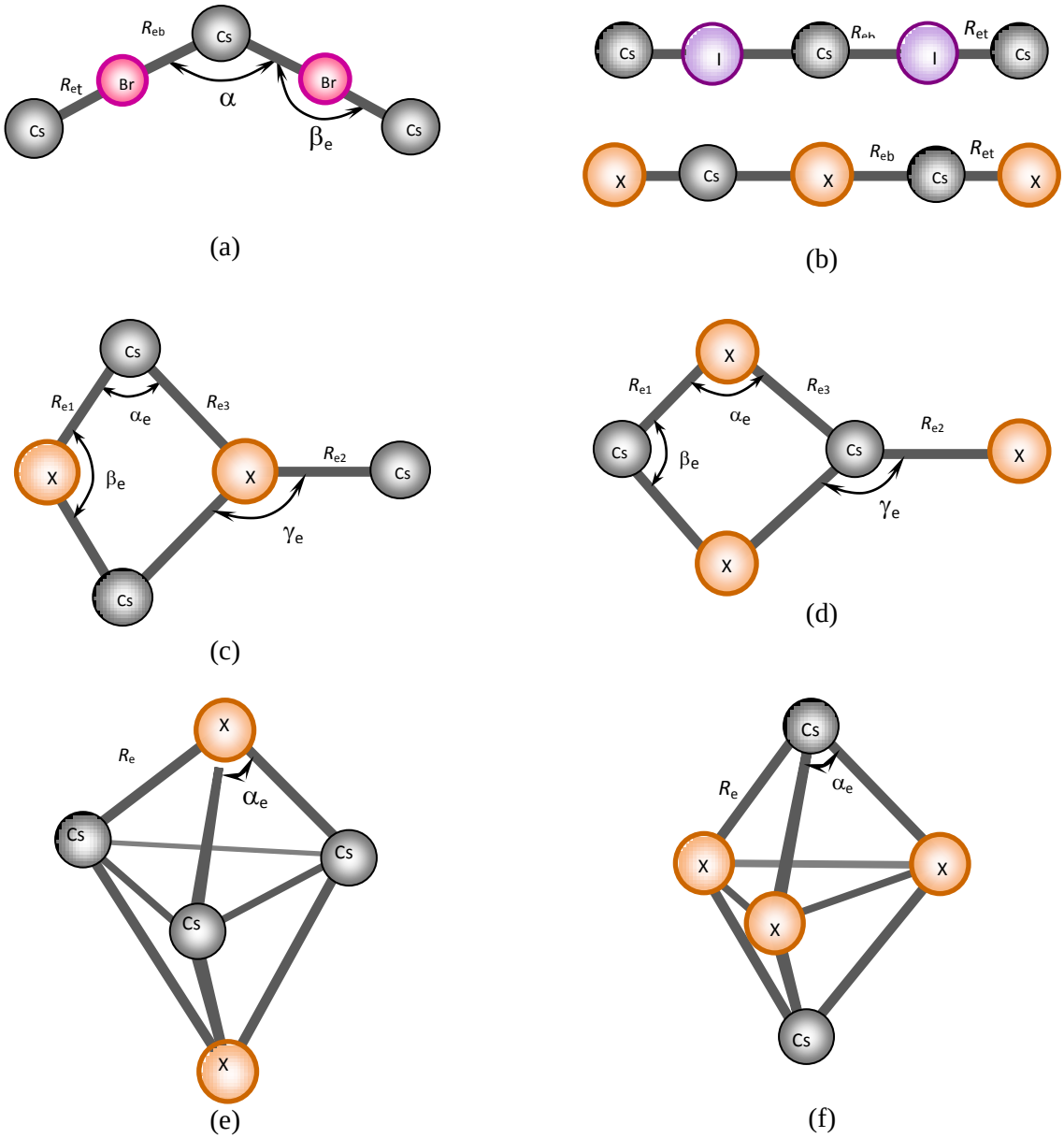

Figure 19: Geometrical equilibrium structures of the isomers for pentaatomic ions: (a) V-shaped, C_{2v}, $Cs_3Br_2^+$, (b) linear, $D_{\infty h}$, $Cs_2Br_3^-$, $Cs_3I_2^+$, and $Cs_2I_3^-$, (c) planar cyclic, C_{2v}, $Cs_3X_2^+$, (d) planar cyclic, C_{2v}, $Cs_2X_3^-$, (e) bipyramidal, D_{3h}, $Cs_3X_2^+$, (f) bipyramidal, D_{3h}, $Cs_2X_3^-$.

Table 22: Properties of the triatomic ions with linear configuration ($D_{\infty h}$) MP2 results.

Property	Cs_2Br^+	$CsBr_2^-$	Cs_2I^+	CsI_2^-
R_e(Cs−X)	3.264	3.345	3.509	3.590
E	-53.38171	-46.90089	-51.39881	-42.95097
ω_1 ($\sum_g^+$)	70	88	65	65
ω_2 ($\sum_u^+$)	138	113	109	98
ω_3 (Π_u)	24	14	19	14
I_2	1.11	1.13	0.81	0.78
I_3	0.31	0.41	0.25	0.27

Notes: R_e(Cs−X) is the internuclear separation, Å; E is the total electron energy, au ω_i are the fundamental frequencies, cm^{-1}; I_i are the IR intensities, $D^2 \cdot amu^{-1} \cdot Å^{-2}$

Table 23: **Properties of the pentaatomic ions, isomers I, MP2 results.**

Property	$Cs_3Br_2^+$ (C_{2v})	Property	$Cs_2Br_3^-$ ($D_{\infty h}$)	$Cs_3I_2^+$ ($D_{\infty h}$)	$Cs_2I_3^-$ ($D_{\infty h}$)
R_{et}(Cs−X)	3.216	R_{et}(Cs−X)	3.282	3.467	3.530
R_{eb}(Cs−X)	3.371	R_{eb}(Cs−X)	3.416	3.622	3.652
α_e(Br−Cs−Br)	143.6				
β_e(Cs−Br−Cs)	179.5				
E	-86.86862		-80.38729	-82.90444	-74.45643
ω_1 (A_1)	138	ω_1 ($\sum_g^+$)	117	106	98
ω_2(A_1)	51	ω_2 ($\sum_g^+$)	45	34	33
ω_3(A_1)	25	ω_3 ($\sum_u^+$)	121	110	101
ω_4(A_1)	8	ω_4 ($\sum_u^+$)	103	74	76
ω_5 (A_2)	23	ω_5 (Π_g)	10	13	14
ω_6(B_1)	24	ω_6 (Π_u)	20	20	16
ω_7(B_2)	137	ω_7 (Π_u)	3	8	10
ω_8(B_2)	79				
ω_9(B_2)	23				
μ_e	9.9				

Notes: R_{et}(Cs−X) and R_{eb}(Cs−X) are the terminal and bridge internuclear distances respectively, Å; α_e(Br−Cs−Br) and β_e(Cs−Br−Cs) are the valence angles in degrees; E is the total electron energy, au: ω_i are the fundamental frequencies, cm^{-1}; μ_e is the dipole moment, D.

The cyclic structure is described by three different internuclear separations Cs−X, which are denoted as R_{e1}, R_{e2}, and R_{e3}, and two independent valence angles α_e and β_e. The internuclear distances of the negative ions are slightly greater than those of positive ions correspondingly.

The relative energy of the cyclic isomers with respect to the isomer I is $\Delta E_{iso} = E_{II} - E_I$ and for all four ions the values of ΔE_{iso} are negative and lie in the range between −8 and −12 kJ·mol^{-1}. This result indicates that the cyclic isomer has lower energy on the PES than the isomer I and is more stable energetically. The vibrational spectra look alike for positive and negative ions both in frequencies and IR intensities.

Table 24: Properties of the pentaatomic ions with cyclic structure of C_{2v} symmetry (isomer II), MP2 results.

Property	$Cs_3Br_2^+$	$Cs_2Br_3^-$	$Cs_3I_2^+$	$Cs_2I_3^-$
R_{e1}(Cs−X)	3.255	3.270	3.510	3.521
R_{e2}(Cs−X)	3.295	3.336	3.548	3.585
R_{e3}(Cs−X)	3.557	3.603	3.797	3.846
α_e	85.6	86.8	88.1	84.6
β_e	99.9	99.1	96.5	100.9
γ_e	135.5	136.3	136.4	135.1
$\Delta_r E_{iso}$	−8.4	−11.6	−9.2	−10.9
ω_1 (A_1)	116	114	92	91
ω_2 (A_1)	111	105	90	88
ω_3 (A_1)	56	65	51	50
ω_4 (A_1)	31	31	25	26
ω_5 (B_1)	33	29	24	25
ω_6 (B_1)	14	10	11	8
ω_7 (B_2)	118	112	95	93
ω_8 (B_2)	65	64	55	54
ω_9 (B_2)	18	22	16	17
μ_e	9.4	6.7	10.8	7.8

Notes: R_{e1}(Cs−X), R_{e2}(Cs−X) and R_{e3}(Cs−X) are internuclear distances, Å; α_e, β_e, and γ_e are the valence angles in degrees; $\Delta_r E_{iso} = E_{II} - E_I$ is the relative energy of the cyclic isomer, kJ·mol^{-1}; ω_i are the normal mode frequencies, cm^{-1}; μ_e is the dipole moment, D.

The isomer III, that is of the bipyramidal shape, is specified by two parameters that are internuclear distance R_e(Cs−X) and valence angle α_e. The internuclear distances for positive ions are slightly shorter than those for negative ions for cesium bromide or equal for iodide. We refer to the magnitudes of ionic radii of Cs^+, Br^-, I^- ions. The bond angles at the vertices are almost

the same and close to right angle. The corresponding vibrational frequencies of $Cs_3X_2^+$ and $Cs_2X_3^-$ ions are close to each other while the frequencies of positive ions are slightly larger than those of negative. The relative energy of bipyramidal isomer with respect to the isomer I is $\Delta_r E_{iso}$ = E_{III}–E_I, the values of $\Delta_r E_{iso}$ are negative and in the range between –30 and –38 kJ·mol^{-1}. Therefore the isomer III is more energetically stable than the linear one for $Cs_2Br_3^-$, $Cs_3I_2^+$, $Cs_2I_3^-$, and V-shaped for $Cs_3Br_2^+$. In addition the bipyramidal isomer has lower energy than cyclic one and thus appeared to be the most energetically stable among three alternative isomers.

Table 25: Properties of the pentaatomic ions with bipyramidal structure of D_{3h} symmetry (isomer III), MP2 results.

Property	$Cs_3Br_2^+$	$Cs_2Br_3^-$	$Cs_3I_2^+$	$Cs_2I_3^-$
R_e(Cs–X)	3.373	3.415	3.673	3.668
α_e	90.0	89.7	88.2	92.5
ΔE_{iso}	–30.32	–38.48	–35.54	–38.14
ω_1 (A_1')	111	104	86	84
ω_2 (A_1')	52	54	49	43
ω_3 (A_2'')	101	98	73	71
ω_4 (E')	99	97	75	80
ω_5 (E')	29	39	29	25
ω_6 (E'')	77	67	57	58

Notes: R_e(Cs–X) is the internuclear distance, Å; α_e is the valence angle in degrees; $\Delta E_{iso} = E_{III} - E_I$ is the relative energy of the bipyramidal isomer, kJ·mol^{-1}; ω_i are the normal mode frequencies, cm^{-1}.

4.3.3 Relative concentration of isomers

To examine the relative concentrations of isomers I, II, and III in saturated vapors over cesium bromide or iodide, thermodynamic calculations were performed. We considered the isomerization reactions I → II and I → III. The relative concentrations x_i of the two isomers in equilibrium vapor was calculated using Eq. (2.5). Similarly, the enthalpies of the isomerization reactions $\Delta_r H°(0)$ were evaluated using isomerization energies ΔE_{iso} and the ZPVE corrections $\Delta\varepsilon$ by use of Eqs. (2.1) and (2.2); the energies ΔE_{iso} were calculated by MP4 method. The values of $\Delta_r \Phi°(T)$ and other thermodynamic functions were calculated in the rigid rotator-harmonic oscillator approximation using the optimized coordinates and vibrational frequencies obtained in

the MP2 calculations as the input parameters. The values of reduced Gibbs free energy and other thermodynamic functions are reported in the Appendix 3. The thermodynamic functions and the relative concentration of the isomers were computed for the temperature range between 700 K and 1600 K related to the experimental condition. The results of calculations of energies and enthalpies of the isomerization reactions $\Delta_r H°(0)$, ZPVE corrections $\Delta\varepsilon$, change in the reduced Gibbs free energies $\Delta_r\Phi°(T)$, and relative concentration $x_i = p_i / p_I$ the isomers are reported in Table 26 for T = 800 K.

Table 26: The energies ΔE_{iso} and enthalpies $\Delta_r H^0(0)$ of the isomerization reactions, change in the reduced Gibbs free energies $\Delta_r\Phi°(T)$, ZPVE corrections $\Delta\varepsilon$, and relative abundances $x_i = p_i/p_I$ (i = II or III) of the isomers (T = 800 K).

Isomerization reaction	ΔE_{iso} (MP4), kJ·mol^{-1}	$\Delta\varepsilon$, kJ·mol^{-1}	$\Delta_r H°(0)$, kJ·mol^{-1}	$\Delta_r\Phi°(T)$, J·mol^{-1}·K^{-1}	$x_i = p_i/p_I$
$Cs_3Br_2^+$ (I) = $Cs_3Br_2^+$ (II)	–5.4	0.32	–5.1	–17.4	0.27
$Cs_3Br_2^+$ (I) = $Cs_3Br_2^+$ (III)	–21.6	0.96	–20.6	–54.8	0.03
$Cs_2Br_3^-$ (I) = $Cs_2Br_3^-$ (II)	–9.2	0.60	–8.6	–43.2	0.02
$Cs_2Br_3^-$ (I) = $Cs_2Br_3^-$ (III)	–33.2	1.21	–32.0	–83.4	0.005
$Cs_3I_2^+$ (I) = $Cs_3I_2^+$ (II)	–5.8	0.32	–5.4	–14.5	0.40
$Cs_3I_2^+$ (I) = $Cs_3I_2^+$ (III)	–27.7	0.74	–26.9	–52.1	0.11
$Cs_2I_3^-$ (I) = $Cs_2I_3^-$ (II)	–7.0	0.39	–6.6	–17.0	0.35
$Cs_2I_3^-$ (I) = $Cs_2I_3^-$ (III)	–28.5	0.82	–27.7	–54.8	0.09

For each isomerization reaction considered the value of $\Delta_r H°(0)$ is negative which means that the isomer in the right hand side of the reactions is more favorable by energy regarding the isomer I. Compared to the results found by the MP2 method the magnitudes of $\Delta_r H°(0)$ by MP4 level are less and are in the range ~20–30 kJ·mol^{-1} for the bipyramidal isomer and ~5–8 kJ·mol^{-1} for cyclic isomer.

The value of x_i represents which isomer out of two is prevailing in the saturated vapor. One can see that $x_i < 1$ for all of the isomerization reactions that implies the isomer I is prevailing compared to the cyclic or bipyramidal. It is important to note here that for the ions $Cs_3Br_2^+$, $Cs_3I_2^+$, and $Cs_2I_3^-$ the isomers I and II are found in comparable amount, but the bipyramidal one

is not abundant. For the ion $Cs_2Br_3^-$ the linear isomer is the most abundant compared with two others and actually only this one among the three exists.

The temperature dependence of the relative concentration x_i has been examined for the temperature range between 700 and 1600 K (Fig. 20). As is seen all relative concentrations of the isomers decrease with temperature increase. For the ion $Cs_3Br_2^+$ at 800 K, the concentration of cyclic isomer is 27% and decreases slowly to about 18% at 1500 K (Fig. 20 a). The concentrations of bipyramidal $Cs_3Br_2^+$ is 3% at 800 K and decreases to 0.7% at 1500 K. For the negative ion $Cs_2Br_3^-$ the concentrations of both cyclic and bipyramidal are very low and decrease further with temperature rise (Fig. 20 b). For the ions $Cs_3I_2^+$ and $Cs_2I_3^-$, a very close appearance of the plots is observed in Figs 20 c, d. There is rather big amount of both cyclic and bipyramidal isomers at temperatures around 700–800 K, and then the relative concentrations are dropping down rapidly when the temperature rises still remaining essential for the cyclic species.

As the three isomers may occur in a comparable amount, the fraction w_i of each isomer out of three was found as well using the following equation:

$$w_i = \frac{p_i}{p_{\mathrm{I}} + p_{\mathrm{II}} + p_{\mathrm{III}}}, \tag{4.1}$$

where p_i (i = I, II, or III) represents the concentration of the isomer of interest. The fraction w_i was expressed through the ratio $x_i = p_i/p_{\mathrm{I}}$ mentioned above:

$$w_i = \frac{x_i}{1 + x_{\mathrm{II}} + x_{\mathrm{III}}}. \tag{4.2}$$

The values of w_i at 800 K were found to be as follows: for $Cs_3Br_2^+$ are 0.77, 0.21 and 0.02; $Cs_3I_2^+$ are 0.66, 0.27 and 0.07 and $Cs_2I_3^-$ are 0.70, 0.24 and 0.06 that is of linear, cyclic and bipyramid isomers, respectively. From these values, we can notice that the isomer I dominates for all ions, while the cyclic is less abundant but still significant in its amount, and the fraction of the bipyramidal does not exceed 10%. Fig. 21 elucidates the influence of temperature on the fraction of isomers w_i. As it is seen raise in temperature increases the amount of linear isomer and decreases slowly that of cyclic isomers. For the bipyramid the fraction decreases rapidly as

temperature elevates. Thus for all ions with temperature increase, the cyclic and bipyramidal isomers are decreasing in their content whereas isomer I is increasing and being predominant.

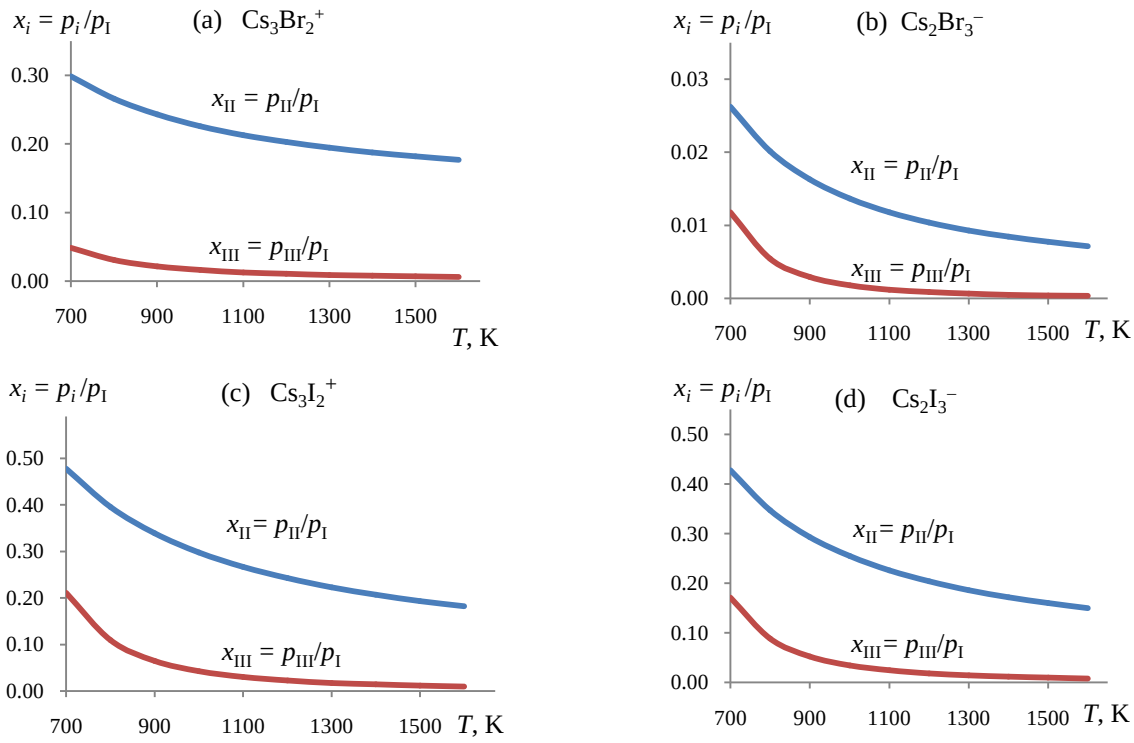

Figure 20: Temperature dependence of the relative amount of pentaatomic ions isomers $x_i = p_i/p_I$ where i = II or III: (a) $Cs_3Br_2^+$; (b) $Cs_2Br_3^-$; (c) $Cs_3I_2^+$; (d) $Cs_2I_3^-$.

Concluding this section it is worth to emphasize the importance of the entropy factor on the relative content of the isomers. The effect of entropy and consequently in reduced Gibbs energy is appeared to be essential and prevailing over the energetic factor. In spite of the higher energetic stability of isomers II and III their relative amount is lower than of the isomer I. It is distinctly seen particularly for the bipyramidal isomer as its energy is lower by ~30 kJ·mol^{-1} than that of the isomer I but its relative concentration is very small in saturated vapor at elevated temperatures. Therefore the considerable decrease in entropy of the isomerization reactions prevails over the energy factor and result in the predominance of the isomers I.

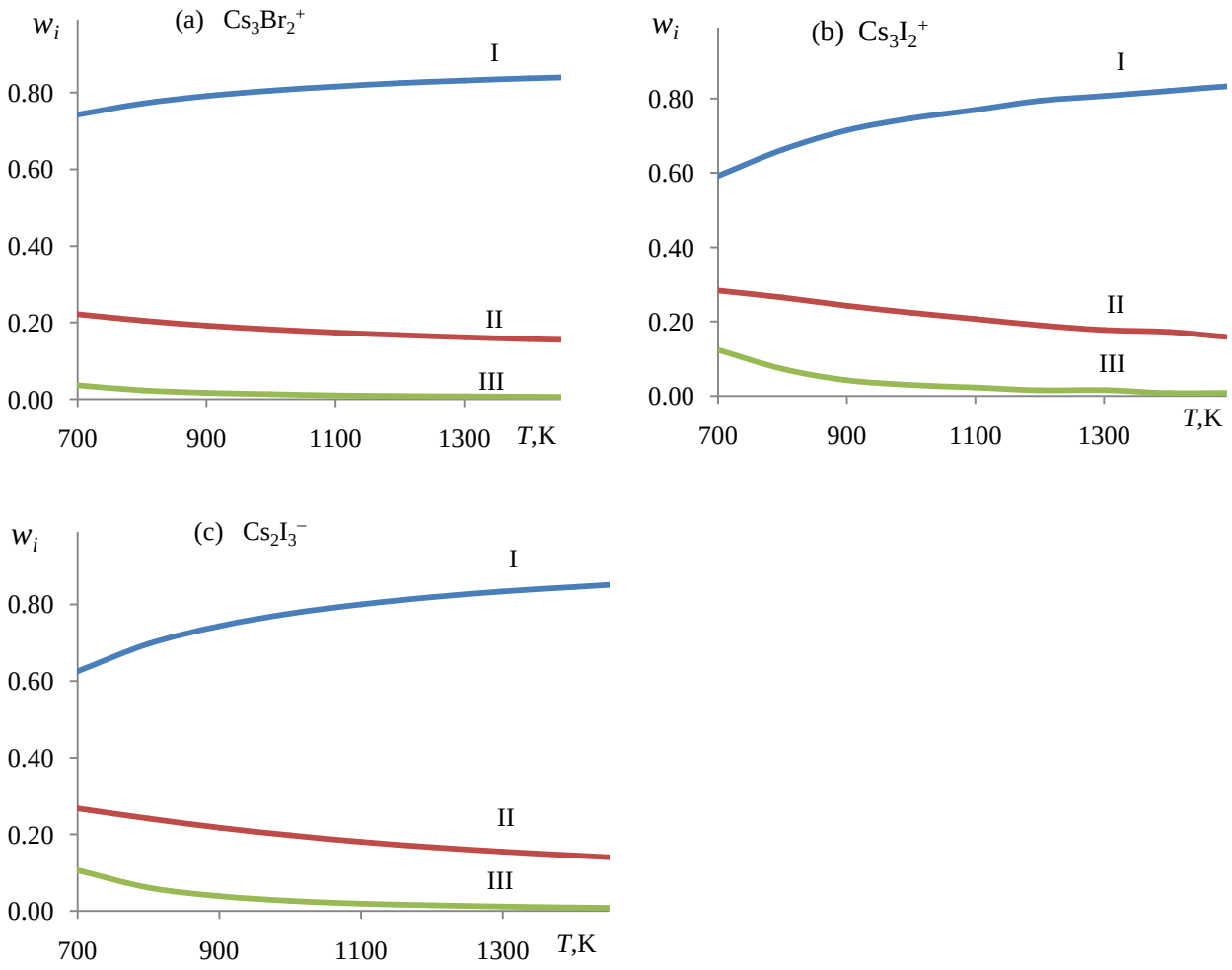

Figure 21: The fractions w_i (i = I, II or III) of isomers *versus* temperature: (a) $Cs_3Br_2^+$; (b) $Cs_3I_2^+$; (c) $Cs_2I_3^-$.

4.3.4 The enthalpies of dissociation reactions and enthalpies of formation of ions

In this section, we have examined the dissociation reactions of the cluster ions with elimination of CsX molecules. The energies of reactions $\Delta_r E$ have been calculated at different theoretical levels, B3LYP5, MP2, MP2C, MP4, MP4C, where in MP2C and MP4C the BSSE correction have been taken into account. The results are presented in Fig. 22. One can see the similar trend in values of $\Delta_r E$ with an enhancement of the theoretical level from B3LYP5 to MP4C *i.e.* the lowest values come from the B3LYP5 method, the highest ones from MP2 following by the further decreasing to the MP4C level. This trend is common either of tri- and pentaatomic ions.

Also the distinct similarity may be observed for the same isomers of pentaatomic ions that is a slight oscillation of $\Delta_r E$ from MP2 to MP4C for isomer I and almost monotonic decrease for both cyclic and bipyramidal isomers. From these results the true value of $\Delta_r E$ comes when approaching the limit that we suppose is close to the MP4C result. The latter appeared to be an intermediate between B3LYP5 and MP2 results. Regarding a certain pentaatomic ion, the change in $\Delta_r E$ is not the same for different isomers that is the change in $\Delta_r E$ from MP2 to MP4C is about 10 kJ·mol^{-1} for the isomers I or II, while that is ~20 kJ·mol^{-1} for the isomers III.

This results in a small decrease of the isomerization energies from MP2 to MP4 and further to MP4C. The BSSE correction itself looks slightly different for three isomers of the same ion; that contributes to the error of computational scheme (Solomonik *et al.*, 2005) and hence to the uncertainties of the theoretical values of the enthalpies of the dissociation reactions accepted here.

The values of $\Delta_r E$ obtained using the MP4C level were taken for calculation of the enthalpies of the reactions $\Delta_r H°(0)$ by Eq. (2.1). The results on $\Delta_r E$, $\Delta_r H°(0)$, ZPVE, and $\Delta_f H°(0)$ are listed in Table 27. The reference thermodynamic data required for the calculations of the enthalpies of formation $\Delta_f H°(0)$ of the cluster ions were retrieved from (Gurvich *et al.*, 2000). The uncertainties of the theoretical values were estimated on the base of the results for the dimer molecules Cs_2X_2 (section 4.3.1).

Regarding the positive and negative triatomic ions with the same halogen, Cs_2Br^+ and $CsBr_2^-$ or Cs_2I^+ and CsI_2^-, have nearly equal enthalpies of reaction respectively, while for the ions with different halogens the values for bromides are higher by 7–10 kJ·mol^{-1} than for iodides. For all ions, the decrease in enthalpies of dissociation is observed from tri- to pentaatomic ions, so triatomic ions are apparently more stable against decomposition than pentaatomic ions.

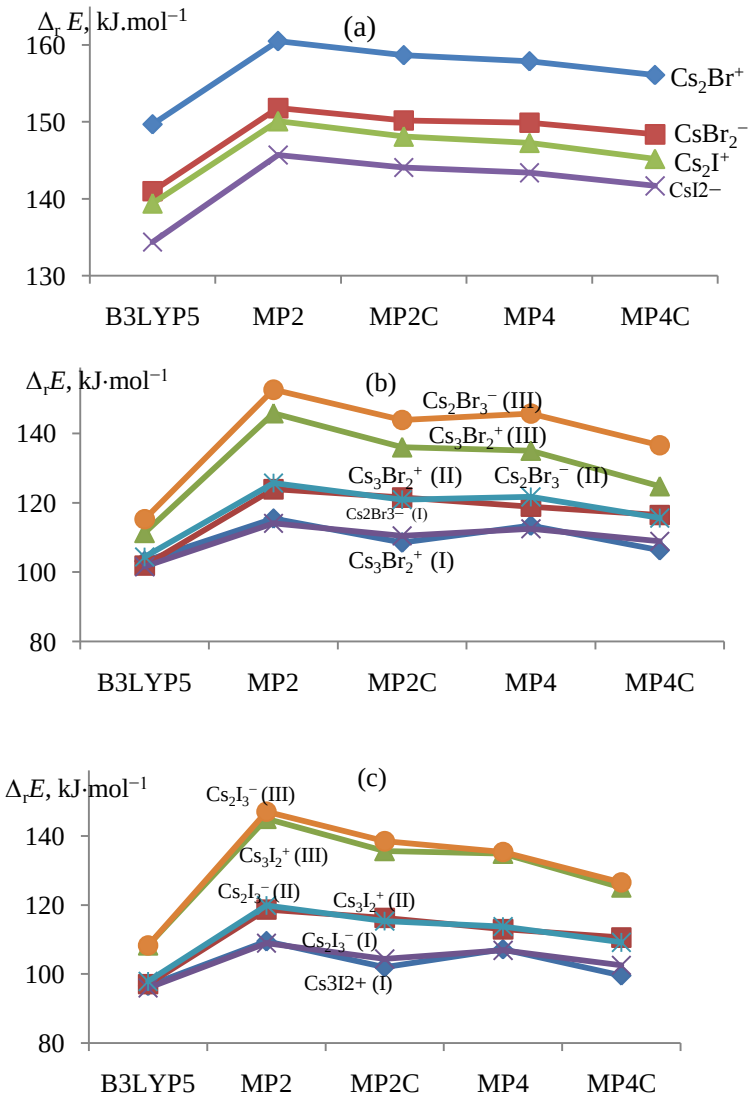

Figure 22: The energies of dissociation reactions of the ions *versus* the level of calculation: (a) triatomic ions; (b) $Cs_3Br_2^+$ and $Cs_2Br_3^-$; (c) $Cs_3I_2^+$ and $Cs_2I_3^-$.

For the pentaatomic ions the dissociation reactions are considered for each of three isomers. Comparing the isomers of the same shape for the positive and negative ions with the same halogen, one can see that the enthalpies are very close to each other, e.g. for $Cs_3Br_2^+$ (I) and $Cs_2Br_3^-$ (I), $\Delta_r H°(0)$ = 106 and 108 kJ·mol^{-1}, respectively or for $Cs_3I_2^+$ (III) and $Cs_2I_3^-$ (III), $\Delta_r H°(0)$ = 124 and 125 kJ·mol^{-1}, respectively. The bigger difference is observed for the bipyramidal isomers of $Cs_3Br_2^+$ and $Cs_2Br_3^-$, 123 and 135 kJ·mol^{-1} which is probably due to the

smaller size of Br than Cs atom and hence the bipyramidal $Cs_2Br_3^-$ ion with three Br atoms in the base has higher stability compared to $Cs_3Br_2^+$ with three Cs atoms in the base.

Comparing the bromides and corresponding iodides with the same shape and charge one can observe the higher values for bromides by 6–10 kJ·mol^{-1}, e.g. for $Cs_3Br_2^+$ (I) and for $Cs_3I_2^+$ (I), $\Delta_r H°(0)$ = 106 and 99 kJ·mol^{-1}, respectively or for $Cs_3Br_2^+$ (III) and $Cs_3I_2^+$ (III), $\Delta_r H°(0)$ = 135 and 125 kJ·mol^{-1}, respectively. The only one exclusion is observed for the enthalpies of dissociation of the bipyramidal ions $Cs_3Br_2^+$ and $Cs_3I_2^+$; 123 and 124 kJ·mol^{-1}, as no decrease from bromide to iodide is there. This result may be explained by a steric factor, the similar size of Cs and I atoms favors the $Cs_3I_2^+$ bipyramid compared to $Cs_3Br_2^+$ built of atoms of rather different size.

It is worth to remind here about the increase of stability of the isomers in the rank I–II–III; the enthalpy of dissociation of the isomer I is less by 6–11 kJ·mol^{-1} than of isomer II and 17–27 kJ·mol^{-1} compared to isomer III. The reason is that the isomers with compact shape are more stable against dissociation.

The experimental data are available in (Sidorova *et al.*, 1979) for ions existing in vapor over cesium iodide where the ion molecular reactions were investigated by mass spectrometric method and the equilibrium constants k_p° for the heterophase reactions involving the tri- and pentaatomic cluster ions were measured. Using these constants we have computed the values of $\Delta_r H°(0)$ by Eq. (3.1).

As an example, an ion molecular reaction for the positive triatomic ion may be expressed as follows:

$$Cs_2I^+ \rightarrow [CsI] + Cs^+, \tag{4.3}$$

where [CsI] corresponds to condensed phase. The equilibrium constant for this reaction is

$$k_p^\circ = \frac{p(Cs^+)}{p(Cs_2I^+)} = \frac{I(Cs^+)}{I(Cs_2I^+)}\sqrt{\frac{m(Cs^+)}{m(Cs_2I^+)}}, \tag{4.4}$$

where *I* and *m* are ion currents and molecular mass of the ions, respectively. The thermodynamic functions of the ions Cs^+ and I^-, and [CsI] were taken from (Gurvich *et al.*, 2000). The enthalpies

of heterophase reactions were converted into enthalpies of gas phase reactions using the enthalpies of sublimation of CsI from (Gurvich *et al.*, 2000). The geometrical parameters and vibrational frequencies of the ions Cs_2I^+, CsI_2^-, $Cs_3I_2^+$, and $Cs_2I_3^-$ needed for the calculation of the thermodynamic functions were taken from our MP2 results.

Table 27: **The dissociation reactions of the ions, energies $\Delta_r E$, enthalpies $\Delta_r H°(0)$, and ZPVE corrections $\Delta\varepsilon$ of the reactions, and enthalpies of formation $\Delta_f H^o(0)$ of the ions; all values are in kJ·mol^{-1}.**

				$\Delta_r H°(0)$		$\Delta_f H°(0)$	
No	**Reaction**	$\Delta_r E$	$\Delta\varepsilon$	**Theoretical**	**Based on expt[a]**	**Theoretical**	**Based on expt[a]**
1	$Cs_2Br^+ = CsBr + Cs^+$	156.1	–0.66	155 ± 5		101 ± 5	
2	$CsBr_2^- = CsBr + CsBr_2^-$	148.4	–0.50	148 ± 5		–552 ± 5	
3	$Cs_2I^+ = CsI + Cs^+$	145.2	–0.58	145 ± 10	150 ± 5	160 ± 10	155 ± 5
4	$CsI_2^- = CsI + I^-$	141.7	–0.46	141 ± 10	146 ± 5	–478 ± 10	–483 ± 5
5	$Cs_3Br_2^+$ (I)$= CsBr + Cs_2Br^+$	106.3	–0.65	106 ± 10		–202 ± 10	
6	$Cs_3Br_2^+$ (II)$= CsBr + Cs_2Br^+$	116.5	–0.96	116 ± 10		–212 ± 10	
7	$Cs_3Br_2^+$ (III)$= CsBr + Cs_2Br^+$	124.8	–1.60	123 ± 10		–219 ± 10	
8	$Cs_2Br_3^-$ (I)$= CsBr + CsBr_2^-$	108.9	–0.47	108 ± 10		–858 ± 10	
9	$Cs_2Br_3^-$ (II)$= CsBr + CsBr_2^-$	115.6	–0.47	115 ± 10		–864 ± 10	
10	$Cs_2Br_3^-$ (III)$= CsBr + CsBr_2^-$	136.6	–1.67	135 ± 10		–884 ± 10	
11	$Cs_3I_2^+$ (I) $= CsI + Cs_2I^+$	99.6	–0.47	99 ± 15	108 ± 12	–88 ± 15	–102 ± 12
12	$Cs_3I_2^+$ (II) $= CsI + Cs_2I^+$	110.6	–0.79	110 ± 15	114 ± 12	–99 ± 15	–108 ± 12
13	$Cs_3I_2^+$ (III) $= CsI + Cs_2I^+$	125.1	–1.21	124 ± 15	135 ± 12	–113 ± 15	–129 ± 12
14	$Cs_2I_3^-$ (I) $= CsI + CsI_2^-$	102.6	–0.48	102 ± 15	114 ± 12	–729 ± 15	–746 ± 12
15	$Cs_2I_3^-$ (II) $= CsI + CsI_2^-$	109.2	–0.87	108 ± 15	118 ± 12	–735 ± 15	–750 ± 12
16	$Cs_2I_3^-$ (III) $= CsI + CsI_2^-$	126.6	–1.30	125 ± 15	138 ± 12	–757 ± 15	–770 ± 12

[a]The values $\Delta_r H°(0)$ "based on experiment" were determined by us on the base of the equilibrium constants from [24] and our thermodynamic functions. The uncertainties for the triatomic ions were taken from (Sidorova *et al.*, 1979) and for pentaatomic estimated by us. In the original work by Sidorova *et al*.,(1979), the enthalpies of the dissociation reactions (3) and (4) were 151.0 ± 5.4 and 151.4 ± 5.4 kJ·mol^{-1}, respectively. These values were found on the basis of the experimental equilibrium constants and estimated geometrical parameters and vibrational frequencies of the ions.

The enthalpies of dissociation calculated through experimental data (Sidorova *et al.*, 1979) are denoted as "based on experiment" hereafter and given in Table 27. As regards the pentaatomic ions, the existence of isomers had not been considered by Sidorova *et al*. (1979). In this work, as we have found the isomers may exist at a comparable amount, the fractions of the isomers, w_i (*i*

= I, II, or III), are taken into account, that is the measured current is multiplied be the fraction, e.g. the ion current for isomer I is $I(Cs_3I_2^+, I) = I(Cs_2I_3^+)w_I$. The values of the ion currents obtained by this way have been used to calculate the equilibrium constant for each isomer and then the enthalpies of reactions $\Delta_r H°(0)$ "based on experiment". It is worth to note that for the pentaatomic ions only a few values of currents had been measured and no statistical treatment was done in (Sidorova *et al.*, 1979).

4.4 Conclusions

The DFT (B3LYP5) and MP2 methods have been used to calculate geometrical parameters and vibrational frequencies of different cluster ions Cs_2X^+, $Cs_3X_2^+$, CsX_2^-, and $Cs_2X_3^-$ (X = Br or I) existing in saturated vapors over cesium bromide and iodide. The results obtained by DFT and MP2 methods do not contradict each other and literature data as well. Nevertheless the MP2 method yields preferable results.

For the pentaatomic ions $Cs_3X_2^+$ and $Cs_2X_3^-$ different isomers of linear, planar cyclic, bipyramidal, and V-shaped were proved to exist in considerable fractions. The properties of the species with the similar structure look alike for positive and negative ions both in vibrational spectra and energetic stability. In spite of the highest energetic stability of the bipyramidal isomer its relative concentration is appeared to be small in saturated vapors at elevated temperatures.

Regarding the enthalpies of dissociation reactions of the dimer molecules and ions, $\Delta_r H°(0)$, the DFT (B3LYP5 and B3P86) methods bring rather underrated values compared with experimental data available. The higher level of calculations MP4C allowed us to approach more reliable results and come to better agreement with the literature data. Still as concerns cesium iodide species — the dimer molecule and ions — detailed analysis of the theoretical and experimental data shows that the experimental values of $\Delta_r H°(0)$ seem to be somehow overrated and it would be desirable to refine them applying advanced experimental techniques.

CHAPTER FIVE

Molecular Clusters Cs_3X_3 and Cs_4X_4 (X = Br, I): Quantum Chemical Study of Structure and Thermodynamic Properties[4]

Abstract: The properties of trimer Cs_3X_3 and tetramer Cs_4X_4 (X = Br, I) molecules have been studied using DFT with B3LYP5 functional and MP2 and MP4 methods. Two equilibrium geometrical structures of trimers, hexagonal (D_{3h}) and 'butterfly-shaped' (C_s), and one for tetramers, distorted cubic (T_d), are confirmed to exist; geometrical parameters and vibrational spectra are determined. The relative concentration of Cs_3X_3 isomers has been evaluated; the butterfly-shaped isomer dominates over hexagonal in saturated vapor in a broad temperature range. The dissociation reactions through different channels have been considered and enthalpies of formation $\Delta_f H°(0)$ of clusters determined: -858 ± 20 kJ·mol^{-1} (Cs_3Br_3), -698 ± 20 kJ·mol^{-1} (Cs_3I_3), -1270 ± 30 kJ·mol^{-1} (Cs_4Br_4) and -1045 ± 30 kJ·mol^{-1} (Cs_4I_4). The Gibbs free energies $\Delta_r G°(T)$ calculated for the dissociation reactions of trimer and tetramer molecules have indicated that these molecules are resistive in narrow temperature range only and decompose spontaneously with temperature increase with elimination of dimer molecules.

5.1 Introduction

The study of alkali halide clusters, ionic and molecular, has been the subject of research over past five decades. This involves both experimental (Butman *et al.*, 2000; Chupka, 1959; Dunaev *et al.*, 2013; Gusarov, 1986; Pogrebnoi *et al.*, 2000; Sidorova *et al.*, 1979; Snelson, 1967) and theoretical (Cohen *et al.*, 1975; Bloomfield *et al.*, 1991; Rupp *et al.*, 1977; Weis *et al.*, 1992; Welch *et al.*, 1976) studies. Most experimental studies have dealt with the identification of cluster species existing in saturated vapor and measurement of equilibrium constants of ion molecular reactions. On the other hand theoretical studies are concern mainly prediction of equilibrium configurations, geometrical parameters, binding energies, and vibrational frequencies. These clusters are of interest because they have unique electronic, optical and magnetic properties which make them to be useful in different applications. For example, cesium chloride thin films were used in fabrication of electronic devices through ion implantation techniques (Lee *et al.*, 2010; Liao *et al.*, 2011; Liu *et al.*, 2013a; Liu *et al.*, 2012; Zhang *et al.*,

[4] Stanley F. Mwanga, Tatiana P. Pogrebnaya and Alexander M. Pogrebnoi, Molecular Clusters Cs_3X_3 and Cs_4X_4 (X = Br, I): Quantum Chemical Study of Structure and Thermodynamic Properties, Revised manuscript submitted to Cogent Chemistry (Taylor & Francis)

2014; Zhang *et al.*, 2012). Cluster ions have been proved to be useful in ionic thrusters (Benson *et al.*, 2009) and magneto-hydrodynamic generators (Kay, 2011a). Besides, cesium and iodine exist among the fission products that may be released in nuclear power plants (Badawi *et al.*, 2012; Lennart *et al.*, 1994; Povinec *et al.*, 2013; Roki *et al.*, 2014; Roki *et al.*, 2013); these byproducts are highly radioactive materials. Thus, evaluations of thermodynamic properties of gaseous species are essential for safety features of a nuclear pressurized reactor. The thermodynamic functions of gaseous species are usually derived by statistical thermodynamics from the geometrical parameters and vibrational frequencies.

Recently, we have theoretically investigated the properties of molecular and ionic clusters of cesium fluoride (Chapter two), cesium chloride (Hishamunda *et al.*, 2012; Pogrebnaya *et al.*, 2012), and cesium bromide and iodide (Chapter four). In these works, the equilibrium geometrical structure, vibrational spectra and thermodynamic properties of the clusters were determined. The dimers and trimers of cesium bromine and iodine have been studied theoretically and experimentally by Groen and Kovács (Groen *et al.*, 2010). Molecular clusters of lithium iodide have been found to exist in vapor over solid lithium iodide (Bencze *et al.*, 1998). However, tetramers of cesium bromide and iodine have not yet studied. We also, anticipate that isomeric forms would exist for trimers of cesium bromine and iodine as it was revealed for cesium fluoride and chloride (Chapter two and three). In this work we present quantum chemical investigation of the properties of trimer Cs_3X_3 and tetramer Cs_4X_4 (X = Br, I) molecules.

5.2 Computational details

Quantum chemical calculations are performed as detailed in sections 2.2, 3.2 and 4.2. We expect that including the diffused functions into valence basis sets of halogen atoms, Br and I, will improve an accuracy of the calculated thermochemical properties of the species as it based on results by (Martin *et al.*, 2001) and our experience as well (Chapter two). The geometry of the species was optimized by B3LYP5 and MP2 methods. A vibrational analysis was performed at the same level of calculations to examine whether the obtained structures correspond to a real minimum energy by the absence of the imaginary frequencies. The visualization of geometrical structure and vibrational spectra the software have been used: MacMolPlt (Bode *et al.*, 1998) and

Chemcraft (Zhurko, and Zhurko, 2014). The enthalpies of the chemical reactions $\Delta_r H°(0)$ were calculated on the basis of energies $\Delta_r E$, and the zero-point vibration energy (ZPVE) correction $\Delta\varepsilon$ as given in Eq. (2.1) and (2.2). This approach is similar to that applied by Curtiss *et al.* (2000). The dissociation energies $\Delta_r E$ of the species were obtained as explained in previous section 2.2. In the DFT calculations, BSSE correction was not considered. According to Liu *et al* (2013b) as well as our findings (Chapter two), the DFT methods are not mush sensitive to the BSSE correction and the latter does not improve the DFT results on energies and enthalpies of dissociation reactions.

5.3 Results and discussions

5.3.1 Trimer Cs_3Br_3 and Cs_3I_3 molecules

For trimer Cs_3X_3 molecules, two equilibrium structures were confirmed to have minima at the potential energy surface (PES): hexagonal planar (D_{3h}) and butterfly-shaped (C_s) (Figs. 23 a, b). The geometrical parameters and vibrational spectra of these structures are compiled in Tables 28, 29. As expected, there is a progressive increase of internuclear separation from bromide to iodide. Regarding the energy, butterfly-shaped isomer possesses lower energy by ~14 kJ·mol^{-1} (Cs_3Br_3) and ~15 kJ·mol^{-1} (Cs_3I_3) than hexagonal (MP2). Thus, butterfly-shaped structure is more energetically stable than hexagonal. Similar isomeric forms were confirmed to exist for Cs_3F_3 and Cs_3Cl_3 as it is described in Chapters two and three. We have evaluated the energy barrier in the path from the C_s ('butterfly') to D_{3h} (hexahonal) configuration. In the molecule within C_s symmetry, the separation between two opposite atoms, Cs_2–X_2 (Fig. 28b), was a variable parameter (transition reaction coordinate). This parameter was varied with a step of 0.5 Å from the distance in the C_s structure up to that in the hexagonal one. All other atom coordinates were optimized at each step. It was revealed that the barrier for the transition was ~6 kJ·mol^{-1} both for Cs_3Br_3 and Cs_3I_3 (DFT/B3LYP5). Heat energy of the molecules at ~350 K is ~3 kJ·mol^{-1}, which is twice less compared to the barrier. The barrier also is much higher regarding vibrational energy quantum, that is ~1 kJ·mol^{-1}.

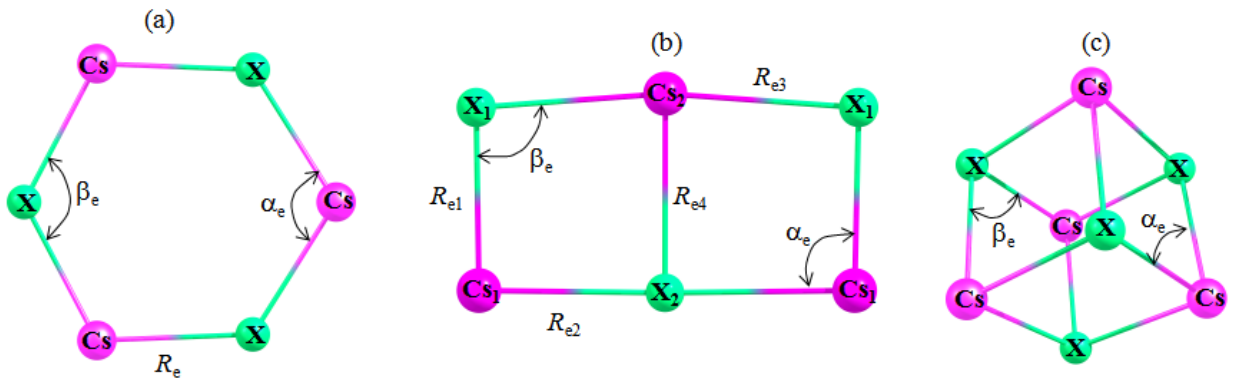

Figure 23: Geometrical structures of the trimers Cs_3X_3 and tetramer Cs_4X_4 (X = Br, I) molecules: (a) Cs_3X_3, planar hexagonal D_{3h}; (b) Cs_3X_3, butterfly-shaped C_s; (c) Cs_4X_4, distorted cube T_d.

The vibrational frequencies determined by B3LYP5 and MP2 methods are given in Tables 28, 29. In most cases a good agreement is observed between the corresponding frequencies found by two methods. Based on our previous experience (Chapter two, three and four) we consider that MP2 results to be more applicable for further consideration and calculation of the thermodynamic functions of the species. The decrease of the corresponding values of ω_i is observed from bromide to iodide. Several low frequencies of ~30 cm^{-1} and less are found in spectra of both isomers of Cs_3X_3: there are ω_3, ω_4, ω_7, ω_8; for hexagonal isomer and, ω_5, ω_6, ω_7, ω_{11}, ω_{12}, for C_s isomer. The assignments of vibrational frequencies for Cs_3X_3 are presented in Figs. 24 and 25 As for hexagonal planar Cs_3X_3, both species have few modes active in IR spectra, Cs−X stretching being of the highest intensity. The bands of medium intensity are wagging X−Cs−X modes with low frequencies, 26 cm^{-1} (Cs_3Br_3) and 23 cm^{-1} (Cs_3I_3). The bands of weak intensity are related to rocking Cs−X−Cs vibrations with low vibration frequency of 12 cm^{-1}. Our computed vibrational spectra for Cs_3X_3 (D_{3h}) can be compared with experimental data in (Groen *et al.*, 2010) where FT-IR spectra of $(CsBr)_n$ and $(CsI)_n$ (n= 1–3) had been measured using matrix isolation technique. For the trimers, the vibrational mode, 110.2 cm^{-1} in Kr and 103.1 cm^{-1} in Xe matrix for Cs_3Br_3 and 86.6 cm^{-1} in Xe for Cs_3I_3 had been recorded. Therefore our values, 118 cm^{-1} (Cs_3Br_3) and 91 cm^{-1} (Cs_3I_3), agree well with the experimental frequencies. Worth to note also that our results for the trimer molecules are in a good agreement with theoretical data (Groen *et al.*, 2010).

For butterfly-shaped isomers the majority of vibrational modes are active in IR spectra although most of them have weak intensity. The bands of highest intensity correspond to Cs−X stretching vibrations; the most intensive bands are observed at 118 cm^{-1} (Cs−Br) and 93 cm^{-1} (Cs−I). Other valence vibrations at 67 cm^{-1} (Cs_3Br_3) and 63 cm^{-1} (Cs_3I_3) possess low intensities. The bending vibrational modes are characterized by weak intensities.

Table 28: Properties of neutral molecules Cs_3X_3 (hexagonal D_{3h}), X = Br, I.

Property	Cs_3Br_3 (D_{3h})		Cs_3I_3 (D_{3h})	
	B3LYP5	**MP2**	**B3LYP5 B2**	**MP2**
R_e(Cs−X)	3.377	3.348	3.626	3.589
α_e(X−Cs−X)	119.3	117.9	123.2	121.8
β_e(Cs−X−Cs)	120.7	122.1	116.8	118.2
$-E$	100.84946	100.43294	94.95303	94.49097
ω_1 (A_1')	103 (0)	114 (0)	86 (0)	91 (0)
ω_2 (A_1')	68 (0)	86 (0)	58 (0)	59 (0)
ω_3 (A_1')	33 (0)	43 (0)	28 (0)	28 (0)
ω_4 (A_2'')	26 (0.61)	26 (0.63)	22 (0.44)	23 (0.46)
ω_5 (E')	110 (1.22)	118 (1.1)	88 (0.97)	91 (0.95)
ω_6 (E')	85 (0.28)	91 (0.06)	71 (0.01)	73 (0.00)
ω_7 (E')	19 (0.24)	12 (0.22)	12 (0.09)	12 (0.08)
ω_8 (E'')	12 (0)	12 (0)	11 (0)	11 (0)
q(Cs)	0.834	0.881	0.800	0.860
q(X)	–0.834	–0.881	–0.800	–0.860

Note: Here and hereafter R_e(Cs–X) is the equilibrium internuclear distance, Å; α_e(X-Cs-X) and β_e(Cs-X-Cs) is valence angles, degs; E is the total electron energy, au; ω_i are vibrational frequencies, cm^{-1}; the values given in parentheses near the frequencies are IR intensities, $D^2 \cdot amu^{-1} \cdot Å^{-2}$.

To consider the electron density distribution, we have calculated the Mullikan atomic charges q by both methods, DFT and MP2 (Tables 28 and 29). One can see the high ionicity of the species as the charges on atoms are about 0.8-0.9 au. For both isomers of Cs_3Br_3 and Cs_3I_3, the MP2 method demonstrates higher ionicity as the charge magnitudes are bigger by 0.03-0.07 au than the corresponding values of q obtained by DFT. It is worth to mention here the dipole moments μ_e as they relate to the electron density distribution (Table 29). The values of μ_e also demonstrate

that the DFT method underrates the ionic character of bonds as μ_e(DFT) < μ_e(MP2). It is evident that this correlation holds due to charges relationship, q(DFT) < q(MP2). If compare two isomers, in the hexagonal one of Cs_3X_3 the absolute values of charges on X and Cs atoms are equal which follows from the high symmetry of the structure. In the isomers of C_s configuration, the electron density distribution is not uniform: according to MP2 results, the side cesium atoms, Cs_1, have slightly smaller charges (by 0.01 au) than the middle Cs_2 atom, while the side halogen atoms X_1 have bigger charge magnitudes (by ~0.02 au) compared to the middle one X_2, that holds for both Cs_3Br_3 and Cs_3I_3 clusters. Ionicity slightly decreases, by 0.01-0.02 au, from the hexagonal to 'butterfly' configuration and from bromide to iodide.

The relative concentration p_{II}/p_I of the isomers in the saturated vapor was evaluated using Eq. (2.5). The values of $\Phi°(T)$ and other thermodynamic functions were calculated using OpenThermo software (Tokarev, 2007-2009) within the 'rigid rotator-harmonic oscillator' approximation; the optimized coordinates and vibrational frequencies obtained by MP2 method were used as the input parameters. The values of reduced Gibbs free energy and other thermodynamic functions are reported in the Appendix 4. The enthalpies of the isomerisation reactions $\Delta_r H°(0)$ were calculated on the basis of isomerisation energies ΔE_{iso} using Eqs. (2.1) and (2.2). The isomerisation energies ΔE_{iso}, ZPVEs $\Delta\varepsilon$, enthalpies $\Delta_r H°(0)$ of isomerisation reactions, change in the reduced Gibbs energies $\Delta_r\Phi°(T)$, and the relative abundance p_{II}/p_I of the isomers at T = 1000 K are presented in Table 30. The value of p_{II}/p_I indicates which of the isomers prevails in saturated vapor. For both species, the butterfly-shaped Cs_3X_3 (C_s) dominates over hexagonal-shaped Cs_3X_3 (D_{3h}) isomer, as the ratio p_{II}/p_I is greater than one.

Table 29: Properties of neutral molecules Cs_3X_3 ('butterfly-shaped', C_s), X = Br, I.

Property	Cs_3Br_3 (C_s)		Cs_3I_3 (C_s)	
	B3LYP5	**MP2**	**B3LYP5**	**MP2**
$R_{e1}(Cs_1–X_1)$	3.303	3.264	3.553	3.517
$R_{e2}(Cs_1–X_2)$	3.429	3.374	3.680	3.615
$R_{e3}(Cs_2–X_1)$	3.487	3.431	3.734	3.674
$R_{e4}(Cs_2–X_2)$	3.737	3.606	3.986	3.842
$\alpha_e(X_1–Cs_1–X_2)$	94.0	92.0	96.5	94.3
$\beta_e(Cs_1–X_1–Cs_2)$	93.2	93.7	90.2	90.8
$\chi_e(Cs_1–X_2–Cs_2–X_1)$	169.0	169.8	172.0	173.1
$-E$	100.85067	100.43813	94.95448	94.49674
ΔE_{iso}	-3.19	-13.63	-3.82	-15.15
ω_1 (A')	109 (1.05)	118 (1.01)	85 (1.00)	93 (0.72)
ω_2 (A')	90 (0.34)	101 (0.36)	75 (0.12)	86 (0.08)
ω_3 (A')	62 (0.10)	67 (0.14)	53 (0.06)	59 (0.07)
ω_4 (A')	44 (0.12)	61 (0.12)	39 (0.11)	50 (0.08)
ω_5 (A')	35 (0.03)	37 (0.23)	27 (0.08)	30 (0.08)
ω_6 (A')	29 (0.29)	31 (0.26)	24 (0.24)	26 (0.30)
ω_7 (A')	5 (0.01)	10 (0.01)	6 (0.00)	7 (0.01)
ω_8 (A'')	112 (0.60)	120 (0.75)	89 (0.77)	95 (0.79)
ω_9 (A'')	104 (0.62)	110 (0.41)	88 (0.00)	93 (0.21)
ω_{10} (A'')	79 (0.02)	86 (0.01)	56 (0.02)	63 (0.03)
ω_{11} (A'')	34 (0.10)	36 (0.10)	27 (0.13)	28 (0.08)
ω_{12} (A'')	16 (0.00)	16 (0.00)	13 (0.00)	13 (0.00)
μ_e	9.92	10.45	10.68	11.31
$q(Cs_1)$	0.814	0.868	0.776	0.851
$q(X_1)$	–0.834	–0.882	–0.778	–0.853
$q(Cs_2)$	0.850	0.880	0.776	0.837
$q(X_2)$	–0.811	–0.852	–0.772	–0.833

Note: $\chi_e(Cs_1–X_2–Cs_2–X_1)$-is the dihedral angle, degs; $\Delta E_{iso} = E(Cs_3X_3, C_S) – E(Cs_3X_3, D_{3h})$ is isomerisation energy, $kJ·mol^{–1}$; μ_e is the dipole moment, D.

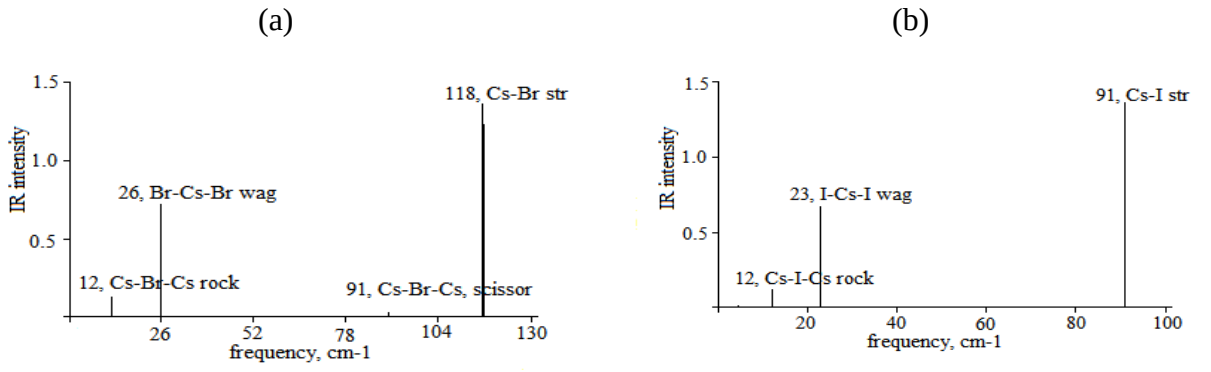

Figure 24: IR spectrum of planar hexagonal isomer Cs_3X_3 (D_{3h}): (a) Cs_3Br_3 and (b) Cs_3I_3.

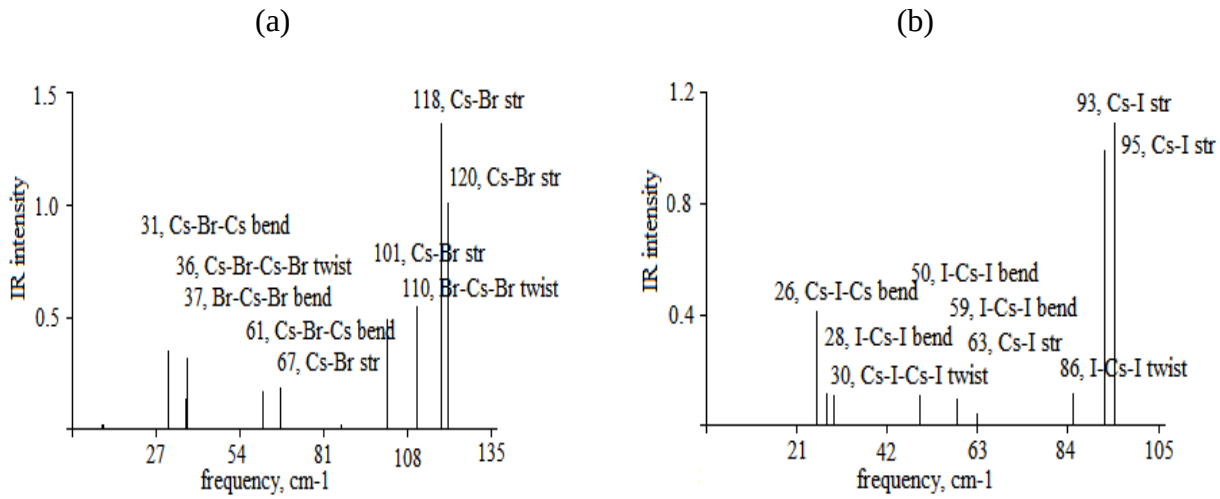

Figure 25: IR spectrum of butterfly-shaped isomer Cs_3X_3 (C_s): (a) Cs_3Br_3 and (b) Cs_3I_3.

The temperature effect on the relative abundance p_{II}/p_I of the isomers is considered for temperature range between 700 K and 1600 K (Fig. 26). As is seen for both species the relative concentration of the butterfly-shaped structure is 3.7 (Cs_3Br_3) and 6.7 (Cs_3I_3) at 700 K and decreases with temperatures rise but still greater than one up to ~1600 K. Thus, the butterfly-shaped structure dominates in vapor in a broad temperature. The relative abundance of isomers is influenced by two factors: the isomerisation energy and entropy $S°$ of species. The lower the ΔE_{iso}, and the bigger $S°$ of the isomer II, give higher ratio of p_{II}/p_I. Thus, the isomer with C_s symmetry dominates being favoured by both of these factors.

Table 30: The energies ΔE_{iso} and enthalpies $\Delta_r H^o(0)$ of the isomerization reactions, change in the reduced Gibbs free energies $\Delta_r\Phi°(T)$, ZPVE corrections $\Delta\varepsilon$, and relative abundances p_{II}/p_I of the isomers (T = 1000 K).

Isomerization reaction	ΔE_{iso}, kJ·mol^{-1}	$\Delta\varepsilon$, kJ·mol^{-1}	$\Delta_r H°(0)$, kJ·mol^{-1}	$\Delta_r\Phi°(T)$, J·mol^{-1}·K^{-1}	p_{II}/p_I
Cs_3Br_3 (D_{3h}) = Cs_3Br_3(C_s)	–13.63	0.35	–13.28	–8.308	1.8
Cs_3I_3 (D_{3h}) = Cs_3I_3(C_s)	–15.15	0.41	–14.74	–5.427	3.1

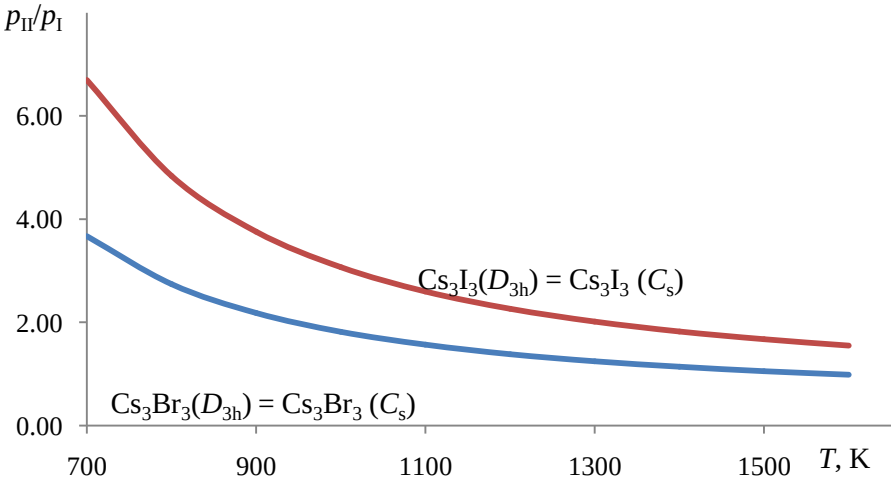

Figure 26: Temperature dependence of the relative concentration of the isomers for trimers Cs_3X_3 (X = Br, I) molecules.

The enthalpies of dissociation reactions $\Delta_r H°(0)$ with the elimination of CsX molecules and enthalpies of formation $\Delta_f H°(0)$ of Cs_3X_3 were calculated for the C_s isomer based on MP4C results. The values of $\Delta_f H°(0)$ for CsX and Cs_2X_2 molecules were taken from (Gurvich *et al.*, 2000). The theoretical values of $\Delta_r H°(0)$ were calculated using Eqs. (2.1) and (2.2).

It is worth to note that the spin-orbit coupling effect may be important for heavy atoms, especially for species with two or more low lying electronic states (Fedorov *et al.*, 2003). In this case the first excited electronic state is far above the ground state, according to the TDDFT

calculations, the first excitation energies are ~4.5 eV (Cs_3Br_3) and ~ 4.1 eV (Cs_3I_3). Therefore the spin-orbit coupling was not taken into account in calculation of thermodynamic properties.

The calculated dissociation energies $\Delta_r E$, ZPVE corrections $\Delta\varepsilon$, enthalpies of the dissociation reactions $\Delta_r H°(0)$, and enthalpies of formation $\Delta_f H°(0)$ of Cs_3X_3 molecules are presented in Table 31. The data determined for Cs_3F_3 (Chapter two) and Cs_3Cl_3 (Chapter three) are included for comparison. Two types of dissociation reactions are considered: (i) with elimination of monomer and dimer and (ii) three monomers. From fluoride to iodide the enthalpies of the dissociation reactions decrease: 129 →121→117→110 kJ·mol^{-1} for the reactions (i), and 301→276→267→253 kJ·mol^{-1} for the reactions (ii). The second type of reactions requires approximately 2.3 times bigger energy than first one due to different number of bonds to be broken. The uncertainties of the $\Delta_r H°(0)$ values may be estimated on the base of the comparison between theoretical and experimental data obtained for Cs_2Br_2, Cs_2I_2, $Cs_3I_2^+$, $Cs_2I_3^-$, and $Cs_4Cl_3^+$ for which the maximum difference between the calculated by MP4C method and experimental data is equal to 16 kJ·mol^{-1}. The enthalpies of formation $\Delta_f H°(0)$ of the trimers found through both types of reactions are close to each other or coincide. The uncertainty was accepted to be ± 20 kJ·mol^{-1}, and the values of $\Delta_f H°(0)$ are as follows: –858 ± 20 kJ·mol^{-1} (Cs_3Br_3) and –698 ± 20 kJ·mol^{-1} (Cs_3I_3).

Table 31: The energies, $\Delta_r E$, ZPVE corrections, $\Delta\varepsilon$, and enthalpies $\Delta_r H°(0)$ of the dissociation reactions, and enthalpies of formation $\Delta_f H°(0)$ of Cs_3X_3 (C_s) (X= F, Cl, Br, I) molecules, all values are in kJ·mol^{-1}.

No	Dissociation reaction	$\Delta_r E$	$-\Delta\varepsilon$	$\Delta_r H°(0)$	$-\Delta_f H°(0)$
1	$Cs_3F_3 = CsF + Cs_2F_2$	130.9	1.57	129	1378
2	$Cs_3F_3 = 3CsF$	304.7	4.22	301	1386
3	$Cs_3Cl_3 = CsCl + Cs_2Cl_2$	121.4	1.16	121	996
4	$Cs_3Cl_3 = 3CsCl$	278.3	2.76	276	996
5	$Cs_3Br_3 = CsBr + Cs_2Br_2$	117.5	0.98	117	858
6	$Cs_3Br_3 = 3CsBr$	268.7	2.14	267	858
7	$Cs_3I_3 = CsI + Cs_2I_2$	111.0	0.93	110	698
8	$Cs_3I_3 = 3CsI$	254.6	1.95	253	698

5.3.2 Tetramers Cs_4Br_4 and Cs_4I_4 molecules

For the tetramers Cs_4X_4 molecules only one equilibrium structure with T_d symmetry was confirmed to exist (Fig. 23 c). This structure is specified by two parameters R_e(Cs–X) and α_e(X–Cs–X). The geometrical parameters and vibrational frequencies of Cs_4X_4 molecules are gathered in Table 32. Similar to trimers, the internuclear separation increases from bromide to iodide, while the corresponding vibrational frequencies decrease as a rule. Due to compactness of the tetramers, there are less low frequencies than for trimers.

The IR spectra of Cs_4X_4 (T_d) are shown in Figs. 27 a, b. As is seen the most of vibration modes are inactive in IR spectra and have zero intensity. The only two modes are active and assigned to X–X wagging and Cs–X–Cs twisting vibrations; the most intensive modes, 85 cm^{-1} (Cs_4Br_4) and 82 cm^{-1} (Cs_4I_4), relate to X–X wagging vibrations, the weaker modes at 95 cm^{-1} (Cs_4Br_4) and 71 cm^{-1} (Cs_4I_4) correspond to Cs–X–Cs twisting vibrations.

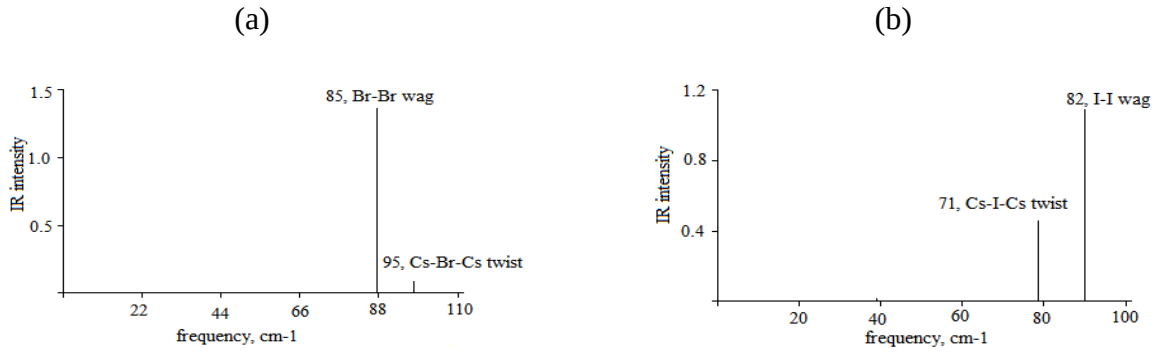

Figure 27: Calculated IR spectra of distorted cube Cs_4X_4 (T_d): (a) Cs_4Br_4 and (b) Cs_4I_4.

The electron density distribution is represented through the Mullikan atomic charges q found by both methods, DFT and MP2 (Table 32). The values of q being about 0.8-0.9 au show a high ionic character of bonds. The observations discussed above for the trimer molecules are valid here as well; the magnitudes of q are higher by MP2 than DFT, the ionicity decreases from bromide to iodide. Compared to the trimer molecules, the charges in tetramers are slightly higher by 0.02-0.03 au.

Table 32: Property of neutral molecule Cs_4X_4 distorted cubic (T_d).

Property	Cs_4Br_4		Cs_4I_4	
	B3LYP5	**MP2**	**B3LYP5**	**MP2**
R_e(Cs−X)	3.512	3.433	3.768	3.678
α_e (X-Cs-X)	90.4	89.6	92.9	91.9
β_e (Cs-X-Cs)	89.6	90.4	87.1	88.0
$-E$	134.50200	133.96752	126.63848	126.04400
ω_1 (A_1)	120 (0)	83 (0)	53(0)	83 (0)
ω_2 (A_1)	(31) (0)	31 (0)	36 (0)	36 (0)
ω_3 (E)	68 (0)	85 (0)	52 (0)	66 (0)
ω_4 (E)	36 (0)	35 (0)	24 (0)	37 (0)
ω_5 (T_1)	65 (0)	84 (0)	51 (0)	66 (0)
ω_6 (T_2)	87 (1.86)	95 (0.24)	66 (1.17)	82 (1.95)
ω_7 (T_2)	83 (0.21)	85 (3.75)	63 (1.59)	71 (0.71)
ω_8 (T_2)	33(0.06)	19 (0.03)	26 (0.06)	26 (0.36)
q(Cs)	0.874	0.909	0.823	0.876
q(X)	–0.874	–0.909	–0.823	–0.876

Three channels of the dissociation of Cs_4X_4 molecules with the elimination of monomer and dimer molecules were considered (Table 33), similarly to trimers, the data of our previous works were included. It can be observed the dissociation into two Cs_2X_2 molecules requires lowest energy than other two channels. For the dissociation into two dimers, the values of $\Delta_r H°(0)$ are less by 39 kJ·mol^{-1} (Cs_4F_4), 35 kJ·mol^{-1} (Cs_4Cl_4), 32 kJ·mol^{-1} (Cs_4Br_4) and 33 kJ·mol^{-1} (Cs_4I_4) compared to the dissociation into monomer plus trimer and by 342 kJ·mol^{-1} (Cs_4F_4), 310 kJ·mol^{-1} (Cs_4Cl_4), 300 kJ·mol^{-1} (Cs_4Br_4) and 286 kJ·mol^{-1} (Cs_4I_4) compared to the dissociation into four CsX molecules. Uncertainties of the enthalpies of reaction and enthalpies of formations were estimated as ± 20 kJ·mol^{-1} and ± 30 kJ·mol^{-1}, respectively. The enthalpies of formation found on the base of three reactions are close to each other, the averaged values of $\Delta_f H°(0)$ were accepted: –1270 ± 30 kJ·mol^{-1} (Cs_4Br_4) and –1043 ± 30 kJ·mol^{-1} (Cs_4I_4).

Table 33: The energies, $\Delta_r E$, ZPVE corrections, $\Delta\varepsilon$, and enthalpies $\Delta_r H°(0)$ of the dissociation reactions, and enthalpies of formation $\Delta_f H°(0)$ of Cs_4X_4 (T_d) (X= F, Cl, Br, I) molecules, all values are in kJ·mol^{-1}.

No	Dissociation reaction	$\Delta_r E$	$-\Delta\varepsilon$	$\Delta_r H°(0)$	$-\Delta_f H°(0)$
1	$Cs_4F_4 = CsF + Cs_3F_3$	210.0	4.00	206	1949
2	$Cs_4F_4 = 2Cs_2F_2$	169.8	2.66	167	1941
3	$Cs_4F_4 = 4CsF$	517.4	7.96	509	1956
4	$Cs_4Cl_4 = CsCl + Cs_3Cl_3$	219	2.15	217	1453
5	$Cs_4Cl_4 = 2Cs_2Cl_2$	183.5	1.71	182	1464
6	$Cs_4Cl_4 = 4CsCl$	497.3	4.9	492	1453
7	$Cs_4Br_4 = CsBr + Cs_3Br_3$	213.0	3.43	210	1265
8	$Cs_4Br_4 = 2Cs_2Br_2$	179.2	1.41	178	1274
9	$Cs_4Br_4 = 4CsBr$	481.7	3.73	478	1267
10	$Cs_4I_4 = CsI + Cs_3I_3$	192.6	1.81	191	1038
11	$Cs_4I_4 = 2Cs_2I_2$	160.0	1.73	158	1054
12	$Cs_4I_4 = 4CsI$	447.3	3.59	444	1038

5.3.3 Trimer and tetramer dissociation: thermodynamic approach

For the most probable channel of dissociation of trimer into elimination of CsX molecule and tetramer molecules into two dimers, the Gibbs free energy change was calculated and plotted vs temperature (Figs. 28, 29). The plots for other two halides, Cs_3X_3 and Cs_4X_4 (X = F and Cl) were included. As seen, the values of $\Delta_r G°$ are positive for rather narrow temperature range; the change of sign occurs at ~ 330 K, 280 K, 240 K and 210 K for Cs_3X_3 and ~390 K, 370 K, 360 K and 250 K for Cs_4X_4 (X = F, Cl, Br and I) respectively. Therefore according the thermodynamic approach, only Cs_3F_3 and all tetramers excluding Cs_4I_4 may exist at the room and moderate temperatures. With temperature rise all trimers Cs_3X_3 dissociate spontaneously into CsX plus Cs_2X_2 while tetramers Cs_4X_4 decompose into two dimeric molecules.

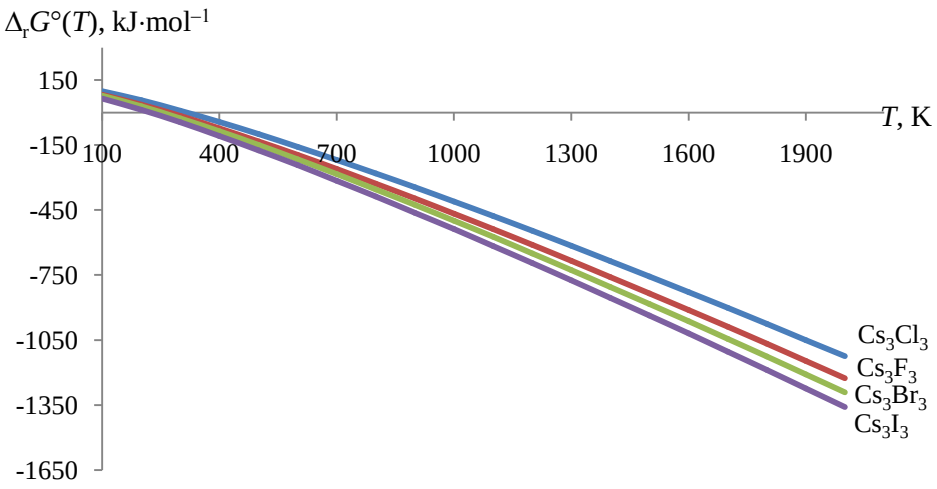

Figure 28: Gibbs free energy change versus temperature for the reaction Cs_3X_3 = CsX + Cs_2X_2 (X =F, Cl, Br and I).

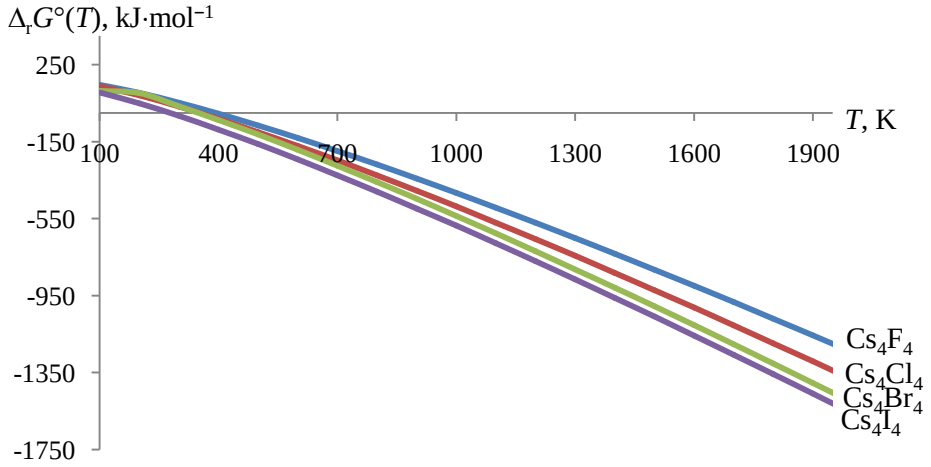

Figure 29: Gibbs free energy change versus temperature for the reaction Cs_4X_4 = 2Cs_2X_2 (X =F, Cl, Br and I).

5.4 Conclusion

The geometrical structure and vibrational spectra of the trimer and tetramer molecules, Cs_3X_3 and Cs_4X_4 (X = Br and I), were determined by B3LYP5 and MP2 methods. The results computed by these two methods were in a good accordance between each other and also in good

agreement with the experimental and theoretical data available in literature for Cs_3X_3. The existence of two isomeric forms, hexagonal and butterfly shaped, for Cs_3X_3 was confirmed, and the latter isomer was found to be most abundant in equilibrium vapor. Thermodynamic properties of Cs_3X_3 and Cs_4X_4 were calculated. Different dissociation channels of the species were considered; among them the most probable appeared to be those with elimination of dimeric molecules. The analysis of Gibbs free energy $\Delta_r G°$ revealed that these cluster molecules are not stable at elevated temperatures; at temperatures greater than 360 K both Cs_3X_3 and Cs_4X_4 dissociate spontaneously into CsX plus Cs_2X_2 and two dimeric molecules, respectively. Tetramers are more stable than trimers, likely due to compact structure close to cubic.

CHAPTER SIX

6.1. General Discussion

For the accurate determination of thermodynamic properties of molecular and ionic clusters, a good prediction of geometrical parameters and vibrational frequencies is needed. Analysis of results obtained using B3LYP5 B2 and MP2 B2 computational levels have shown in our findings that the results are reasonably good compare to experimental data available. As presented in Fig. 30, the agreement between our theoretical results of internuclear distance, R_e (Cs–X) for diatomic molecule CsX (X = F, Cl, Br and I) with experimental data obtained using microwave spectra (Huber *et al.*, 2001) are good. As seen in Fig. 30 a, the values of R_e (Cs–X) calculated by B3LYP5 and MP2 methods a decrease is noticeable as one moving from basis set B1 to B2; the values computed using B2 being much closer to experimental data. Regarding the methods themselves, the comparison are shown in Figs. 30 b, c for calculated R_e (Cs–X) of CsX and dimers Cs_2X_2. As it can be observed the calculated values of R_e (Cs–X) for both CsX and Cs_2X_2 molecules decrease monotonically from B3LYP5 B2 to literature data, whereby the values obtained by MP2 B2 being rather close to reference values.

The calculated vibrational frequencies of CsX molecules and experimental data by microwave spectra (Huber *et al.*, 2001) are shown in Fig. 31. There is an increase of vibrational frequencies from B1 to B2 within both B3LYP5 and MP2 methods. The values calculated employing B2 is seen to be closer to experimental data. As well the calculated values of vibrational frequencies of CsX molecules using B2 only are presented together with experimental data (Fig. 31 b). A progression increase of vibrational frequencies from B3LYP5 B2 to experimental data is noticed.

Thus, for both geometrical parameters and vibrational frequencies the results calculated by B3LYP5 B2 and MP2 B2 do not contradict each other, but it is worth note that the results by MP2 B2 are preferable as there are much closer to experimental values.

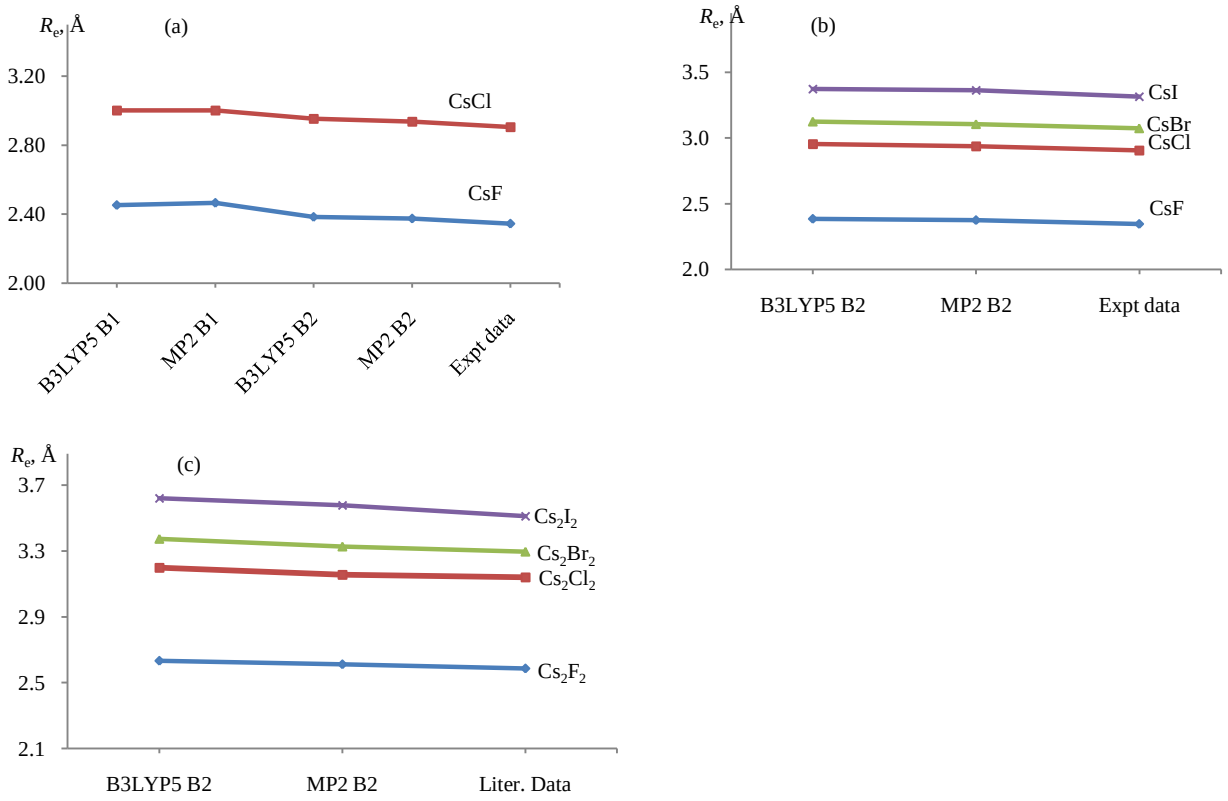

Figure 30: Internuclear separation R_e (Cs–X) of diatomic molecules CsX and dimers Cs_2X_2 versus computation levels: (a) CsF and CsCl using basis sets B1 and B2; (b) CsX with B2; (c) Cs_2X_2 with B2.

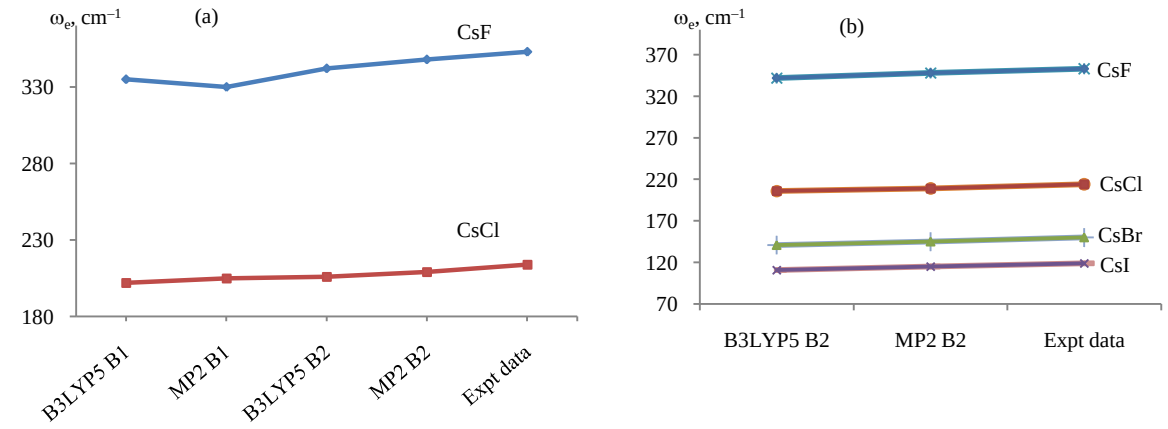

Figure 31: Vibrational frequencies ω_e of diatomic molecules versus computation levels: (a) CsF and CsCl using basis B1 and B2; (b) CsX with B2.

Further analysis of the results obtained with B3LYP5 B2 and MP2 B2 methods were made through evaluation of thermodynamic properties such as enthalpies of dissociation reactions $\Delta_r H°(0)$ and comparison with literature data or values based on experimental data. The advanced method MP4 was also incorporated. Moreover, the accurate prediction of dissociation energies involving the basis set superposition error (BSSE) correction as proposed by Boys and Bernardi (Boys *et al.*, 1970) was applied. Though, it was used only for MP2 B2 and MP4 B2 as that approach is more effective with Møllel-Plesset perturbation theory (Szczęśniak *et al.*, 1986). It has also been observed that increasing electron correlation from MP2 to MP4 reduces the BSSE (Lee, 1999). Thus, employing MP4 method improves the prediction of the dissociation energies, as MP4 has high recover of the correlation energy. The calculated enthalpies of dissociation reactions $\Delta_r H°(0)$ for Cs_2X_2 molecules are compared with reference values and those for ionic clusters for cesium chloride and iodide are compared with values based on experimental data. As is seen in Fig. 32 the values of $\Delta_r H°(0)$ for all Cs_2X_2 molecules form similar patterns, increase from B3L3P5 B2 to MP2 B2 followed by a slightly oscillation behaviour in series MP2 B2–MP2C B2–MP4 B2 –MP4C B2. The values obtained by MP4C B2 are found a bit lower than reference value except that of Cs_2F_2 which is slight higher. However, taking into account the estimated uncertainties limits the values obtained by MP4C B2 agree well with reference data On the other hand B3LYP5 B2 method gave worse results.

For selected ionic clusters our theoretical $\Delta_r H°(0)$ are compared with corresponding values based on experimental data (Fig. 33). Similar trends as those of Cs_2X_2 molecules are seen. Although the differences is noted between the values obtained by MP4C B2 and the one based on experiment data for the two classes of species. For cesium chloride cluster ions, the $\Delta_r H°(0)$ based on experimental data are lower than of MP4C B2 method except for $Cs_4Cl_3^+$ (Fig. 33 a); in contrary to cesium iodide cluster ions whereby the values of $\Delta_r H°(0)$ based on experimental data are higher (Fig. 33 b). In spite of these discrepancies the values of $\Delta_r H°(0)$ obtained by MP4C B2 agree well with experimental data within uncertainties limits. Surprising is the good agreement between the values obtained by B3LYP5 B2 and that based on experimental data for tri- and pentaatomic ions of cesium chloride. But generally, the enthalpies of dissociation reaction obtained by MP2C B2 and MP4C B2 are seen to be more reliable.

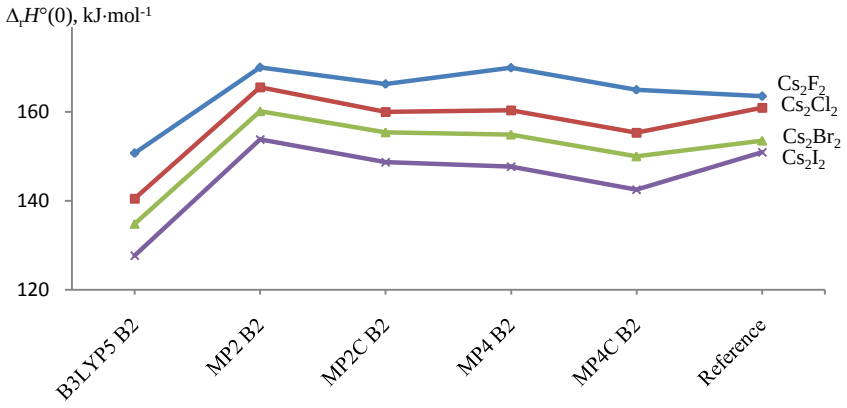

Figure 32: Calculate enthalpies of dissociation reactions Cs_2X_2 = 2CsX, $\Delta_r H°(0)$ versus calculation levels.

Different geometrical configurations of molecular and ionic clusters for cesium halides have been confirmed with minima PES using B3LYP5 B2 and MP2 B2 methods. Our calculated internuclear separation for both molecules and ionic clusters increases with: (1) increasing halogen size, (2) increasing number of atoms (3) within the same number of atoms for ionic clusters, negative ions have slighter higher internuclear separation than positive ions.

For all trimers Cs_3X_3 of cesium halides two equilibrium structures were confirmed to exist. Other clusters with isomeric forms were pentaatomic $Cs_3X_2^+$ and $Cs_2X_3^-$ ions and heptaatomic $Cs_4X_3^+$ ion. The relative concentrations of isomers are found to be influenced by two factors, namely isomerisation energies ΔE_{iso} and entropy $S°$ of the species. Our findings revealed that butterfly-shaped isomer prevails over hexagonal for trimers, in pentaatomic $Cs_3X_2^+$ and $Cs_2X_3^-$ ions the linear (or angular shaped) isomer dominates over cyclic and bipyramidal. The calculated relative abundances of butterfly-shaped Cs_3X_3 (C_s) isomers slightly decrease with temperature rise, while those of linear/angular isomers of pentaatomic $Cs_3X_2^+$ and $Cs_2X_3^-$ ions increase. Among the two isomers for heptaatomic $Cs_4X_3^+$ ion, polyhedral structure (C_{3v}) dominated over two cycled with mutually perpendicular planes (D_{2d}) within the temperature ranges of 700−1000 K and thereafter the concentrations of D_{2d} structure increases at a significant rate with temperature rise.

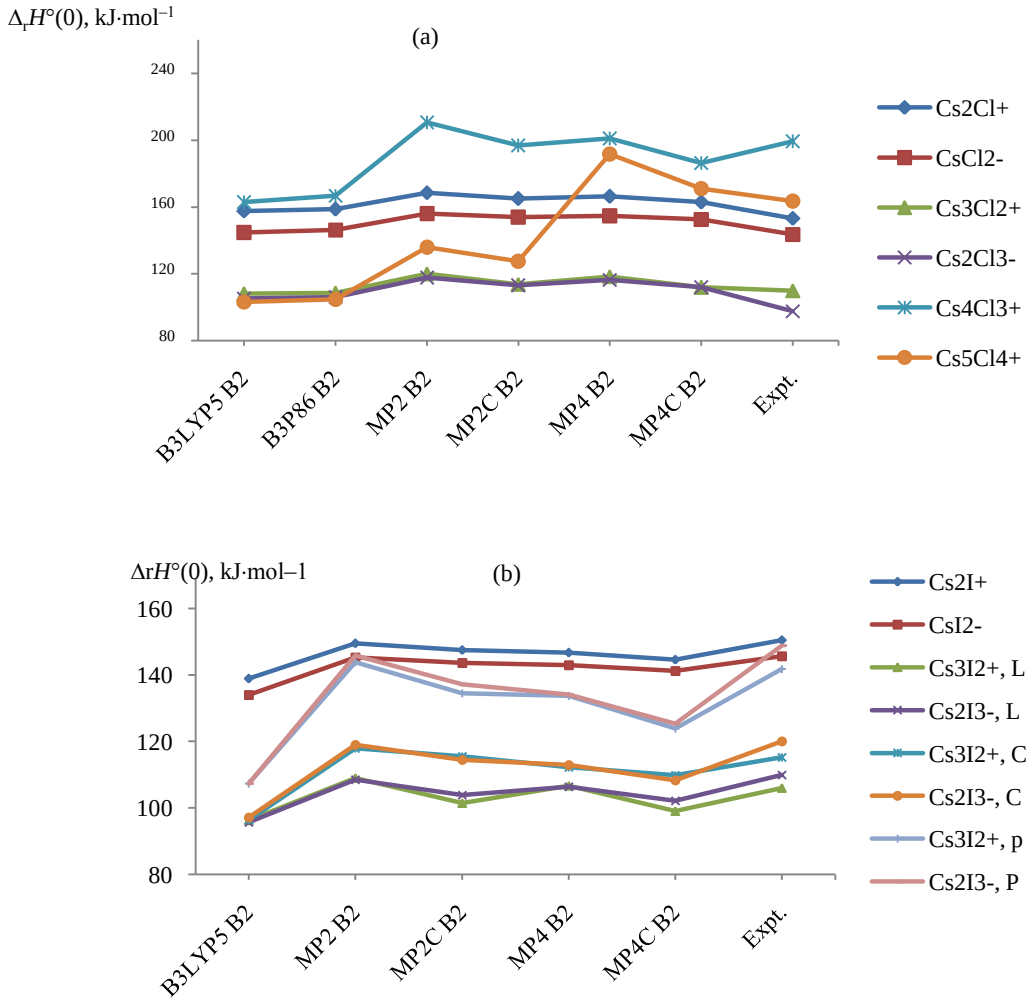

Figure 33: Calculated enthalpies of dissociation reactions $\Delta_r H°(0)$ for ionic clusters versus the calculation levels: (a) cesium chloride; (b) cesium iodide, (where letters L, C and P stand for linear (V−shaped), cyclic and pyramidal structure respectively).

Gibbs free energies of dissociation reactions show that most probable channel for trimers Cs_3X_3 is the elimination of CsX molecule and for tetramer molecules dissociation into two dimers Cs_2X_2. This analysis is important for understanding the stability of trimers and tetramers of cesium halide molecules in vapor. Therefore, these molecules withstand at a narrow temperatures range. Most of them decompose spontaneously at below or above room temperature to their most probable dissociation channel.

The enthalpy of formation $\Delta_f H°(0)$ of molecular and ionic clusters are calculated and the results are presented in Fig. 34. As seen in Figs. 34 a, b the values of $\Delta_f H°(0)$ decrease with increasing halogen size. The decrease is due to lessen of electron affinity with halogen size. For triatomic ions Cs_2X^+ (X = Cl, Br, I) the values of $\Delta_f H°(0)$ were found to be positive (Fig. 34 b).

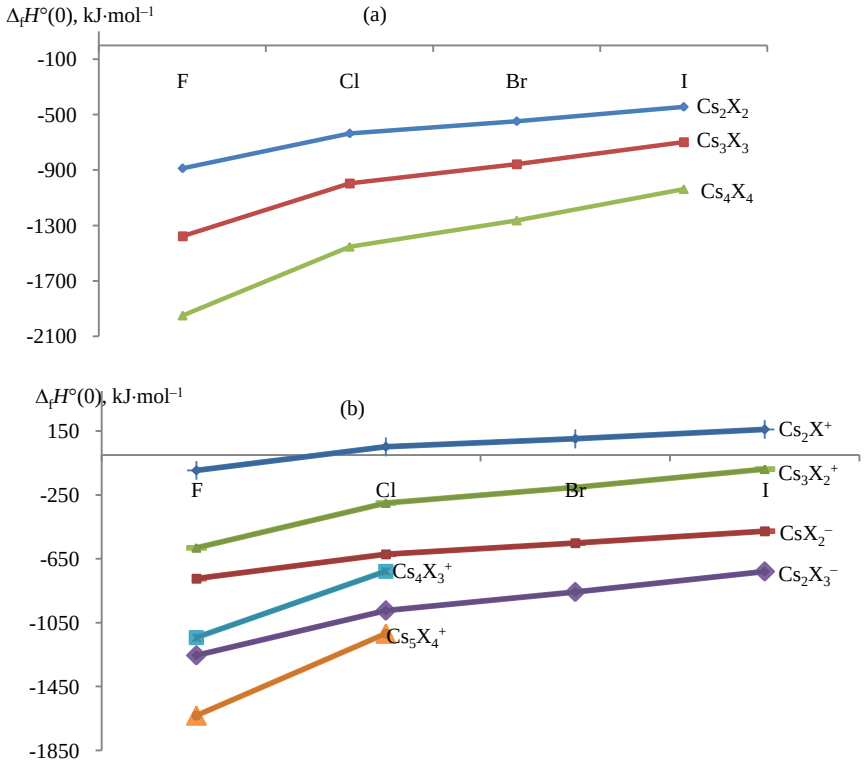

Figure 34: Enthalpies of formation of cesium halides versus halogen: (a) molecular, (b) ionic clusters.

Further analysis of $\Delta_f H°(0)$ of molecules $(CsX)_n$ and ionic clusters $X^-(CsX)_n$ and $Cs^+(CsX)_n$ versus number *n* of CsX molecules within the species are plotted in Fig. 35. The values of $\Delta_f H°(0)$ at $n = 1$ correspond to the enthalpies of formation of CsX molecules (Fig. 35 a) and X^- and Cs^+ ions at $n = 0$ (Figs. 35 b, c). The calculated values of $\Delta_f H°(0)$ for molecules and ions increase with number of CsX molecules attached; almost linear trend is seen. This trend might be used for the estimation of enthalpies of formation of heavier cluster molecules and ions that could be generated under the same conditions.

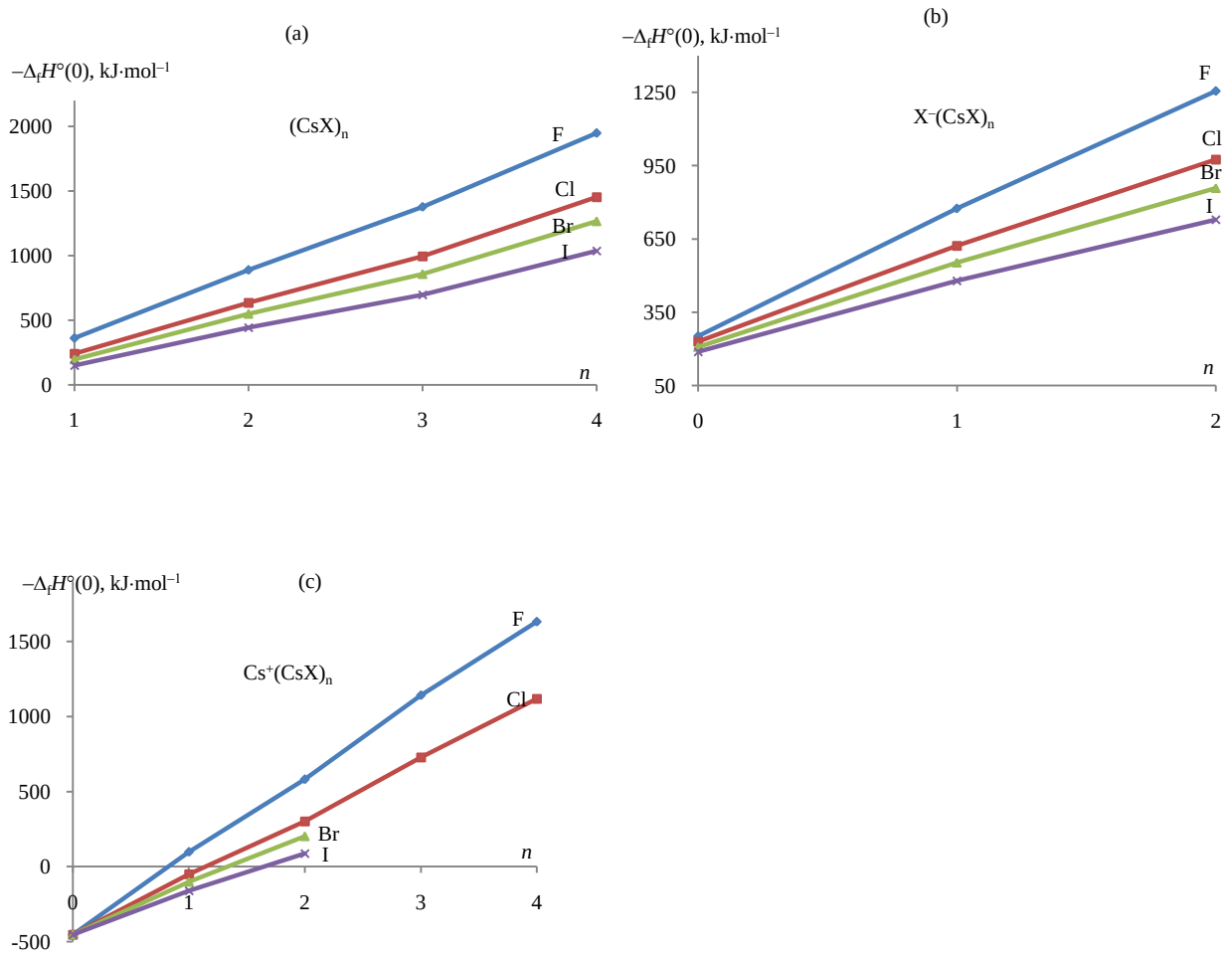

Figure 35: Enthalpies of formation $\Delta_f H°(0)$ of cluster molecules and ions of cesium halides versus *n*, the number of CsX attached: (a) $(CsX)_n$; (b) $X^-(CsX)_n$ and $Cs^+(CsX)_n$.

6.2. Conclusion

Our studies constitute fundamental researches that promote the development of cluster assembled materials as one of the viable building blocks. The results of this work may be useful for modelling of industrial processes.

The appropriateness of quantum chemical methods, DFT/B3LYP5 and MP2, for determination of the structure, vibrational spectra and thermodynamic properties of molecular and ionic clusters of cesium halides was demonstrated. Notably, the results obtained by MP2 method with extended basis set showed good agreement with available experimental data.

For trimer molecules, pentaatomic positive and negative ions and heptaatomic positive ions different isomers are confirmed to exist in saturated vapor over cesium halides. The relative abundance of the isomers was determined. The most abundant isomer was found to be butterfly-shaped for trimer molecules, linear or angular structure for both positive and negative pentaatomic ions, and polyhedral for heptaatomic ions.

Enthalpies of dissociation reactions $\Delta_r H°(0)$ and enthalpies of formation $\Delta_f H°(0)$ of molecular and ionic clusters were calculated using MP4 perturbation theory involving basis set superposition error correction. For the enthalpies $\Delta_r H°(0)$ of dissociation of Cs_nX_n molecules and $Cs_nX_{n-1}^+$ and $Cs_{n-1}X_n^-$ ions with elimination of CsX molecule, even-odd oscillation behaviour was observed; for even number *n* the enthalpies $\Delta_r H°(0)$ were higher than those for odd *n*. Regarding enthalpies of formation, we found that the values of $\Delta_f H°(0)$ decrease from fluorides to iodides and increase with the number of CsX molecules attached.

6.3. Recommendations

Further studies of molecular and ionic clusters of inorganic compound may be recommended:

1. Floppy nonrigid structures and low bending frequencies are found for some species. Advanced approximations like anharmonic oscillator and direct summation methods are to be used for the calculations of thermodynamic functions.
2. Theoretical enthalpies of reactions were compared with values based on experimental equilibrium constants available. Still some data either theoretical or experimental are to be obtained/refined using more advanced quantum chemical methods, e.g. CCSD (T), and up-to date experimental techniques as well.
3. Extending the characterization of the molecular and ionic clusters of cesium halides by studying these systems in aqueous and other media and determining the spectroscopic properties of cesium halide clusters in solvents.

REFERENCES

Aguado, A. (2001). An ab Initio Study of the Structures and Relative Stabilities of Doubly Charged $[(NaCl)_m (Na)_2]^{2+}$ Cluster Ions. *The Journal of Physical Chemistry B, 105*(14), 2761-2765.

Alexandrova, A. N., Boldyrev, A. I., Fu, Y. J., Yang, X., Wang, X. B., and Wang, L. S. (2004). Structure of the $Na_xCl^-_{x+1}$ (x = 1–4) clusters via ab initio genetic algorithm and photoelectron spectroscopy. *The Journal of Chemical Physics, 121*(12), 5709-5719.

Anil K. Kandalam, Puru Jena, Xiang Li, Soren M. Eustis, and Bowen, K. H. (2008). Photoelectron spectroscopy and theoretical studies of $[Co_m(pyrene)_n]^-$ (m = 1,2 and n = 1,2) complexes. *Journal of Chemical Physics, 129*, 134308-134318.

Badawi, M., Xerri, B., Canneaux, S., Cantrel, L., and Louis, F. (2012). Molecular structures and thermodynamic properties of 12 gaseous cesium-containing species of nuclear safety interest: Cs_2, CsH, CsO,Cs_2O, CsX, and Cs_2X_2 (X = OH, Cl, Br, and I). *Journal of Nuclear Materials, 420*(1), 452-462.

Bartlett, N. (1962). Xenon Hexafluoroplatinate (V) Xe^+[Ptf6] (p. 218): Royal Society of Chemistry Thomas Graham House, Science Park, Milton Rd, Cambridge Cb4 0wf, Cambs, England.

Bartlett, R. J. (1989). Coupled-cluster approach to molecular structure and spectra: a step toward predictive quantum chemistry. *The Journal of Physical Chemistry, 93*(5), 1697-1708.

Becke, A. D. (1993). Density-functional thermochemistry. III. The role of exact exchange. *The Journal of Chemical Physics, 98*(7), 5648-5652.

Bencze, L., Lesar, A., and Popovic, A. (1998). The evaporation thermodynamics of lithium iodide. Mass spectrometric and ab initio studies. *Rapid communications in mass spectrometry, 12*(14), 917-930.

Benson, S. W., and Patterson, M. J. (2009). *NASA's Evolutionary Xenon Thruster (NEXT) Ion Propulsion Technology Development Status in 2009.* Paper presented at the 31st International Electric Propulsion Conference, Ann Arbor, MI, IEPC Paper.

Bergman, H., Ostmark, H., Ekvall, K., and Langlet, A. (1993). *A study of the sensitivity and decomposition of keto-RDX.* Paper presented at the Proceedings of the 10th Symposium (International) on Detonation.

Bode, B. M., and Gordon, M. S. (1998). MacMolPlt version 7.4.2. *Journal Molecular Graphics and Modeling, 16,* 133-138.

Boys, S. F., and Bernardi, F. (1970). The calculation of small molecular interactions by the differences of separate total energies. Some procedures with reduced errors. *Molecular. Physical, 19,* 553-556.

Bruce, S. A., and Lester, A. (1976). Matrix reactions of alkali metal fluoride molecules with fluorine. Infrared and Raman spectra of the trifluoride ion in the $M^+F_3^-$ species. *Journal of the American Chemical Society, 98* 1591–1593. doi: 10.1021/ja00422a058

Butman, M., Kudin, L., Smirnov, A., and Munir, Z. (2000). Mass spectrometric study of the molecular and ionic sublimation of cesium iodide single crystals. *International Journal of Mass Spectrometry, 202*(1), 121-137.

Castleman, A., and Bowen, K. (1996). Clusters: Structure, energetics, and dynamics of intermediate states of matter. *The Journal of Physical Chemistry, 100*(31), 12911-12944.

Castleman, A., and Jena, P. (2006). Clusters: A bridge between disciplines. *Proceedings of the National Academy of Sciences, 103*(28), 10552-10553.

Castleman Jr, A., and Khanna, S. (2009). Clusters, Superatoms, and Building Blocks of New Materials. *The Journal of Physical Chemistry C, 113*(7), 2664-2675.

Chupka, W. A. (1959). Dissociation energies of some gaseous alkali halide complex ions and the hydrated ion $K(H_2O)^+$. *Journal Chemical Physical, 10,* 458–465.

Cohen, A. J., and Gordon, R. G. (1975). Theory of the lattice energy, equilibrium structure, elastic constants, and pressure-induced phase transitions in alkali-halide crystals. *Physical Review B, 12*(8), 3228.

Cordfunke, E. H. P., and Konings, R. J. M. (1990). Thermochemical Data for Reactor Materials and Fission Products, *Elsevier Science Pub. Co., Inc.*

Cramer, C. J. (2004). *Essentials of Computation Chemistry Theories and Models.*

Curtiss, L. A., Redfern, P. C., and Frurip, D. J. (2000). Theoretical methods for computing enthalpies of formation of gaseous compounds. *Reviews in Computational Chemistry, Volume 15,* 147-211.

Dickey, R. P., Maurice, D., Cave, R. J., and Mawhorter, R. (1993). A theoretical investigation of the geometries, vibrational frequencies, and binding energies of several alkali halide dimers. *The Journal of Chemical Physics, 98*(3), 2182-2190.

Dorsett, H., and White, A. (2000). Overview of molecular modelling and ab initio molecular orbital methods suitable for use with energetic materials.

Dunaev, A. M., Kudin, L. S., Butman, M. F., and Motalov, V. B. (2013). Alkali Halide Work Function Determination by Knudsen Effusion Mass Spectrometry. *The Electrochemical Society Transactions, 46*(1), 251−258. doi: 10.1149/04601.0251ecst

Fedorov, D. G., Koseki, S., Schmidt, M. W., and Gordon, M. S. (2003). Spin-orbit coupling in molecules: chemistry beyond the adiabatic approximation. *International Reviews in Physical Chemistry, 22*(3), 551-592.

Feller, D. (1996). The role of databases in support of computational chemistry calculations. *Journal of computational chemistry, 17*(13), 1571-1586.

Fernandez-Lima, F. A., Nascimento, M. A. C., and Silveira, E. F. d. (2012). Alkali halide clusters produced by fast ion impact. *Nuclear Instruments and Methods in Physics Research Section B: Beam Interactions with Materials and Atoms, 273*, 102-104.

Frank, J. (1999). Introduction to Computational Chemistry. *Editorial Offices October*.

Frisch, M. J., Del Bene, J. E., Binkley, J. S., and Schaefer III, H. F. (1986). Extensive theoretical studies of the hydrogen-bonded complexes $(H_2O)_2$, $(H_2O)_2H^+$, $(HF)_2$, $(HF)_2H^+$, F_2H^-, and $(NH_3)_2$. *The Journal of Chemical Physics, 84*(4), 2279-2289.

Galhena, A. S., Jones, C. M., and Wysocki, V. H. (2009). Influence of cluster size and ion activation method on the dissociation of cesium iodide clusters. *International Journal of Mass Spectrometry, 287*(1), 105-113.

Giri, S., Behera, S., and Jena, P. (2014). Superhalogens as Building Blocks of Halogen-Free Electrolytes in Lithium-Ion Batteries. *Angewandte Chemie International Edition, 53*(50), 13916-13919.

Gorokhov, L. N. (1972). *Development of high-temperature mass spectrometry methods and thermodynamic investigations of alkali metal halides.* (Chemical Sciences Doctoral Dissertation), Moscow

Granovsky, A. (2012a). Firefly version 8.1.0, www. from http://classic.chem.msu.su/gran/firefly/index.html

Granovsky, A. A. (2012b). Firefly version 8.0.0, www. from http://classic.chem.msu.su/gran/firefly/index.html

Grant, G. H., and Richards, W. G. (1995). *Computational chemistry*: Oxford University Press.

Groen, C. P., and Kovács, A. (2010). Matrix-isolation FT-IR study of $(CsBr)_n$ and $(CsI)_n$ (n = 1–3). *Vibrational Spectroscopy, 54*(1), 30-34.

Gurvich, L. V., Yungman, V. S., Bergman, G. A., Veitz, I. V., Gusarov, A. V., Iorish, V. S., Leonidov, V. Y., Medvedev, V. A., Belov, G. V., Aristova, N. M., Gorokhov, L. N., Dorofeeva, O. V., Ezhov, Y. S., Efimov, M. E., Krivosheya, N. S., Nazarenko, I. I., Osina, E. L., Ryabova, V. G., Tolmach, P. I., Chandamirova, N. E., and Shenyavskaya, E. A. (2000). Thermodynamic Properties of Individual Substances. Ivtanthermo for Windows Database on Thermodynamic Properties of Individual Substances and Thermodynamic Modeling Software, Version 3.0 (Glushko Thermocenter of RAS, Moscow, 1992–2000).

Gusarov, A. V. (1986). *Equilibrium ionization in vapors of inorganic compounds and the thermodynamic properties of ions.* (Chemical sciences doctoral dissertation), VNITsPV, Moscow.

Haaland, A. (2008). *Molecules and Models: The molecular structures of main group element compounds* doi:10.1093/acprof:oso/9780199235353.001.0001

Hargittai, M. (2000). Molecular structure of metal halides. *Chemical Reviews, 100*(6), 2233-2302.

Hartley, J., and Fink, M. (1987). An electron diffraction study of alkali bromide vapors. *The Journal of Chemical Physics, 87*(9), 5477-5482.

Hartley, J., and Fink, M. (1988). An electron diffraction study of alkali iodide vapors. *The Journal of Chemical Physics, 89*(10), 6053-6057.

Hebert, A., Lovas, F., Melendres, C., Hollowell, C., Story Jr, T., and Street Jr, K. (1968). Dipole moments of some alkali halide molecules by the molecular beam electric resonance method. *The Journal of Chemical Physics, 48*(6), 2824-2825.

Hehre, W. J. (1986). *Ab initio molecular orbital theory*: Wiley-Interscience.

Hilpert, K. (1990). Chemistry of inorganic vapors *Noble Gas and High Temperature Chemistry* (pp. 197): Springer.

Hilpert, K., and Niemann, U. (1997). High temperature chemistry in metal halide lamps. *Thermochimica acta, 299*(1), 49-57.

Hishamunda, J., Girabawe, C., Pogrebnaya, T., and Pogrebnoi, A. (2012). Theoretical study of properties of Cs_2Cl^+, $CsCl_2^-$, $Cs_3Cl_2^+$, and $Cs_2Cl_3^-$ ions: Effect of Basis set and Computation Method. *Rwanda Journal, 25*(1), 66-85.

Hohenberg, P., and Kohn, W. (1964). Inhomogeneous electron gas. *Physical Review, 136*(3B), B864.

Holthausen, M., and Koch, W. (2000). A Chemist's guide to density functional theory: Wiley-VCH: Weinheim, Germany.

Huber, K., and Herzberg, G. (2001). Constants of Diatomic Molecules (data prepared by JW Gallagher and RD Johnson, III) in NIST Chemistry WebBook, NIST Standard Reference Database Number 69, eds. *PJ Linstrom and WG Mallard, July*. from webbook.nist.gov

Huber, K. P., and Herzberg, G. (1976). Diatomic Constants for $^{133}Cs^{19}F$. from http://webbook.nist.gov/cgi/cbook.cgi?ID=C13400130&Units=SI&Mask=1000#Diatomic

Huh, S., and Lee, G. (2001). Mass Spectrometric Study of Negative, Positive, and Mixed KI Cluster Ions by Using Fast Xe Atom Bombardment. *Journal-Korean Physical Society, 38*(2), 107-110.

Jansen, H., and Ros, P. (1969). Non-empirical molecular orbital calculations on the protonation of carbon monoxide. *Chemical Physics Letters, 3*(3), 140-143.

Jensen, F. (2007). *Introduction to computational chemistry*: John Wiley & Sons.

Kay, T. P. (2011). *Magnetohydrodynamic engergy conversion device using solar radiation as an energy source,* US Patent No. US 7,982,343 B2.

Khanna, S., and Jena, P. (1993). Assembling crystals from clusters. *Physical review letters, 71*(1), 208-301.

Khanna, S., and Jena, P. (1995). Atomic clusters: Building blocks for a class of solids. *Physical Review B, 51*(19), 13705.

Knight, D., Zidan, R., Lascola, R., Mohtadi, R., Ling, C., Sivasubramaniam, P., Kaduk, J., Hwang, S., Samanta, D., and Jena, P. (2013). Stabilization of Hydrogen Rich, Yet Highly Pyrophoric Al $(BH4)_3$ via the Synthesis of the Hypersalt $K[Al(BH_4)_4]$. *Journal Physical Chemestry C, 117*, 19905-19915.

Kohn, W., and Sham, L. J. (1965). Self-consistent equations including exchange and correlation effects. *Physical Review*, *140*(4A), A1133.

Konings, R., Booij, A., and Cordfunke, E. (1991). High-temperature infrared study of the vaporization of CsI, CdI_2 and Cs_2 CdI_4. *Vibrational Spectroscopy, 2*(4), 251-255.

Krasnov, K. S., Philippenko, N. V., Bobkova, V. A., Lebedeva, N. L., Morozov, E. V., Ustinova, T. I., and Romanova, G. A. (1979). *Handbook Molecular Constants of Inorganic Compounds* (Krasnov, K. S. Ed.).

Kudin, L. S., Burdukovskaya, G. G., Krasnov, K. S., and Vorob'ev, O. V. (1990). Mass spectrometric study of the ionic composition of saturated potassium chloride vapor. Enthalpies of formation of the K_2Cl^+, $K_3Cl_2^+$, KCl_2^-, and $K_2Cl_3^-$ ions. *Russian Journal Physical Chemistry, 64*, 484 –489.

L.A. Bloomfield, C.W.S. Conover, Y.A. Yang, Y.J. Twu, and Phillips, N. G. (1991). Experimental and theoretical studies of the structure of alkali halide clusters. *Atoms, Molecules and Clusters, 20*, 93-96.

Lee, C.-J., Han, J.-I., Choi, D.-K., and Moon, D.-G. (2010). Transparent organic light-emitting devices with CsCl capping layers on semitransparent Ca/Ag cathodes. *Materials Science and Engineering: B, 172*(1), 76-79.

Lee, C., Yang, W., and Parr, R. G. (1988). Development of the Colle-Salvetti correlation-energy formula into a functional of the electron density. *Physical Review B, 37*(2), 785.

Lee, J. S. (1999). On the effectiveness of function counterpoise method in the calculation of He–He interaction energies. *Bull Korean Chemical Society, 20*, 241-243.

Leininger, T., Nicklass, A., Küchle, W., Stoll, H., Dolg, M., and Bergner, A. (1996). The accuracy of the pseudopotential approximation: Non-frozen-core effects for spectroscopic constants of alkali fluorides XF (X= K, Rb, Cs). *Chemical Physics Letters*, *255*(4), 274-280.

Lennart, D., and Kjell, J. (1994). Specific features of cesium chemistry and physics affecting reactor accident source term predictions: Organisation for Economic Co-Operation and Development-Nuclear Energy Agency, Committee on the safety of nuclear installations-OECD/NEA/CSNI, Le Seine Saint-Germain, 12 boulevard des Iles, F-92130 Issy-les-Moulineaux (France).

Liao, Y.-x., Liu, J., Wang, B., and Yi, F.-t. (2011). Multiform structures with silicon nanopillars by cesium chloride self-assembly and dry etching. *Applied Surface Science, 257*(24), 10489-10493.

Lisek, I., Kapała, J., and Miller, M. (1998). Thermodynamic study of the CsCl–$NdCl_3$ system by Knudsen effusion mass spectrometry. *Journal of alloys and compounds, 278*(1), 113-122.

Liu, B., and McLean, A. (1973). Accurate calculation of the attractive interaction of two ground state helium atoms. *The Journal of Chemical Physics, 59*(8), 4557-4558.

Liu, J., Ashmkhan, M., Dong, G., Wang, B., and Yi, F. (2013a). Fabrication of micro-nano surface texture by CsCl lithography with antireflection and photoelectronic properties for solar cells. *Solar Energy Materials and Solar Cells, 108*, 93-97.

Liu, W., Ferguson, M., Yavuz, M., and Cui, B. (2012). Porous TEM windows fabrication using CsCl self-assembly. *Journal of Vacuum Science & Technology B, 30*(6), 06F201.

Liu, Y., Zhao, J., Li, F., and Chen, Z. (2013b). Appropriate description of intermolecular interactions in the methane hydrates: an assessment of DFT methods. *Journal of computational chemistry, 34*(2), 121-131.

Martin, J. M., and Sundermann, A. (2001). Correlation consistent valence basis sets for use with the Stuttgart–Dresden–Bonn relativistic effective core potentials: The atoms Ga–Kr and In–Xe. *The Journal of Chemical Physics, 114*(8), 3408-3420.

Mayer, I., and Turi, L. (1991). An analytical investigation into the bsse problem. *Journal of Molecular Structure: THEOCHEM, 227*, 43-65.

Michael, F. L., and Allan, J. L. (1994). Principles of Plasma Discharges and Materials Processing (pp. 512–540): John Wiley & Sons. Inc., New York, NY.

Miller, M., Niemann, U., and Hilpert, K. (1994). Study of the Heterocomplexes in the Vapor of the Na-Sn-Br-I System and Their Relevance for Metal Halide Lamps. *Journal of the Electrochemical Society, 141*(10), 2774-2778.

Møller, C., and Plesset, M. S. (1934). Note on an approximation treatment for many-electron systems. *Physical Review*, *46*(7), 618.

Motalov, V. B., Pogrebnoi, A. M., and Kudin, L. S. (2001). Molecular and ionic associates in vapor over rubidium chloride. *Russian Journal Physical Chemestry*, *75*, 1407–1412.

Parks, E., Inoue, M., and Wexler, S. (1982). Collision induced dissociation of CsI and Cs_2I_2 to ion pairs by Kr, Xe, and SF6. *The Journal of Chemical Physics*, *76*(3), 1357-1379.

Parr, R. G., and Yang, W. (1989). *Density-functional theory of atoms and molecules* (Vol. 16): Oxford university press.

Patterson, M. (2004). Ion Propulsion. Retrieved August, 30, 2013, from http://www.grc.nasa.gov/WWW/ion/

Perdew, J. P. (1986). Density-functional approximation for the correlation energy of the inhomogeneous electron gas. *Physical Review B, 33*(12), 8822.

Perdew, J. P., and Zunger, A. (1981). Self-interaction correction to density-functional approximations for many-electron systems. *Physical Review B, 23*(10), 5048.

Peterson, K. A., and Dunning Jr, T. H. (1995). Benchmark calculations with correlated molecular wave functions. VII. Binding energy and structure of the HF dimer. *The Journal of Chemical Physics*, *102*(5), 2032-2041.

Pogrebnaya, T., Pogrebnoi, A., and Kudin, L. (2007). Theoretical study of the structure and stability of the Na_2Cl^+, $NaCl_2^-$, $Na_3Cl_2^+$, and $Na_2Cl_3^-$ ions. *Journal of Structural Chemistry*, *48*(6), 987-995.

Pogrebnaya, T., Pogrebnoi, A., and Kudin, L. (2008). Calculation of the thermodynamic characteristics of ions in vapor over sodium fluoride. *Russian Journal of Physical Chemistry A*, *82*(1), 75-82.

Pogrebnaya, T., Pogrebnoi, A., and Kudin, L. (2010). Structural and thermodynamic characteristics of ionic associates in vapors over sodium bromide and iodide. *Journal of Structural Chemistry*, *51*(2), 231-237.

Pogrebnaya, T. P., Hishamunda, J. B., Girabawe, C., and Pogrebnoi, A. M. (2012). Theoretical study of structure, vibration spectra and thermodynamic properties of cluster ions in vapors over potassium, rubidium and cesium chlorides *Chemistry for Sustainable Development* (pp. 353-366): Springer.

Pogrebnoi, A. M., Kudin, L. S., and Kuznetsov, A. Y. (2000). Enthalpies of Formation of the Ions Present in the Saturated Vapor over Cesium Chloride. *Russian Journal of Physical Chemistry, 74*, 1728-1730

Pogrebnoi, A. M., Pogrebnaya, T. P., Kudin, L. S., and Tuyizere, S. (2013). Structure and thermodynamic properties of positive and negative cluster ions in saturated vapor over barium dichloride. *Molecular Physics*, 111(21), 3234-3245.

Pople, J., Seeger, R., and Krishnan, R. (1977). Variational configuration interaction methods and comparison with perturbation theory. *International Journal of Quantum Chemistry, 12*(S11), 149-163.

Povinec, P. P., Aoyama, M., Biddulph, D., Breier, R., Buesseler, K., Chang, C., Golser, R., Hou, X., Ješkovský, M., and Jull, A. (2013). Cesium, iodine and tritium in NW Pacific waters-a comparison of the Fukushima impact with global fallout. *Biogeosciences Discussions, 10*(4), 5481-5496.

Purvis III, G. D., and Bartlett, R. J. (1982). A full coupled-cluster singles and doubles model: The inclusion of disconnected triples. *The Journal of Chemical Physics, 76*(4), 1910-1918.

Rao, B., Khanna, S., and Jena, P. (1999). Designing new materials using atomic clusters. *Journal of Cluster Science, 10*(4), 477-491.

Roki, F.-Z., Ohnet, M.-N., Fillet, S., Chatillon, C., and Nuta, I. (2014). Critical assessment of thermodynamic properties of CsI solid, liquid and gas phases. *The Journal of Chemical Thermodynamics, 70*, 46-72.

Roki, F., Ohnet, M., Fillet, S., Chatillon, C., and Nuta, I. (2013). Knudsen cell mass spectrometric study of the Cs 2 IOH (g) molecule thermodynamics. *The Journal of Chemical Thermodynamics, 65*, 247-264.

Rupp, M., and Ahlrichs, R. (1977). Theoretical investigation of structure and stability of oligomers of LiH, NaH, LiF, and NaF. *Theoretica chimica acta, 46*(2), 117-127.

Sarkas, H. W., Kidder, L. H., and Bowen, K. H. (1995). Photoelectron spectroscopy of color centers in negatively charged cesium iodide nanocrystals. *The Journal of Chemical Physics, 102*(1), 57-66.

Schmidt, M. W., Baldridge, K. K., Boatz, J. A., Elbert, S. T., Gordon, M. S., Jensen, J. H., Koseki, S., Matsunaga, N., Nguyen, K. A., Su, S. J., Windus, T. L., Dupuis, M., and Montgomery, J. A. (1993). General Atomic and Molecular Electronic Structure System. *Journal. Computational. Chemestry, 14*, 1347-1363. doi: doi:10.1002/jcc.540141112.

Schuchardt, K. L., Didier, B. T., Elsethagen, T., Sun, L., Gurumoorthi, V., Chase, J., Li, J., and Windus, T. L. (2007). Basis set exchange: a community database for computational sciences. *Journal of chemical information and modeling, 47*(3), 1045-1052. doi: 10.1021/ci600510j.

Sidorova, I., Gusarov, A., and Gorokhov, L. (1979). Ion-molecule equilibria in the vapors over cesium iodide and sodium fluoride. *International Journal of Mass Spectrometry and Ion Physics, 31*(4), 367-372. doi: 10.1016/0020-7381(79)80073-X.

Snelson, A. (1967). Infrared spectrum of LiF, Li2F2, and Li3F3 by matrix isolation. *The Journal of Chemical Physics, 46*(9), 3652-3656.

Solomonik, V. G., Smirnov, A. N., and Mileev, M. A. (2005). Structure, vibrational spectra, and energetic stability of LnX_4^- (Ln = La, Lu; X = F, Cl, Br, I) ions. *Koordinats. Khim., 31*, 218-228

Srivastava, A. K., and Misra, N. (2014a). Novel $(Li_2X)^+(LiX_2)^-$ supersalts (X= F, Cl) with aromaticity: a journey towards the design of a new class of salts. *Molecular Physics, 112*(19), 2621-2626.

Srivastava, A. K., and Misra, N. (2014b). Novel Li_3X_3 supersalts (X= F, Cl, Br & I) and their alkalide characteristics. *New Journal of Chemistry*.

Szalay, P. G. (2005). Configuration Interaction: Corrections for Size-Consistency. *Encyclopedia of Computational Chemistry*.

Szczęśniak, M., and Scheiner, S. (1986). Correction of the basis set superposition error in SCF and MP2 interaction energies. The water dimer. *The Journal of Chemical Physics, 84*(11), 6328-6335.

Tao, F. M., and Pan, Y. K. (1991). Validity of the function counterpoise method and ab initio calculations of van der Waals interaction energy. *The Journal of Physical Chemistry, 95*(9), 3582-3588.

Timoshenko, M., and Akopyan, M. (1974). Photoelectron spectra of cesium halogenides. *High Energy Chemistry, 8*(3), 211-214.

Tokarev, K. L. (2007-2009). "OpenThermo", v.1.0 Beta 1 (C) ed. .

Trapp, C., Atkins, P., Cady, M., and Guinta, C. (2006). *Physical Chemistry Instructor's Solutions Manual*

Tsuchiya, S., Green, M., and Syms, R. (2000). Structural fabrication using cesium chloride island arrays as a resist in a fluorocarbon reactive ion etching plasma. *Electrochemical and Solid-State Letters, 3*(1), 44-46.

Unemoto, A., Matsuo, M., and Orimo, S. i. (2014). Complex hydrides for electrochemical energy storage. *Advanced Functional Materials, 24*(16), 2267-2279.

Van Duijneveldt, F. B., van Duijneveldt-van de Rijdt, J. G., and van Lenthe, J. H. (1994). State of the art in counterpoise theory. *Chemical Reviews, 94*(7), 1873-1885.

Viswanathan, R., and Hilpert, K. (1984). Mass Spectrometric Study of the Vaporization of Cesium Iodide and Thermochemistry of $(CsI)_2(g)$ and $(CsI)_3(g)$. *Berichte der Bunsengesellschaft für physikalische Chemie, 88*(2), 125-131.

Wang, Y.-L., Wang, X.-B., Xing, X.-P., Wei, F., Li, J., and Wang, L.-S. (2010). Photoelectron Imaging and Spectroscopy of MI_2^- (M= Cs, Cu, Au): Evolution from Ionic to Covalent Bonding. *The Journal of Physical Chemistry A, 114*(42), 11244-11251.

Watts, J. D., Gauss, J., and Bartlett, R. J. (1993). Coupled-cluster methods with noniterative triple excitations for restricted open-shell Hartree–Fock and other general single determinant reference functions. Energies and analytical gradients. *The Journal of Chemical Physics, 98*(11), 8718-8733.

Weis, P., Ochsenfeld, C., Ahlrichs, R., and Kappes, M. M. (1992). Abinitio studies of small sodium–sodium halide clusters, Na_nCl_n and Na_nCl_{n-1} ($n \leq 4$). *The Journal of Chemical Physics, 97*(4), 2553-2560.

Welch, D., Lazareth, O., Dienes, G., and Hatcher, R. (1976). Alkali halide molecules: Configurations and molecular characteristics of dimers and trimers. *The Journal of Chemical Physics, 64*(2), 835-839.

Woodruff, D. P. (2007). *Atomic clusters: from gas phase to deposited* (Vol. 12): Elsevier.

Woon, D. E., Dunning Jr, T. H., and Peterson, K. A. (1996). Abinitio investigation of the N2–HF complex: Accurate structure and energetics. *The Journal of Chemical Physics, 104*(15), 5883-5891.

Yang, J., and Kestner, N. R. (1991). Accuracy of counterpoise corrections in second-order intermolecular potential calculations. 1. Helium dimer. *The Journal of Physical Chemistry, 95*(23), 9214-9220.

Yang, Y., Bloomfield, L., Jin, C., Wang, L., and Smalley, R. (1992). Ultraviolet photoelectron spectroscopy and photofragmentation studies of excess electrons in potassium iodide cluster anions. *The Journal of Chemical Physics, 96*(4), 2453-2459.

Zhang, X., Liu, J., Wang, B., Zhang, T., and Yi, F. (2014). Fabrication of silicon nanotip arrays with high aspect ratio by cesium chloride self-assembly and dry etching. *AIP Advances, 4*(3), 031335.

Zhang, Y., Li, J., Wei, T., Liu, J., Yi, X., Wang, G., and Yi, F. (2012). Enhancement in the light output power of GaN-based light-emitting diodes with nanotextured indium tin oxide layer using self-assembled cesium chloride nanospheres. *Japanese Journal of Applied Physics, 51*(2R), 020204.

Zhurko, G., and Zhurko, D. (2014). Chemcraft (version 1.7, build 382).

APPENDICES

The thermodynamic functions of the molecular and ionic clusters were obtained for temperatures 298.15 K and between 800–1500 K. The values of the molar heat capacity $c°_p$, the Gibbs reduced free energy Φ°, and entropy $S°$ are given in $J·mol^{-1}·K^{-1}$, and the enthalpy increment $H°(T)–H°(0)$ is in $kJ·mol^{-1}$; absolute temperature T is in kelvins. For the species existing in different isomeric forms, the thermodynamic functions are given for the most abundant isomers.

Appendix 1: Thermodynamic functions of the molecular and ionic clusters of cesium fluoride

The thermodynamic functions of the molecular and ionic clusters Cs_3F_3, Cs_4F_4, Cs_2F^+, CsF_2^-, $Cs_3F_2^+$, $Cs_2F_3^-$, $Cs_4F_3^+$, and $Cs_5F_4^+$ are given in Tables A1.1−A1.8.

Table A1.1. Thermodynamic functions of the Cs_3F_3 (C_s)

T	$c°_p$	Φ°	$S°$	$H°(T)–H°(0)$
298.15	306.464	395.502	500.294	31.244
800	808.314	508.071	629.352	97.025
900	908.314	522.429	644.942	110.262
1000	1008.314	535.390	658.902	123.512
1100	1108.314	547.203	671.54	136.771
1200	1208.314	558.052	683.084	150.038
1300	1308.314	568.083	693.707	163.311
1400	1408.314	577.412	703.546	176.587
1500	1508.314	586.130	712.709	189.868

Table A1.2. Thermodynamic functions of the Cs_4F_4 (T_d)

T	$c°_p$	Φ°	$S°$	$H°(T)–H°(0)$
298.15	175.894	402.743	540.240	40.995
800	181.904	553.390	717.705	131.452
900	182.114	572.862	739.144	149.654
1000	182.274	590.467	758.340	167.873
1100	182.384	606.531	775.718	186.106
1200	182.474	621.300	791.591	204.349
1300	182.534	634.969	806.199	222.599
1400	182.614	647.689	819.728	240.855
1500	182.644	659.583	832.327	259.116

Table A1.3. Thermodynamic functions of the Cs_2F^+ ($D_{\infty h}$)

T	$c°_p$	$\Phi°$	$S°$	$H°(T)–H°(0)$
298.15	60.383	263.406	315.742	15.604
800	62.060	318.265	376.402	46.510
900	62.121	325.139	383.716	52.719
1000	62.164	331.329	390.263	58.934
1100	62.201	336.961	396.19	65.152
1200	62.221	342.125	401.603	71.373
1300	62.241	346.895	406.585	77.597
1400	62.256	351.325	411.198	83.822
1500	62.275	355.462	415.494	90.049

Table A1.4. Thermodynamic functions of the CsF_2^- (C_{2v})

T	$c°_p$	$\Phi°$	$S°$	$H°(T)–H°(0)$
298.15	56.489	261.568	311.424	14.865
800	57.949	313.434	368.112	43.743
900	57.998	319.895	374.940	49.540
1000	58.046	325.711	381.054	55.343
1100	58.071	330.998	386.587	61.148
1200	58.100	335.843	391.640	66.956
1300	58.113	340.317	396.291	72.766
1400	58.128	344.471	400.597	78.577
1500	58.134	348.347	404.607	84.389

Table A1.5. Thermodynamic functions of the $Cs_3F_2^+$ (C_{2v}, V-shaped)

T	$c°_p$	$\Phi°$	$S°$	$H°(T)–H°(0)$
298.15	104.308	374.906	463.611	26.448
800	107.514	468.660	568.595	79.948
900	107.629	480.482	581.266	90.706
1000	107.717	491.138	592.611	101.473
1100	107.791	500.836	602.881	112.249
1200	107.829	509.737	612.261	123.029
1300	107.877	517.960	620.894	133.814
1400	107.902	525.601	628.889	144.603
1500	107.931	532.738	636.334	155.394

Table A1.6. Thermodynamic functions of the $Cs_2F_3^-$ (C_{2h}, Z-shaped)

T	$c°_p$	$\Phi°$	$S°$	$H°(T)–H°(0)$
298.15	104.582	376.883	467.040	26.880
800	107.566	471.611	572.164	80.443
900	107.674	483.501	584.840	91.205
1000	107.750	494.212	596.189	101.977
1100	107.816	503.957	606.462	112.755
1200	107.853	512.897	615.845	123.538
1300	107.896	521.151	624.479	134.326
1400	107.912	528.822	632.476	145.116
1500	107.947	535.983	639.922	155.909

Table A1.7. Thermodynamic functions of the $Cs_4F_3^+$ (C_{3v})

T	$c°_p$	$\Phi°$	$S°$	$H°(T)–H°(0)$
298.15	152.314	412.004	534.919	36.647
800	157.154	544.798	688.348	114.840
900	157.324	561.798	706.869	130.564
1000	157.424	577.148	723.451	146.303
1100	157.514	591.142	738.462	162.052
1200	157.624	603.998	752.173	177.810
1300	157.634	615.888	764.79	193.573
1400	157.714	626.946	776.476	209.342
1500	157.734	637.282	787.358	225.114

Table A1.8. Thermodynamic functions of the $Cs_5F_4^+$ (C_{3v})

T	$c°_p$	$\Phi°$	$S°$	$H°(T)–H°(0)$
298.15	200.304	479.982	640.757	47.935
800	206.76	654.093	842.594	150.801
900	206.98	676.418	866.961	171.489
1000	207.13	696.582	888.779	192.197
1100	207.23	714.966	908.529	212.919
1200	207.37	731.859	926.569	233.652
1300	207.47	747.483	943.17	254.393
1400	-462.91	762.017	958.546	275.140
1500	207.57	775.602	972.864	295.893

Appendix 2: Thermodynamic functions of the molecular and ionic clusters of cesium chloride

The thermodynamic functions of the molecular and ionic clusters Cs_2Cl_2, Cs_3Cl_3, Cs_4Cl_4, $Cs_4Cl_3^+$, and $Cs_5Cl_4^+$ are given in Tables A2.1−A2.5.

Table A2.1. Thermodynamic functions of the Cs_2Cl_2 (D_{2h})

T	$c°_p$	$\Phi°$	$S°$	$H°(T)–H°(0)$
298.15	81.703	319.033	389.901	21.1292
700	82.876	382.709	460.268	54.2914
800	82.943	393.111	471.339	62.5825
900	82.981	402.356	481.11	70.8788
1000	83.016	410.676	489.855	79.1787
1100	83.045	418.240	497.768	87.4813
1200	83.054	425.173	504.994	95.7858
1300	83.073	431.572	511.643	104.092
1400	83.087	437.514	517.799	112.399
1500	83.106	443.060	523.531	120.707
1600	83.101	448.259	528.894	129.016

Table A2.2. Thermodynamic functions of the Cs_3Cl_3 (C_s)

T	$c°_p$	$\Phi°$	$S°$	$H°(T)–H°(0)$
298.15	131.014	434.0219	548.044	33.996
700	132.654	536.3131	660.748	87.104
800	132.744	552.9993	678.468	100.375
900	132.804	567.827	694.107	113.652
1000	132.854	581.167	708.102	126.935
1100	132.874	593.2905	720.765	140.222
1200	132.904	604.4022	732.328	153.511
1300	132.924	614.6578	742.967	166.802
1400	132.944	624.1787	752.818	180.095
1500	132.944	633.0633	761.990	193.390
1600	132.974	641.3929	770.571	206.685

Table A2.3. Thermodynamic functions of the Cs_4Cl_4 (T_d)

T	$c°_p$	$\Phi°$	$S°$	$H°(T)–H°(0)$
298.15	180.144	457.9011	610.64	45.5391
700	182.414	596.235	765.616	118.567
800	182.524	618.964	789.981	136.814
900	182.604	639.184	811.485	155.071
1000	182.654	657.393	830.728	173.335
1100	182.724	673.955	848.14	191.604
1200	182.754	689.143	864.04	209.877
1300	182.754	703.166	878.668	228.153
1400	182.794	716.192	892.214	246.431
1500	182.804	728.352	904.826	264.711
1600	182.854	739.754	916.624	282.992

Table A2.4. Thermodynamic functions of the $Cs_4Cl_3^+$ (C_{3v})

T	$c°_p$	$\Phi°$	$S°$	$H°(T)–H°(0)$
298.15	155.674	456.3205	590.509	40.0083
700	157.544	577.1123	724.388	103.093
800	157.634	596.8658	745.432	118.853
900	157.734	614.425	764.005	134.622
1000	157.784	630.229	780.625	150.396
1100	157.804	644.5957	795.663	166.174
1200	157.764	657.765	809.395	181.956
1300	157.764	669.9213	822.029	197.74
1400	157.904	681.2094	833.728	213.526
1500	157.824	691.744	844.62	229.314
1600	157.774	701.6206	854.81	245.103

Table A2.5. Thermodynamic functions of the $Cs_5Cl_4^+$ (C_{3v})

T	$c°_p$	$\Phi°$	$S°$	$H°(T)–H°(0)$
298.15	205.114	550.455	728.102	52.966
700	207.344	710.059	904.373	136.020
800	207.484	736.119	932.070	156.761
900	207.554	759.274	956.511	177.513
1000	207.594	780.111	978.383	198.272
1100	207.614	799.049	998.172	219.035
1200	207.724	816.405	1016.240	239.802
1300	207.714	832.429	1032.870	260.573
1400	207.754	847.299	1048.260	281.345
1500	207.664	861.177	1062.590	302.119
1600	207.674	874.191	1076.000	322.895

Appendix 3: Thermodynamic functions of the cluster ions of cesium bromide and iodide

The thermodynamic functions of cluster ions Cs_2X^+, CsX_2^-, $Cs_3X_2^+$, $Cs_2X_3^-$ (X = Br, I) are given in Tables A3.1−A3.16.

Table A3.1. Thermodynamic functions of Cs_2Br^+ ($D_{\infty h}$)

T	Φ°	$S°$	$H°(T) - H°(0)$
298.15	295.239	352.864	17.181
700	345.678	405.922	42.171
800	353.739	414.240	48.401
900	360.877	421.579	54.631
1000	367.282	428.145	60.863
1100	373.089	434.085	67.096
1200	378.401	439.508	73.329
1300	383.296	444.498	79.563
1400	387.835	449.118	85.796
1500	392.065	453.419	92.031
1600	396.027	457.442	98.265

Table A3.2. Thermodynamic functions of $CsBr_2^-$ ($D_{\infty h}$)

T	Φ°	$S°$	$H°(T) - H°(0)$
298.15	297.551	355.651	17.323
700	348.273	408.736	42.324
800	356.363	417.056	48.555
900	363.522	424.396	54.786
1000	369.943	430.962	61.019
1100	375.765	436.903	67.252
1200	381.089	442.327	73.485
1300	385.994	447.317	79.719
1400	390.542	451.937	85.954
1500	394.779	456.238	92.188
1600	398.748	460.262	98.423

Table A3.3. Thermodynamic functions of $Cs_3Br_2^+$ (V-shaped, C_{2v})

T	Φ°	S°	$H°(T) - H°(0)$
298.15	435.304	533.967	29.416
700	522.016	625.898	66.897
800	535.923	640.315	76.862
900	548.242	653.034	86.830
1000	559.300	664.414	96.800
1100	569.332	674.710	106.770
1200	578.510	684.110	116.742
1300	586.970	692.758	126.715
1400	594.817	700.766	136.689
1500	602.131	708.221	146.663
1600	608.983	715.195	156.637

Table A3.4. Thermodynamic functions of $Cs_2Br_3^-$ (linear, $D_{\infty h}$)

T	Φ°	S°	$H°(T) - H°(0)$
298.15	453.6812	557.533	30.963
700	544.552	653.058	75.954
800	559.072	668.032	87.168
900	571.926	681.242	98.384
1000	583.459	693.061	109.602
1100	593.917	703.754	120.821
1200	603.483	713.517	132.041
1300	612.296	722.498	143.262
1400	620.469	730.814	154.483
1500	628.087	738.556	165.704
1600	635.220	745.799	176.926

Table A3.5. Thermodynamic functions of $Cs_3Br_2^+$ (cyclic, C_{2v})

T	Φ°	S°	$H°(T) - H°(0)$
298.15	418.579	516.190	29.103
700	504.685	608.116	3290.293
800	518.535	622.532	1388.692
900	530.811	635.252	842.065
1000	541.834	646.632	592.264
1100	551.836	656.927	451.532
1200	560.990	666.327	362.226
1300	569.430	674.975	300.905
1400	577.259	682.983	256.380
1500	584.559	690.438	222.694
1600	591.397	697.412	196.462

Table A3.6. Thermodynamic functions of $Cs_2Br_3^-$ (cyclic, C_{2v})

T	$\Phi°$	$S°$	$H°(T) - H°(0)$
298.15	415.791	513.565	29.151
700	501.997	605.507	72.457
800	515.857	619.924	83.254
900	528.141	632.644	94.053
1000	539.170	644.024	104.854
1100	549.177	654.320	115.657
1200	558.336	663.720	126.461
1300	566.780	672.368	137.265
1400	574.612	680.376	148.070
1500	581.914	687.831	158.876
1600	588.754	694.805	169.682

Table A3.7. Thermodynamic functions of $Cs_3Br_2^+$ (bipyramidal, D_{3h})

T	$\Phi°$	$S°$	$H°(T) - H°(0)$
298.15	382.493	478.083	28.500
700	467.417	569.957	71.778
800	481.156	584.371	82.572
900	493.344	597.088	93.369
1000	504.298	608.467	104.169
1100	514.244	618.762	114.970
1200	523.350	628.161	125.773
1300	531.750	636.808	136.576
1400	539.543	644.815	147.381
1500	546.813	652.270	158.185
1600	553.625	659.244	168.991

Table A3.8. Thermodynamic functions of $Cs_2Br_3^-$ (bipyramidal, D_{3h})

T	$\Phi°$	$S°$	$H°(T) - H°(0)$
298.150	376.844	472.659	28.567
700	461.910	564.564	71.858
800	475.663	578.979	82.653
900	487.863	591.698	93.451
1000	498.825	603.077	104.252
1100	508.778	613.373	115.054
1200	517.891	622.772	125.857
1300	526.296	631.420	136.661
1400	534.095	639.427	147.465
1500	541.368	646.882	158.271
1600	548.184	653.856	169.076

Table A3.9. Thermodynamic functions of Cs_2I^+ ($D_{\infty h}$)

T	$\Phi°$	$S°$	$H°(T) - H°(0)$
298.15	303.678	362.054	17.405
700	354.570	415.166	42.417
800	362.676	423.487	48.649
900	369.848	430.827	54.881
1000	376.280	437.395	61.115
1100	382.110	443.336	67.348
1200	387.442	448.760	73.582
1300	392.353	453.750	79.817
1400	396.906	458.371	86.051
1500	401.148	462.672	92.286
1600	405.121	466.696	98.521

Table A3.10. Thermodynamic functions of CsI_2^- ($D_{\infty h}$)

T	$\Phi°$	$S°$	$H°(T) - H°(0)$
298.15	309.246	368.052	17.533
700	360.392	421.184	42.554
800	368.523	429.506	48.787
900	375.715	436.848	55.020
1000	382.163	443.416	61.254
1100	388.006	449.358	67.488
1200	393.347	454.782	73.722
1300	398.267	459.772	79.957
1400	402.828	464.393	86.191
1500	407.078	468.695	92.426
1600	411.056	472.719	98.661

Tabe A3.11. Thermodynamic functions of $Cs_3I_2^+$ (linear, $D_{\infty h}$)

T	$\Phi°$	$S°$	$H°(T) - H°(0)$
298.150	446.083	550.685	31.187
700	537.413	646.280	76.207
800	551.977	661.257	87.424
900	564.868	674.470	98.642
1000	576.429	686.291	109.862
1100	586.911	696.986	121.082
1200	596.497	706.749	132.303
1300	605.327	715.731	143.525
1400	613.514	724.048	154.747
1500	621.145	731.791	165.969
1600	628.288	739.033	177.192

Table A3.12. Thermodynamic functions of $Cs_2I_3^-$ (linear, $D_{\infty h}$)

T	Φ°	S°	H°(T) – H°(0)
298.15	445.83	550.755	31.283
700	537.355	646.374	76.313
800	551.940	661.353	87.531
900	564.845	674.567	98.750
1000	576.418	686.388	109.970
1100	586.909	697.083	121.191
1200	596.504	706.847	132.412
1300	605.341	715.829	143.634
1400	613.534	724.146	154.857
1500	621.170	731.889	166.079
1600	628.318	739.132	177.302

Table A3.13. Thermodynamic functions of $Cs_3I_2^+$ (cyclic, C_{2v})

T	Φ°	S°	H°(T) – H°(0)
298.15	428.610	528.018	29.638
700	515.792	620.054	72.983
800	529.746	634.476	83.784
900	542.103	647.199	94.586
1000	553.192	658.582	105.390
1100	563.248	668.879	116.194
1200	572.448	678.281	127.000
1300	580.926	686.930	137.805
1400	588.788	694.939	148.612
1500	596.115	702.394	159.418
1600	602.978	709.369	170.225

Table A3.14. Thermodynamic functions of $Cs_2I_3^-$ (cyclic, C_{2v})

T	Φ°	S°	H°(T) – H°(0)
298.15	438.302	537.833	29.675
700	525.557	629.876	73.023
800	539.519	644.299	83.824
900	551.882	657.022	94.626
1000	562.975	668.405	105.430
1100	573.035	678.703	116.235
1200	582.238	688.105	127.040
1300	590.719	696.754	137.846
1400	598.582	704.762	148.652
1500	605.912	712.218	159.459
1600	612.777	719.193	170.266

Table A3.15. Thermodynamic functions of $Cs_3I_2^+$ (bipyramidal, D_{3h})

T	Φ°	S°	$H°(T) - H°(0)$
298.15	391.065	489.077	29.222
700	486.032	589.692	72.562
800	499.910	604.113	83.362
900	512.209	616.836	94.164
1000	523.251	628.219	104.968
1100	533.269	638.516	115.772
1200	542.437	647.918	126.577
1300	550.889	656.567	137.382
1400	558.726	664.575	148.189
1500	566.034	672.031	158.995
1600	572.879	679.005	169.802

Table A3.16. Thermodynamic functions of $Cs_2I_3^-$ (bipyramidal, D_{3h})

T	Φ°	S°	$H°(T) - H°(0)$
298.15	401.919	500.054	29.259
700	488.365	592.077	72.599
800	502.251	606.499	83.399
900	514.554	619.221	94.200
1000	525.600	630.604	105.004
1100	535.621	640.901	115.808
1200	544.792	650.303	126.613
1300	553.245	658.952	137.419
1400	561.085	666.960	148.225
1500	568.395	674.416	159.031
1600	575.241	681.390	169.838

Appendix 4: Thermodynamic functions of the molecular clusters of cesium bromide and iodide

The thermodynamic functions of the molecular clusters Cs_3Br_3, Cs_3I_3, Cs_4Br_4, and Cs_4I_4 are given in Tables A4.1−A4.4.

Table A4.1. Thermodynamic functions of Cs_3Br_3 (butterfly shaped, C_S)

T	Φ°	S°	H°(T) – H°(0)
298.15	461.617	579.868	35.257
700	566.487	692.948	88.523
800	583.427	710.687	101.808
900	598.454	726.340	115.097
1000	611.955	740.344	128.389
1100	624.212	753.015	141.683
1200	635.434	764.583	154.979
1300	645.784	775.226	168.275
1400	655.386	785.081	181.573
1500	664.342	794.256	194.871
1600	672.733	802.839	208.170

Table A4.2. Thermodynamic functions of Cs_2I_3 (butterfly shaped, C_S)

T	Φ°	S°	H°(T) – H°(0)
298.15	487.441	608.317	36.039
700	593.880	721.553	89.3708
800	610.974	739.301	102.662
900	626.119	754.959	115.956
1000	639.716	768.968	129.252
1100	652.051	781.641	142.549
1200	663.340	793.212	155.847
1300	673.745	803.857	169.146
1400	683.394	813.713	182.446
1500	692.392	822.889	195.746
1600	700.819	831.473	209.046

Table A4.3. Thermodynamic functions of Cs_4Br_4 (distorted cube, T_d)

T	$\Phi°$	$S°$	$H°(T) - H°(0)$
298.15	678.367	678.527	47.801
700	833.842	834.015	121.043
800	858.234	858.408	139.311
900	879.755	879.930	157.584
1000	899.010	899.186	175.860
1100	916.432	916.608	194.140
1200	932.338	932.515	212.421
1300	946.973	947.150	230.704
1400	960.522	960.700	248.988
1500	973.137	973.315	267.274
1600	984.939	985.117	285.560

Table A4.4. Thermodynamic functions of Cs_4I_4 (distorted cube, T_d)

T	$\Phi°$	$S°$	$H°(T) - H°(0)$
298.15	696.365	709.431	46.703
700	839.398	839.572	121.846
800	863.799	863.974	140.120
900	885.326	885.502	158.398
1000	904.586	904.763	176.679
1100	922.011	922.188	194.961
1200	937.919	938.097	213.245
1300	952.555	952.733	231.531
1400	966.107	966.285	249.817
1500	978.723	978.902	268.104
1600	990.525	990.704	286.392